LEVEL II

(12) B.S.

Contract No. (15) N00014-79-C-0021

(6) DETERMINATION OF THE EFFECT OF COMPOSITION, STRUCTURE AND ELECTROCHEMICAL MASS TRANSPORT PROPERTIES ON ADHESION AND CORROSION INHIBITION OF PAINT FILMS.

Annual Progress Report No. 2,
For the Period Nov 79 - Oct 80,
(31)

Prepared for
UNITED STATES NAVY
Naval Ocean Research and Development Activity
Bay St. Louis, MS 39520

(11) Dec 80

(12) 110

By:
ELECTROCHEMICAL TECHNOLOGY CORP.
3935 Leary Way N.W.
Seattle, WA 98107

(10) ROBERT T. RUGGERI
THEODORE R. BECK Principal Investigator

Unclassified

SECURITY CLASSIFICATION OF THIS PAGE (When Data Entered)

REPORT DOCUMENTATION PAGE	READ INSTRUCTIONS BEFORE COMPLETING FORM
1. REPORT NUMBER	2. GOVT ACCESSION NO. AD-A095293	3. RECIPIENT'S CATALOG NUMBER
4. TITLE (and Subtitle) Determination of the Effect of Composition, Structure and Electrochemical Mass Transport Properties on Adhesion and Corrosion Inhibition of Paint Films	5. TYPE OF REPORT & PERIOD COVERED Annual Nov. 1, 1979 to Oct. 31, 1980
	6. PERFORMING ORG. REPORT NUMBER
7. AUTHOR(s) R. T. Ruggeri and T. R. Beck	8. CONTRACT OR GRANT NUMBER(s) N00014-79-C-0021
9. PERFORMING ORGANIZATION NAME AND ADDRESS Electrochemical Technology Corp. 3935 Leary Way N.W. Seattle, WA 98107	10. PROGRAM ELEMENT, PROJECT, TASK AREA & WORK UNIT NUMBERS
11. CONTROLLING OFFICE NAME AND ADDRESS United States Navy Naval Ocean Research and Development Activity Bay St. Louis, MS 39520	12. REPORT DATE December 1980
	13. NUMBER OF PAGES 112
14. MONITORING AGENCY NAME & ADDRESS (if different from Controlling Office)	15. SECURITY CLASS. (of this report) Unclassified
	15a. DECLASSIFICATION/DOWNGRADING SCHEDULE

16. DISTRIBUTION STATEMENT (of this Report)

Reproduction in whole or in part is permitted for any purpose of the United States Government

DISTRIBUTION STATEMENT A
Approved for public release;
Distribution Unlimited

17. DISTRIBUTION STATEMENT (of the abstract entered in Block 20, if different from Report)

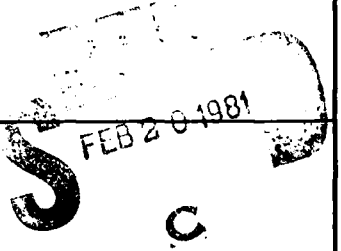

18. SUPPLEMENTARY NOTES

None

19. KEY WORDS (Continue on reverse side if necessary and identify by block number)

Paint, polyurethane, vinyl, diffusion, corrosion, mass transport, sodium ion, chloride ion, water, permeation, permeability coefficient, diffusivity

20. ABSTRACT (Continue on reverse side if necessary and identify by block number)

Mass transport properties of five different paints have been investigated. Water permeability coefficients have been obtained using ASTM methods. Water diffusion coefficients have been measured for two paints, a vinyl resin and a polyurethane. The results strongly suggest that the diffusivity changes with position across these paints. A permeability model encompassing these facts is presented. —> cont

DD FORM 1 JAN 73 1473 EDITION OF 1 NOV 65 IS OBSOLETE

Unclassified

SECURITY CLASSIFICATION OF THIS PAGE (When Data Entered)

Cont.

Permeability coefficients and transference numbers for the transport of sodium and chloride ions have been measured in one type of polyurethane paint. The evidence is that two thirds of the current passing through the polyurethane films is not carried by either sodium or chloride. A model has been proposed in which the additional current is carried by ions resulting from dissociation of a neutral compound. The transport parameters will be related to chemical and structural properties of the paints to obtain a fundamental understanding of the corrosion mechanism.

TABLE OF CONTENTS

ACKNOWLEDGMENT

Most of the experimental work in the second year was done in house by chemical technician, J. H. Mabe. The Department of Chemical Engineering, University of Washington, provided facilities for scintillation counting of radioisotope samples. Professor J. C. Seferis and student, A. R. Wedgewood, continued to provide consulting on physical and mechanical properties of paint films. P. Olson, Experimental Research Equipment Co., made the high pressure reverse osmosis apparatus and other special equipment necessary to carry out the work. S. Drake typed the report.

Special appreciation is extended to Dr. Edward J. Green, Program Director, Chemical Oceanography Division, Naval Ocean Research and Development Activity, Bay St. Louis, Mississippi, for his continued support and encouragement of this program.

1.0 INTRODUCTION

This second annual progress report describes work completed for the Naval Ocean Research and Development Activity between November 1, 1979 and October 31, 1980. The first annual progress report (1) concentrated primarily on the quantitative description of the chemical and physical structure as well as the adhesive properties of paints. This second report describes work investigating the mass transport properties of detached paint films. Both the transport properties and the structural features of paints are important to our ultimate objective; a quantitative understanding of the mechanism of corrosion under paint films.

An understanding of the corrosion mechanism requires an investigation of the physical and electrochemical conditions at the interface where corrosion is taking place. Measurement of the interfacial conditions is invariably difficult. Various spectroscopic methods can be used to investigate the paint-metal interface, but ordinary physical probes invariably upset the natural corrosion process at the measurement point. Consequently, a means of deducing the local conditions at the interface from measurements made at remote sites is required. It is proposed to establish the conditions at the paint-metal interface through the use of a mathematical model (2).

The mathematical model was created to quantitatively describe the transport of all mobile species through paint films. The films are described as a homogeneous diffusion barrier controlling the transport of corrosion products and reactants. The transport processes are quantitatively described in terms of a series of transport parameters, diffusion coefficients, transference numbers, etc., which in turn depend on the chemical and physical properties of the paints. The mass transport characteristics of the paints under study are currently being determined, and will be related later to the chemical and physical structure of paints. Then a quantitative relationship will have been established between the physical properties of the paint, the external conditions (electrolyte concentration, potential, etc.), and the local conditions at the corroding surface. The local conditions must then be related to the actual corrosion

processes occurring at the paint-metal interface. Completion of these steps will constitute development of a practical, quantitative model of corrosion under paints which can be used as a framework to evaluate and improve paint performance.

The first annual report discussed the chemical and physical structure and adhesive properties of the paints under study. This report concentrates on the measurement of transport properties, specifically, water diffusion, and sodium and chloride ion migration. Water transport is important because of the key role water plays throughout the corrosion process; it affects adhesion, the corrosion reaction, paint swelling, and solute solubility, as well as other properties. Ion transport is primarily related to the passage of current. At this time water permeability experiments have been conducted with all paint types. Hittorf experiments to establish ionic transference numbers and permeability coefficients have been performed with two paints, but primarily with one type of polyurethane. Limited data have been obtained on the thermodynamic variables, water solubility and ionic capacity. An apparatus has been constructed to determine the water diffusivity in paint films. Extensive tests have been conducted with two different designs of this apparatus, and two types of paint have been investigated. These experiments are described in Sect. 3 as well as in the two published papers related to this work and included in appendix B.

Future plans involve continuing the measurements of transport properties as well as establishing their relationship to the structural features of paint. The mathematical model has already been completed, and, when a full set of transport parameters becomes availabe, quantitative evaluation of the corrosion process will begin. The final step will then be to correlate actual corrosion experience with the results of model calculations.

2.0 SUMMARY

This report describes a continuation of work to determine the mechanism of painted-metal corrosion and the role of the physical and chemical structure of paint. In the past year, work has been concentrated on the transport of water and solute ions through detached paint films. The investigation consisted of five separate test measurements made on unpigmented and uninhibited paints of commercial and military interest.

Water diffusivity has been determined at various temperatures and relative humidities with a special apparatus. Two distinct experimental techniques have been tested. The first measured the water absorption of a vinyl resin with an electrobalance, and the diffusivity was then calculated. The water diffusivity in this vinyl resin is independent of relative humidity. The equilibrium water solubility of the resin has been shown to depend greatly on the plasticizer (tricresyl phosphate) content.

The second experimental technique for determining water diffusivity utilized a quartz crystal oscillator to measure micro mass changes. These tests showed that the diffusivity of water in one type of polyurethane was also independent of relative humidity (water concentration); however, the diffusivity is a function of film thickness. A possible explanation is that the physical properties of paints vary in the direction normal to the paint-metal interface, and that a dense low-diffusivity skin may form at the paint-air interface as the paint dries.

Water permeability coefficients have been measured employing the standard ASTM method E96-66. These data generally support the conclusion that the paint properties vary with position across the film.

The ionic capacity of one type of polyurethane has been determined using a radiotracer technique. These results are considered preliminary, but an upper bound has been established for the ionic capacity of 10^{-2} m mole/g-paint.

Hittorf experiments have determined the water and ion permeability coefficients for the polyurethane. Transference numbers for sodium and

chloride ions have also been measured. These tests show that roughly 2/3 of the total current is carried by "secondary" ions other than sodium or chloride. Conventional membrane theory offers no explanation as to the identity of the secondary ions.

Transference numbers have been measured for polyurethane membranes in hydrogen iodide (HI) and sodium chloride solutions. The results are consistent with those of Hittorf experiments discussed above. The transference number for hydrogen ion in HI is 0.98. The transference numbers of both hydrogen and sodium change abruptly at solution concentrations near 10^{-2} N indicating a change in the diffusion mechanism at that concentration.

Two papers discussing the experiments and interpreting this work have been presented to professional groups in the past year. These papers are included in this report as Appendix B.

3.0 RESULTS AND DISCUSSION

The work performed in the past year has centered on determining the transport properties of paint films. The same paint designations as were presented in the first annual progress report (1) have been used. The paint compositions have not been included. As in the first report, no pigments or corrosion inhibitors have been used. The work description has been divided into six major categories; each is individually discussed.

3.1 Water Diffusivity

3.1.1 Theory

The diffusivity of water in a polymer film can be obtained in several ways. One is to measure the permeability coefficient (P) and the dimensionless solubility (S) in separate experiments and calculate the diffusivity (D).

$$D = \frac{P}{S} \text{ cm}^2/\text{s} \tag{1}$$

Another way is to measure the rate of water uptake or loss following a change in the external partial pressure of water. This method has the advantage that the diffusivity is obtained directly without evaluating the solubility (3, 4).

The mathematics describing diffusion into a thin, flat sheet have been discussed by Crank (3). The pertinent equation can be written

$$R_w = \frac{W_\infty - W_t}{W_\infty - W_o} = \sum_{n=o}^{\infty} \frac{8}{(2n+1)^2\pi^2} \exp\left[-\frac{(2n+1)^2\pi^2}{4} \frac{Dt}{\ell^2}\right] \tag{2}$$

where W_∞ = weight at infinite time (g)
W_o = weight at time zero (g)
W_t = weight at time t (g)
D = diffusion coefficient (cm^2/s)
2ℓ = film thickness (cm)

At long times,

$$\frac{Dt}{\ell^2} \gg 1 \tag{3}$$

Eq. 2 simplifies to

$$R_w = \frac{8}{\pi 2} \exp\left[-\frac{\pi^2}{4}\frac{Dt}{\ell^2}\right] \tag{4}$$

Under these conditions a plot of $\ell n(R_w)$ vs time (t) produces a straight line, and the diffusivity can be calculated from the slope. The primary disadvantage of this technique is the uncertainty in choosing a value for W_∞. The results are very sensitive to W_∞. A second method employing the initial slope $d(R_w)/d\sqrt{t}$ can be used if initial slope data are available. Both of these methods have been used, but it was most advantageous to obtain the best fit of all the data to a finite series. The finite-series results based on Eq. 2 are subject to fewer errors than those obtained by either the long-time or initial-slope methods. The primary disadvantage of using a finite series is that at short times many terms must be evaluated. This disadvantage has been circumvented by employing a programmable calculator to evaluate the series to a prescribed accuracy and search for the best value of the diffusivity.

3.1.2 Experimental

During the past year a humidity apparatus has been built for the purpose of measuring the diffusivity of water in polymers at various temperatures and relative humidities. This equipment was designed so that the polymer film experiences a step change in relative humidity at a constant temperature ($\pm 0.5°C$). The apparatus was constructed of Plexiglas and insulated with corrugated cardboard. A schematic diagram is shown in Fig. 1.

The humidity apparatus consists of two chambers. The polymer is initially placed inside the smaller chamber (219 cm^3) formed by pressing a metal cup against a metal "hat" connected to the roof of the large chamber or "box." The cup can be lowered and removed from the box through

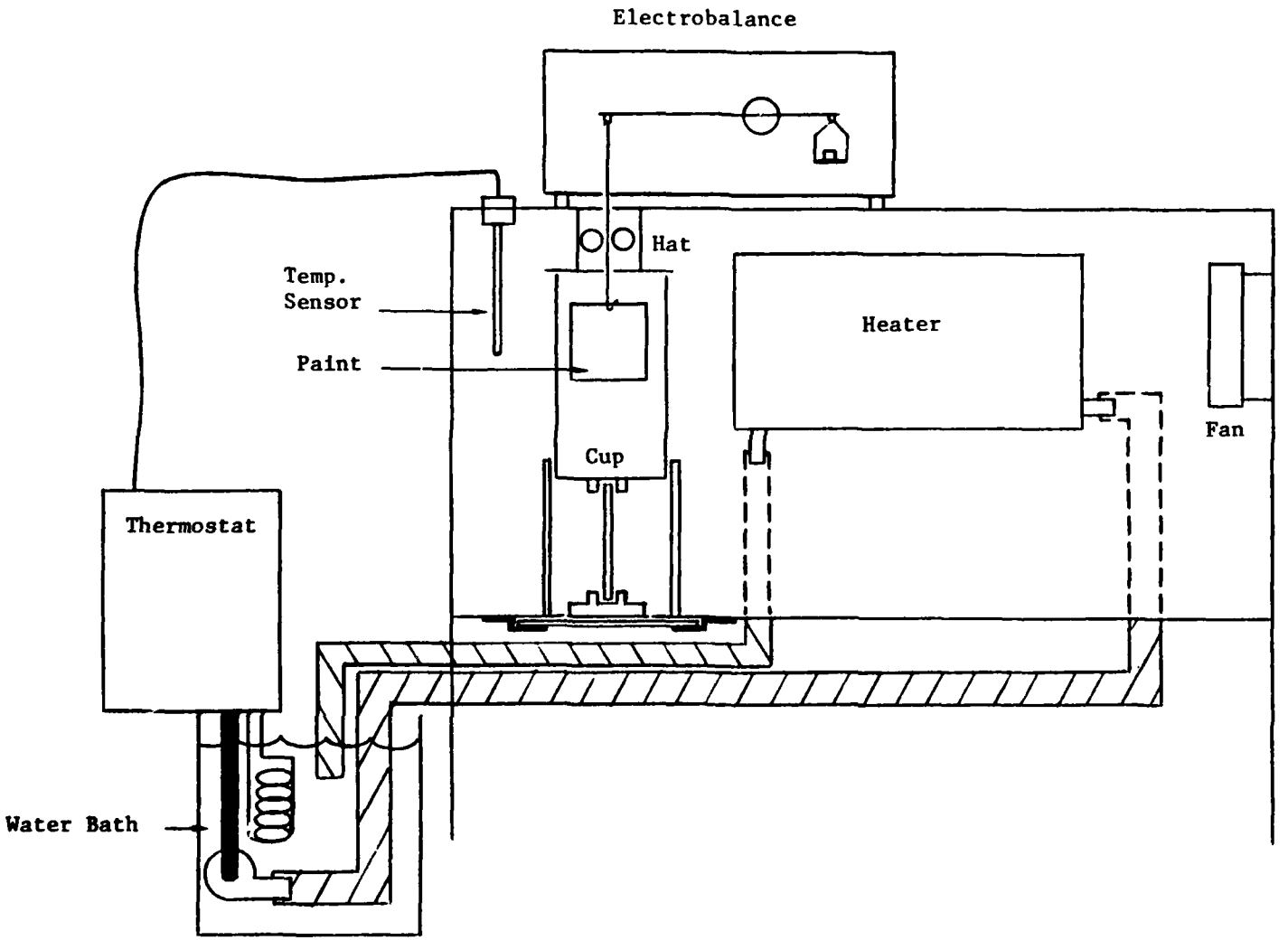

Fig. 1. Humidity chamber and accessories for diffusivity determination.

a hole in the floor. The volume of the box (15 ℓ) is large compared to that of the cup. During the course of the experiment, a membrane is allowed to come to equilibrium with the atmosphere inside the cup. At time zero, the cup is lowered and the atmosphere inside the cup is mixed with that in the large chamber by a fan. The atmosphere surrounding the membrane changes from that inside the cup to near that inside the large chamber in a short time (< 1 s). The change in weight of the membrane is recorded as a function of time after this step change, and the results are analyzed using Eq. 2 to determine the diffusivity.

Two methods have been used to determine the water absorbed by the polymer. Fig. 1 illustrates the first method employing a Cahn electrobalance, model gram-1501. Paint films weighing about 30 mg were hung on a nichrome wire in the humidity chamber. The wire was passed through a hole in the top of the humidity chamber to the electrobalance weighing beam. The electrobalance measured the change in mass of the paint film during the absorption process. This technique proved successful, but several disadvantages were inherent with this method.

(1) The fan circulating the air inside the chamber had to be turned off when electrobalance measurements were being taken. This changed the steady-state heat balance on the chamber, allowed convection currents and thermal gradients to develop, and introduced the possibility of air-side diffusion resistance.

(2) The gram-model Cahn is manually balanced, and the procedure requires several seconds to complete. This reduced the number of data points which could be obtained, particularly in the early stages of the diffusion process. The manual balancing method is not well suited for fast transient measurements, and the accuracy of the measurements suffers because the electrobalance is in balance for only an instant.

The advantage of using the electrobalance is that it measures mass directly, and despite the drawbacks mentioned above, reasonable results have been obtained.

The second method of measuring the absorbed water is indirect, observing the frequency change of a quartz-crystal oscillator. Soxman (5) indicates that the frequency of an AT-cut quartz crystal can be considered to depend only on the crystal mass for small changes in frequency ($\Delta f < 2\%$). A quartz crystal can thus be made to act as an exceedingly sensitive microbalance. A commercially available oscillator (Sloan Thickness Monitor, Digital Sensor Head, #900010) was mounted inside the humidity chamber. Small, thin films of paint were placed on several preweighed gold-coated crystals. After the paint had dried ($t > 7$ days) the painted crystals were weighed and the dry-film mass determined by difference. The crystals were then placed in the oscillator and subjected to a step function in relative humidity. The frequency change with time was recorded on a General Radio, model 1191, frequency counter and the results analyzed using Eq. 2 with

$$R_w = \frac{f_\infty - f_t}{f_\infty - f_o} \tag{5}$$

This crystal-oscillator method enjoys several advantages over the electrobalance technique:

(1) The fan can remain on after the cup has been dropped, while the absorption process is in progress. This insures smaller thermal and humidity gradients in both space and time within the humidity chamber.

(2) Highly precise frequency measurements can be made at constant, relatively short, intervals throughout the course of an experiment. This allows higher precision, especially in the critical "short-time" ($Dt/\ell^2 < 0.5$) region.

The primary disadvantages of the oscillator method are

(1) The films on the gold-coated crystals are thinner than commercial paint applications.

(2) The crystal frequency is sensitive to some parameters not related to the partial pressure of water, i.e., temperature, paint

film shape and position, etc.

(3) The measured frequency (fm) is the average frequency over the measuring period ($t_1 < t < t_2$):

$$fm = \frac{\int_{t_1}^{t_2} f\,dt}{t_2 - t_1} \qquad (6)$$

Both the second and third disadvantages can be circumvented through good experimental technique and more elaborate data manipulation, but the first disadvantage is inherent in the crystal-oscillator technique. A combination of the two experimental techniques appears best at this time.

3.1.3 Results and Discussion

To date, one paint type (VR3) has been tested in the humidity chamber using the Cahn electrobalance. The results have been analyzed in two ways using both Eq. 2 and 4. Typical results showing weight change as a function of time are illustrated in Fig. 2. The "long-time" approximation for the same series of experiments is presented in Fig. 3 showing that the data are fairly well represented by Eq. 4. The two methods of data reduction are compared in Table 1. The standard deviation of the "long-time" diffusivity experiments is 20% while that for the "complete-formula" (Eq. 2) result is 25%. The reason for the apparently higher steady-state weight gain in experiment 11 is not clear. It first appeared to be drift in the electrobalance calibration, but the instrument was frequently zeroed and undetected drift is considered unlikely. In any case, the accuracy of these results is about ±25%.

Tables 1 and 2 show diffusivity results for the same VR3 sample, but the temperatures are slightly different. Data for a different piece of VR3 are shown in Table 3. These data can be compared to those in Table 1 at the same temperature. They indicate that the variation in diffusivity between individual pieces of VR3 may be as great as a factor of two.

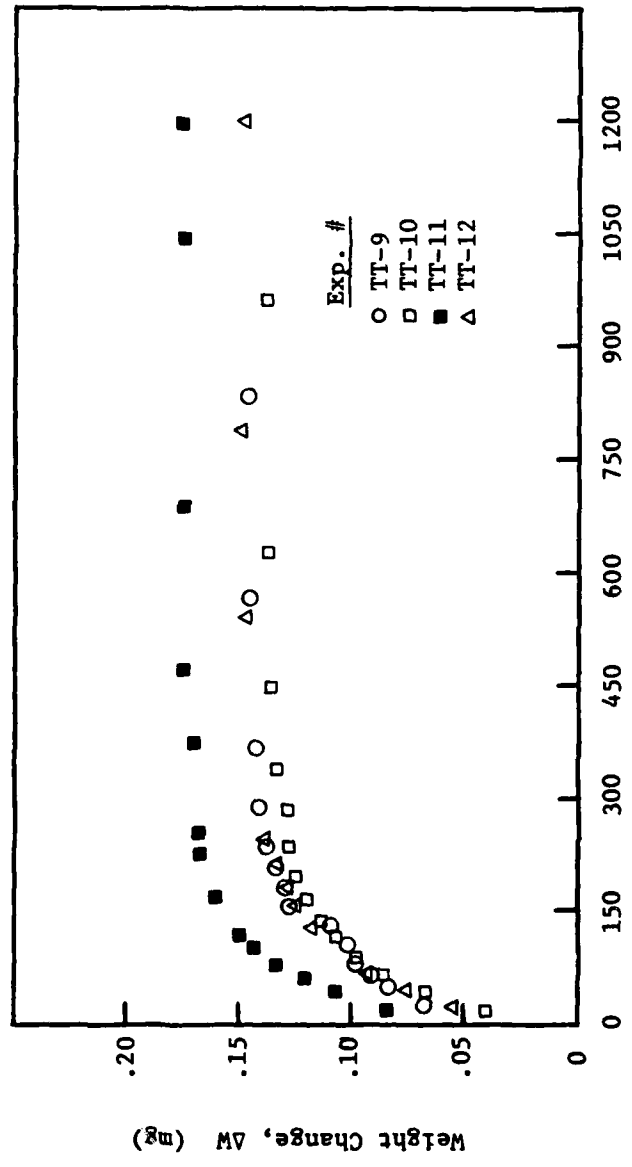

Fig. 2. Four water diffusivity experiments with VR3. Humidity step change from 0% to 83% RH at 22°C. Thickness = 3.20 x 10^{-3} cm.

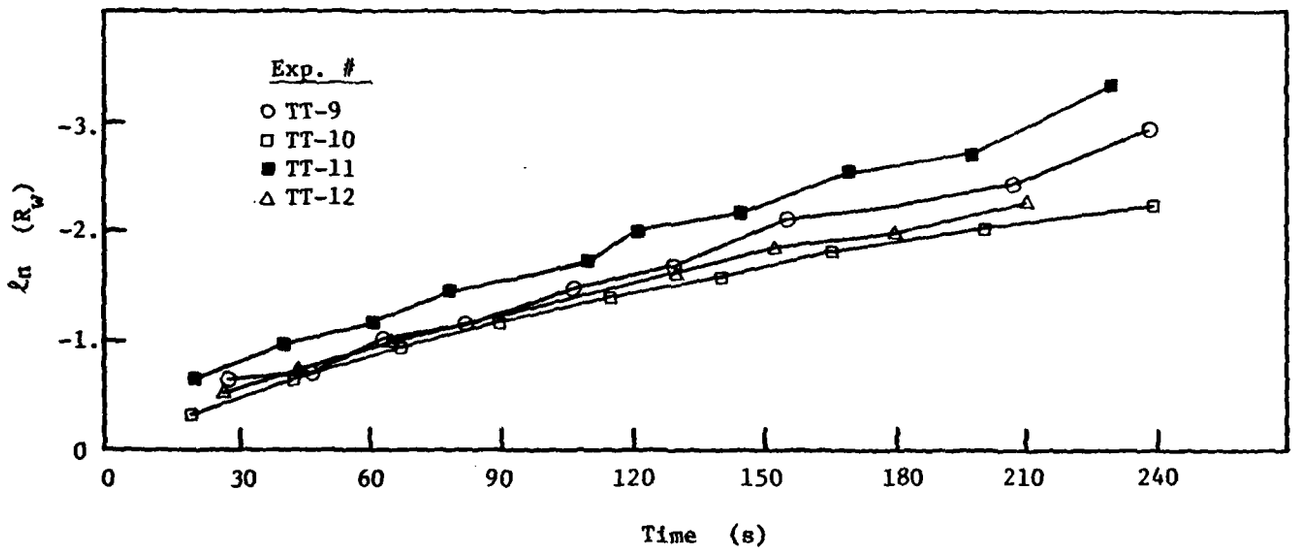

Fig. 3. Long-time approximation (Eq. 4) data for the four experiments shown in Fig. 2. $R_w = (W_\infty - W_t) / (W_\infty - W_o)$, thickness = 3.20×10^{-3} cm.

Table 1

Humidity Chamber Results for a VR3 Free Film

3.20×10^{-3} cm Thick

Experiment Number	Relative Humidity (%)	Temp. (C°)	Days at These Conditions	Diffusivity (cm^2/sec)		Dry Weight (mg)
				Long Time Approximation (eq. 4)	Complete Formula (eq. 2)	
9	83.6	22.0	3	4.98×10^{-8}	4.85×10^{-8}	29.111
10	83.5	22.3	4	3.32×10^{-8}	3.86×10^{-8}	29.112
11	83.5	22.3	5	4.98×10^{-8}	6.59×10^{-8}	29.106
12	83.4	22.7	6	3.74×10^{-8}	4.44×10^{-8}	29.106
Mean 9-12	83.5	22.3	4.5	4.25×10^{-8}	4.93×10^{-8}	29.109

Table 2

Humidity Chamber Results for a VR3 Free Film

3.20×10^{-3} cm Thick

Experiment Number	Relative Humidity %	Temp. (C°)	Days at These Conditions	Diffusivity (cm^2/sec)		Dry Weight (mg)
				Long Time Approximation (eq. 4)	Complete Formula (eq. 2)	
6	82.9	25.4	1	6.64×10^{-8}	7.45×10^{-8}	29.100
7	83.1	24.5	2	6.64×10^{-8}	9.14×10^{-8}	29.100
8	82.9	25.2	3	1.33×10^{-7}	1.66×10^{-7}	29.096
Mean 6-8	83.0	25.0	2	8.85×10^{-8}	1.11×10^{-7}	29.099

Table 3

Humidity Chamber Results for a VR3 Free Film
3.58×10^{-3} cm Thick

Experiment Number	Relative Humidity %	Temp. (C°)	Days at These Conditions	Diffusivity (cm^2/sec)		Dry Weight (mg)
				Long Time Approximation (eq. 4)	Complete Formula (eq. 2)	
14	83.6	22.0	4	5.71×10^{-8}	8.46×10^{-8}	26.902
15	83.5	22.3	5	5.19×10^{-8}	7.29×10^{-8}	26.891
Mean 14-15	83.6	22.2	4.5	5.45×10^{-8}	7.88×10^{-8}	26.897

Fig. 4 shows a sequence of experiments with VR3 in which the steady-state weight gain was observed to decrease from day to day while the experimental conditions were maintained constant. It appeared that the solubility of water in VR3 was decreasing significantly as the paint aged at 33°C. This decreasing solubility coincided with a slight decrease in dry-film weight as shown in Table 4. It was subsequently shown by infrared spectroscopy that the VR3 film had lost the plasticizer, tricresyl phosphate (TCP). Originally the paint film contained 9.5% by weight TCP. By observing the height of the 1580 cm^{-1} absorption peak, the TCP content of the used VR3 film was calculated to be 8.4%, a 1.1% change. This change in weight can be compared with the 1.3% change in dry-film weight observed during the course of the humidity-chamber experiments (TT-14 through TT-28). It therefore appears that the solubility of water in VR3 is quantitatively linked to the amount of plasticizer in the film, and that tricresyl phosphate can be lost when the films are subjected to even modest temperature increases. It is interesting to note, however, that the diffusivity did not change with plasticizer loss (Table 4). The indication is that tricresyl phosphate controls the water solubility, and consequently the permeability coefficient (Eq. 1) but not the diffusivity.

A comparison of the results shown in Tables 4 and 5 illustrates another point. These data are for the same paint film but different relative humidities, and, within the precision of these experiments, the water diffusivity is not a function of water concentration. This is a somewhat surprising result in view of the more general exponential dependence of organic-compound diffusivities on concentration (6, 7). The results shown here clearly demonstrate that in the region of relative humidity investigated ($50\% < RH < 93\%$), the water diffusivity in VR3 is not a strong function of water concentration. This fact is further illustrated in Fig. 5 which shows that diffusivity does not depend on relative humidity.

The fact that the diffusivity is independent of relative humidity allows one to combine data, collected at several values of the relative humidity, in order to construct an Arrhenius plot. When an Arrhenius plot is made of these data, an activation energy of 5.2 kcal/mole is

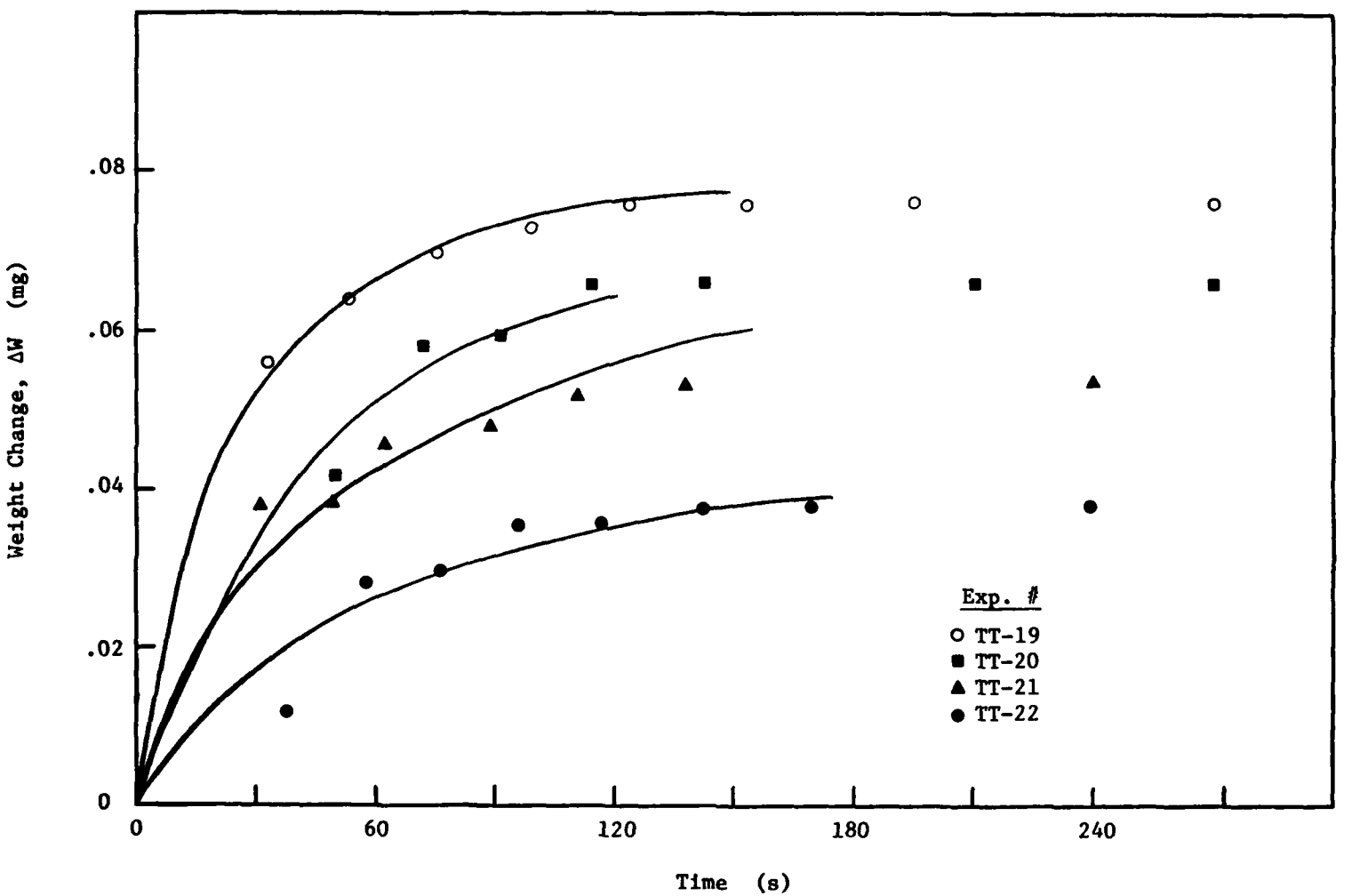

Fig. 4. Weight change vs time for a VR3 film 3.58 x 10^{-3} cm thick. Humidity step change from 0% to 55% RH at 33°C. Solid lines are best fit of data for the first ≈180 s. The four experiments were conducted on four consecutive days.

Table 4

Humidity Chamber Results for a VR 3 Free Film
3.58×10^{-3} cm Thick

Experiment Number	Relative Humidity %	Temp. (C°)	Days at These Conditions	Diffusivity (cm^2/sec) Long Time Approximation (eq. 4)	Diffusivity (cm^2/sec) Complete Formula (eq. 2)	Dry Weight (mg)
19	54.7	33.4	1	1.04×10^{-7}	1.51×10^{-7}	26.650
20	54.7	33.6	2	1.09×10^{-7}	9.60×10^{-8}	26.644
21	54.6	33.9	3	3.64×10^{-8}	6.02×10^{-8}	26.640
22	55.3	31.6	4	4.67×10^{-8}	6.05×10^{-8}	26.632
Mean 19-22	54.8	33.1	2.5	7.40×10^{-8}	9.20×10^{-8}	26.641

Table 5

Humidity Chamber Results for a VR3 Free Film
3.58×10^{-3} cm Thick

Experiment Number	Relative Humidity %	Temp. (C°)	Days at These Conditions	Diffusivity (cm^2/sec) Long Time Approximation (eq. 4)	Diffusivity (cm^2/sec) Complete Formula (eq. 2)	Dry Weight (mg)
27	93	32.5	1	7.79×10^{-8}	9.21×10^{-8}	26.546
28	93	33.3	2	1.20×10^{-7}	1.31×10^{-7}	26.542
29	93	33.7	3	8.14×10^{-8}	8.98×10^{-8}	26.522
Mean 27-29	93		2	9.29×10^{-8}	1.04×10^{-7}	26.537

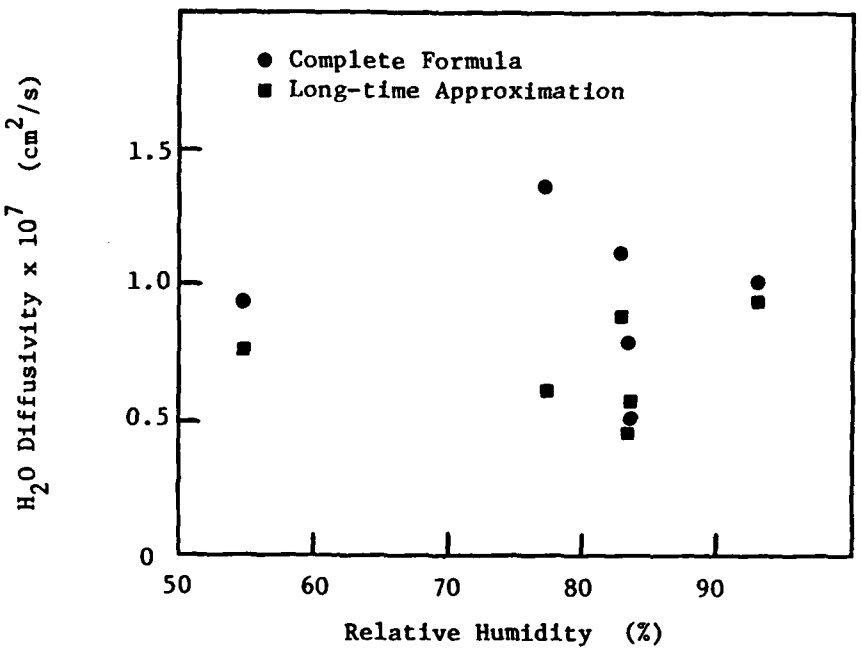

Fig. 5. Water diffusivity vs relative humidity for all VR3 films. Both the long-time approximation and complete-formula data are shown.

obtained, but the data are highly scattered. The scatter is clearly illustrated in Fig. 6 which shows diffusivity as a function of temperature. These electrobalance results are reasonable, but higher precision was sought, so a second experimental technique for measuring water diffusivities was investigated.

The second method of obtaining diffusivities utilized a quartz-crystal oscillator as a sensitive mass-change detector. At this time only preliminary experiments have been conducted with the crystal oscillator. All tests employed gold-coated quartz crystals and a polyurethane paint (0 PUR). A series of tests was conducted to determine which physical parameters affected the crystal-oscillator frequency. Fig. 7 shows the effect of temperature on a crystal at 0% relative humidity. A least-squares-straight-line fit to these data yields a temperature coefficient (γ_T):

$$\gamma_T = -3.8 \text{ Hz/°C} \tag{7}$$

This is in good agreement with the value, -3.3 Hz/°C, reported by King (8). This approximate value has been confirmed with other crystals, and relative humidity has little effect on the temperature coefficient as shown in Fig. 8.

The next series of tests involved determining the effect of humidity on unpainted gold-coated crystals. Fig. 9 shows the frequency change versus time for one crystal subjected to a step change in humidity of 84%. The scatter of 5 Hz in the steady-state frequency is typical. Fig. 10 shows the steady-state frequency change of unpainted crystals as a function of relative humidity. The crystal frequency can decrease as much as 27 Hz at 100% RH.

The unpainted-crystal voltage coefficient (γ_V) of the oscillator has also been determined:

$$\gamma_V = -40 \text{ Hz/V} \tag{8}$$

Finally, the temperature coefficient of a painted crystal at 0% RH was determined to be about -25 Hz/°C. This is about ten times greater than for an unpainted crystal, but the result is based on a small number of tests and may need to be revised later. In any case the changes

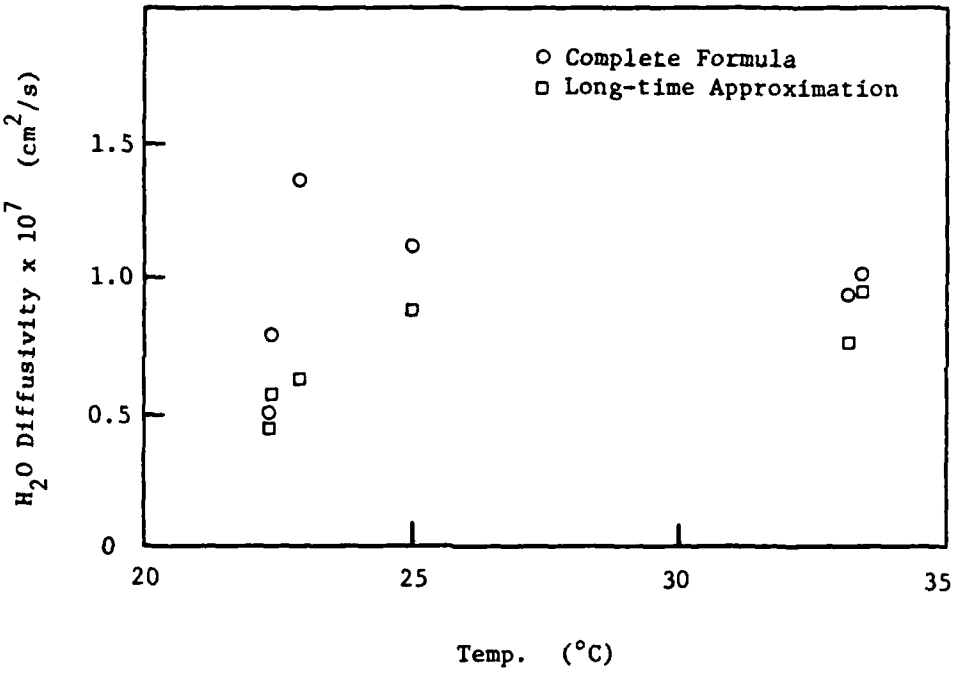

Fig. 6. Water diffusivity vs temperature for all VR3 films. Both the long-time approximation and complete formula data are shown.

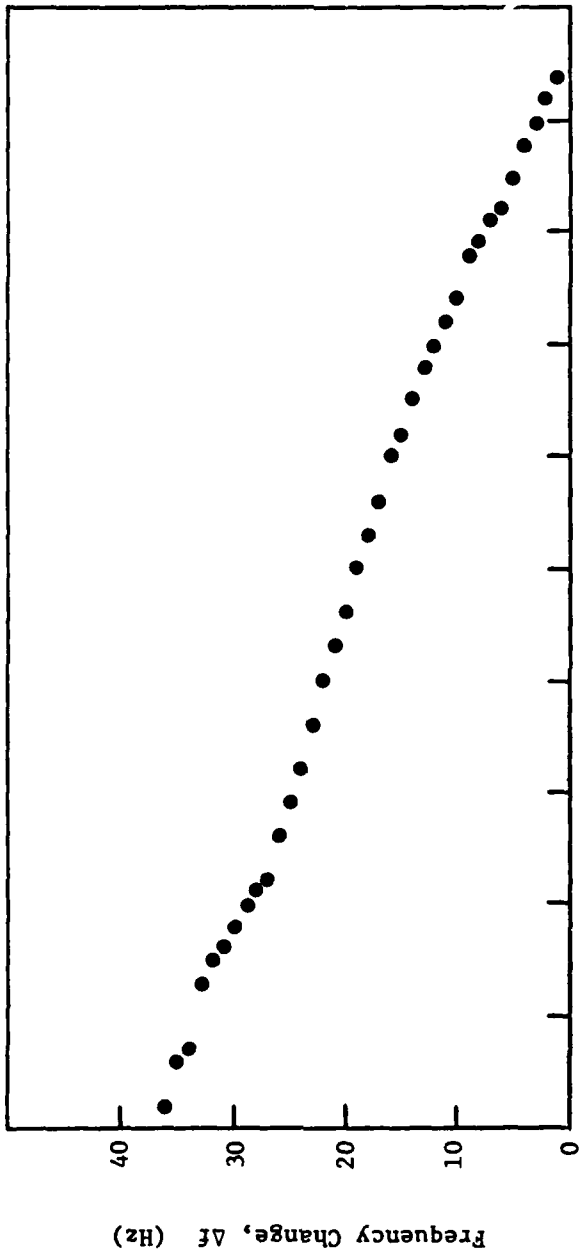

Fig. 7. Uncoated-crystal frequency change vs temperature at 0% relative humidity. Least-squares-straight-line slope = -3.8 Hz/°C.

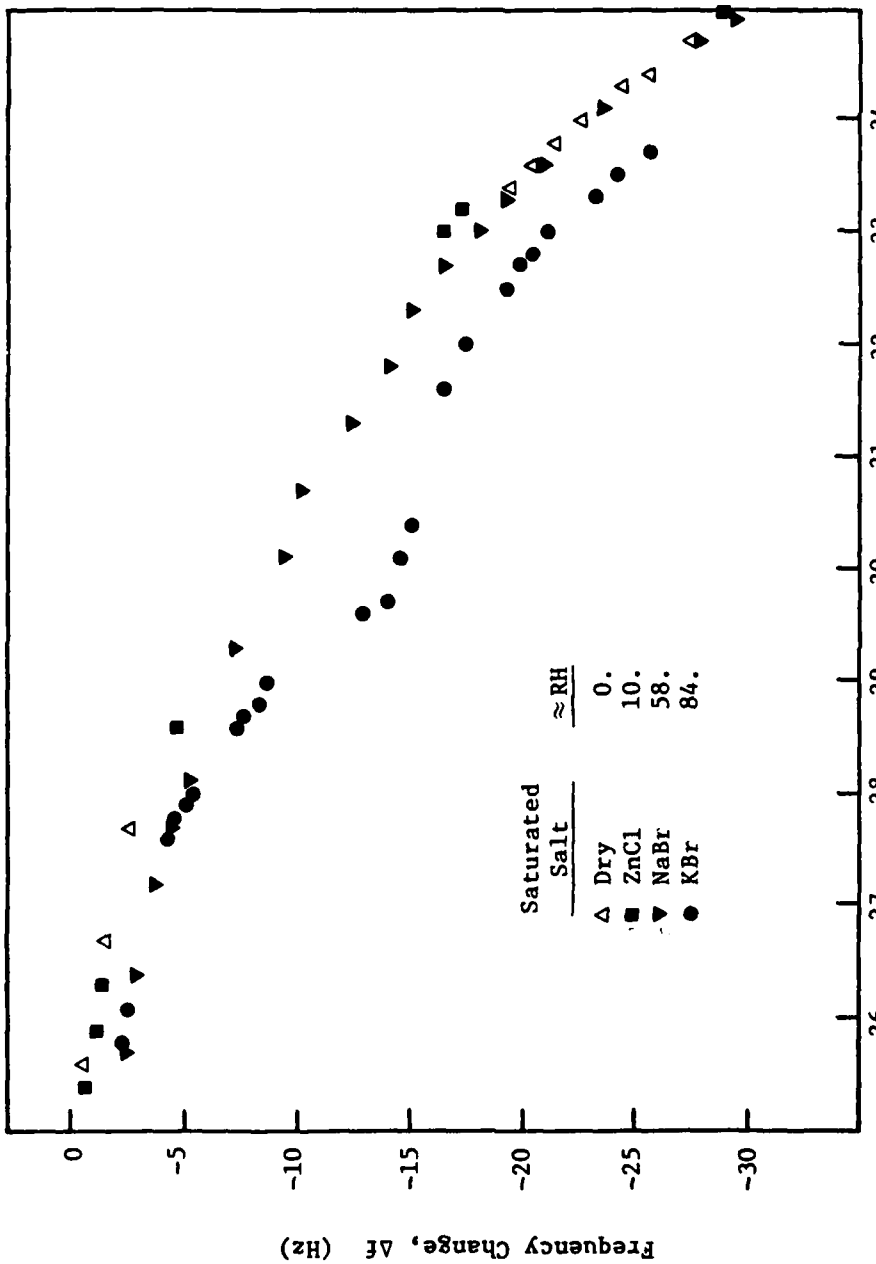

Fig. 8. Uncoated-crystal frequency change vs temperature over various saturated salt solutions (approximately constant relative humidities).

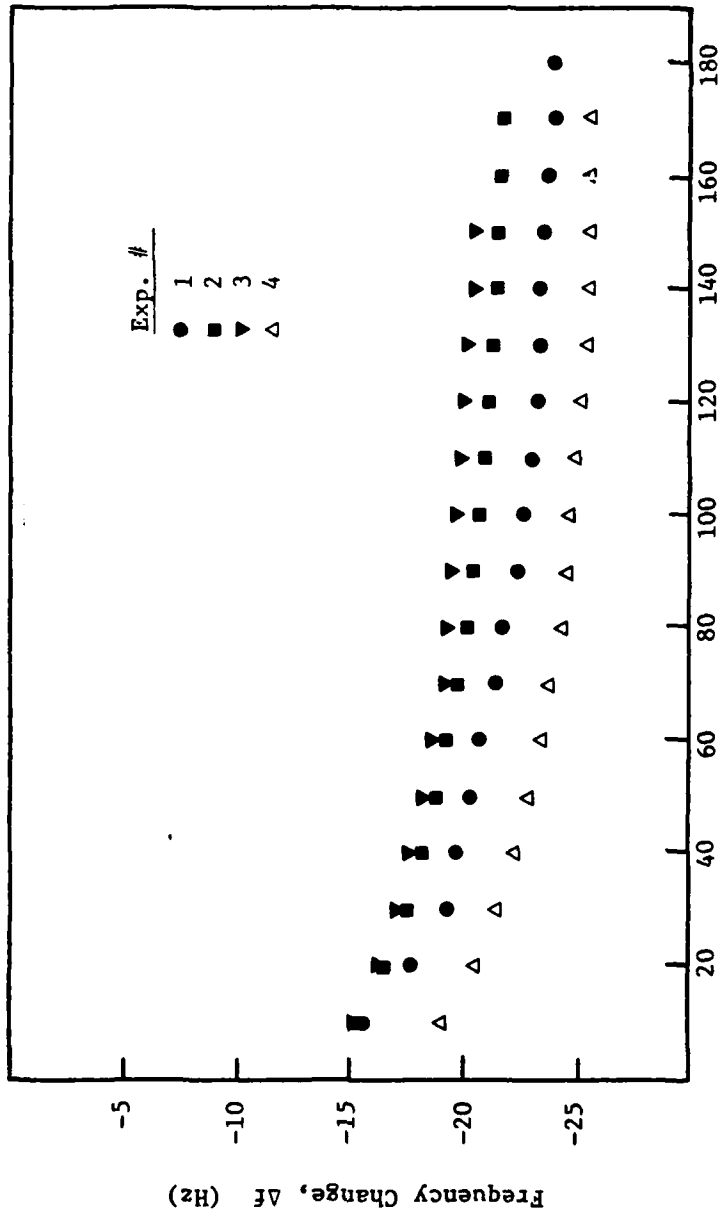

Fig. 9. Uncoated-crystal frequency change vs time after a relative humidity step change, 0% to 84% RH, at 27°C.

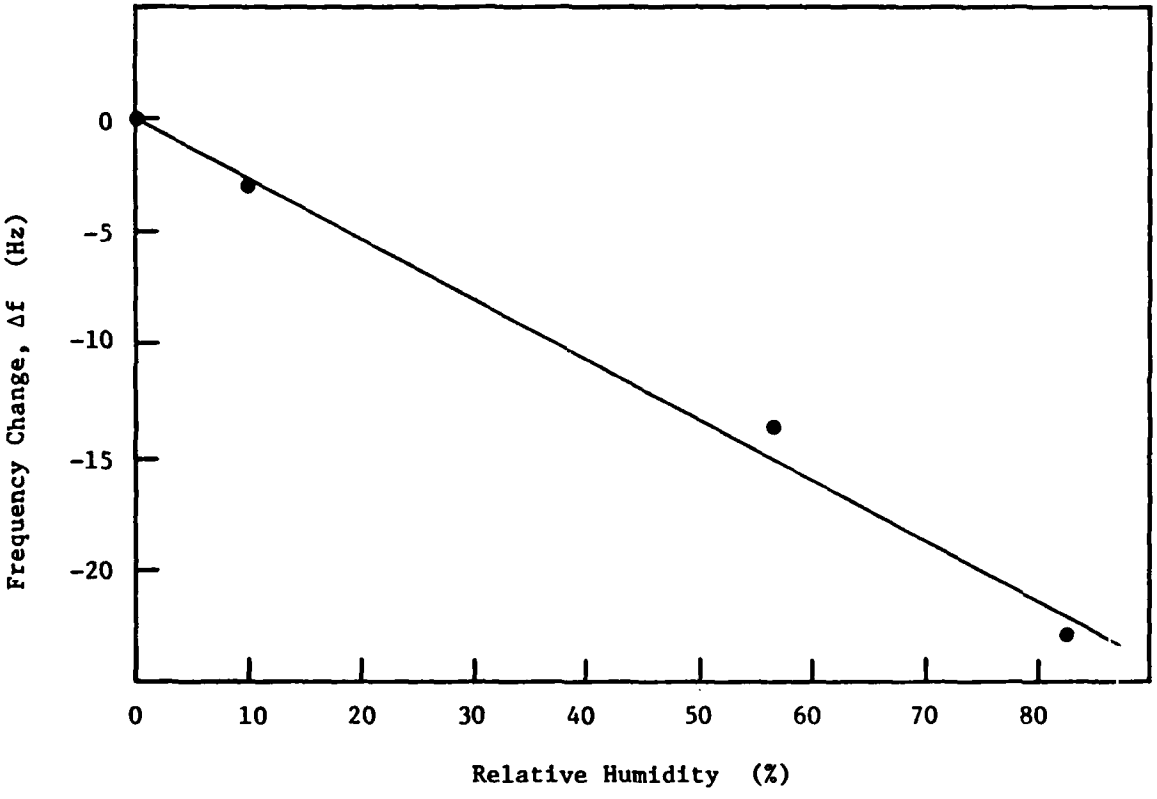

Fig. 10. Uncoated-crystal steady-state frequency change vs relative humidity at 27°C. Least-squares slope = -0.267 Hz/% RH.

introduced by changing temperature and voltage can be minimized by good experimental technique. Furthermore, the sum of all these external effects is small with respect to the frequency change (≈400 Hz) experienced when a painted crystal is exposed to a relative humidity step function from 0% to 50% RH.

Fig. 11 shows the results of two diffusivity experiments with O PUR; increasing relative humidity (0% ⟶ 83% RH), and decreasing humidity (83% ⟶ 0% RH) at 26°C. The results are plotted as the absolute value of frequency change versus time. Both experiments are very close except at long times. The long-time discrepancies are not entirely clear, but they are possibly related to either small temperature effects (≈25 Hz possible) or to slight discrepancies in humidity difference as a result of temperature differences or dessicant condition. The fact that the initial slopes of the two curves are nearly identical indicates that the diffusivity is not a function of concentration between 0% and 83% relative humidity (26°C). Crank (3) has discussed the formal description of this aspect of diffusion.

Fig. 12 shows the same data as Fig. 11 plotted as reduced frequency change (R_w) versus time. The theoretical curves based on a best diffusivity are also shown. The typical trend is for the experimental points to fall below the theoretical curve at short times and slightly above at longer times. This is also indicated in Fig. 11 in which a constant frequency has not been reached after 80 seconds. The data have been extended to times on the order of 600 seconds, and the frequency continues to change slowly. The slow frequency drift makes determination of the long-time frequency (f_∞) difficult, and is one reason the theoretical curves (Fig. 12) do not more closely coincide with the experimental data.

The cause of the long-time frequency drift is currently under investigation, but it appears likely that it occurs because diffusivity depends on position inside the paint films. This hypothesis is further supported by comparing the magnitudes of the diffusivities obtained in diffusion cup and crystal oscillator experiments. The diffusion cup results performed on thick ($\approx 2.5 \times 10^{-3}$ cm) membranes of O PUR indicate the diffusivity is about 10^{-8} cm^2/s. The diffusivities obtained from crystal-

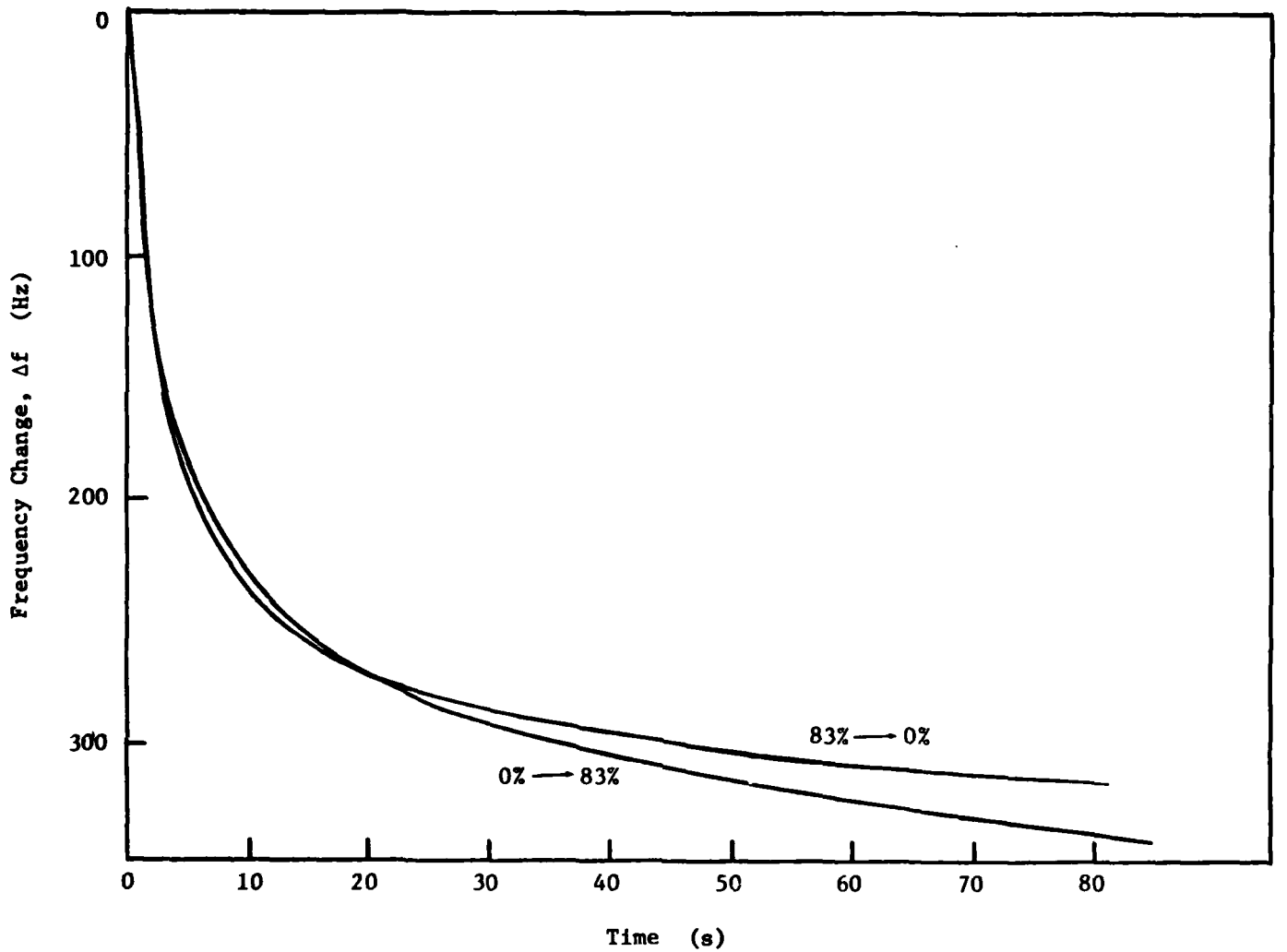

Fig. 11. Absolute value of frequency change vs time for step up and step down humidity changes between 0% and 83% RH. O PUR painted crystal at 26°C.

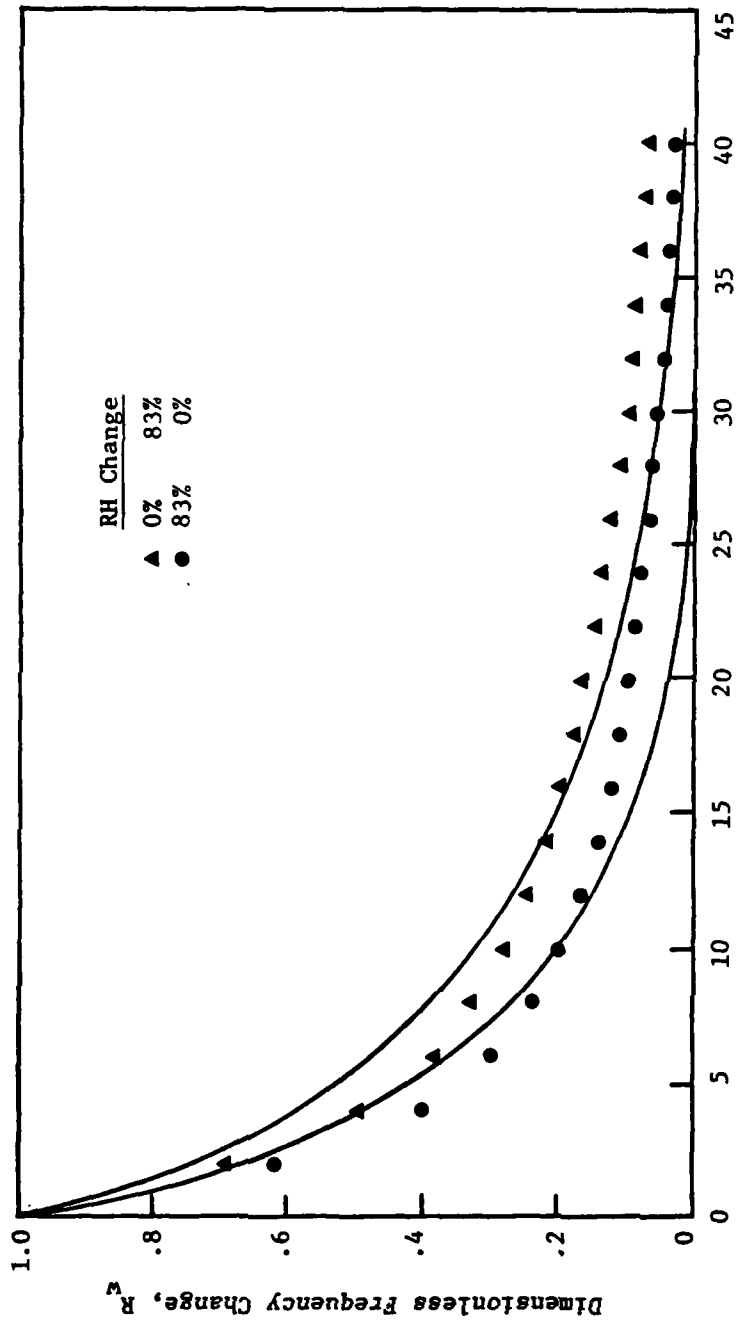

Fig. 12. Dimensionless frequency change vs time for two relative humidity step changes of magnitude 83% RH. O PUR at 25 C. $R_w = (f_\infty - f_t) / (f_\infty - f_o)$.

frequency experiments are one order of magnitude smaller ($\approx 10^{-9}$ cm^2/s) for paint films about 10^{-4} cm thick. The low diffusivity of thin films suggests that at least two regions of different diffusivity are present in O PUR paint films. Several models compatible with these data are possible, and we expect elucidation of how they relate to the structure of polyurethane films as more complete data become available.

The water diffusivity experiments have all been based on an analysis of the transient response of paint films to a step function in relative humidity. For this purpose a thermostated humidity chamber was designed and constructed. Preliminary tests have been performed using one of two additional pieces of equipment; a Cahn electrobalance, or a crystal oscillator. These tests show the unsteady-state technique to be a valuable tool for investigating diffusion in polymers. The results indicate that the diffusivity of water in one type of polyurethane (O PUR) is independent of concentration, but is probably a function of position inside the paint film. Experiments in this area are continuing, and more complete results are expected for O PUR as well as other paint membranes.

3.2 Water Permeability

3.2.1 Theory

The permeability of a membrane material to a mobile species has historically been described in terms of the activity difference of the mobile species across the membrane, the membrane thickness, and the permeability coefficient. For the most part, the equations describing the process have been derived for gaseous diffusants. As Crank and Park (4) point out, however, the same equations can be used to describe the diffusion of liquids. The following equations apply:

$$F = P \frac{da}{dx} \tag{10}$$

where F = diffusion flux (mole/cm^2-s)

P = differential permeability coefficient (cm^2/s)

a = diffusant activity (mole/cm^3)

The liquid activity can also be expanded in terms of a dimensionless *activity coefficient* (γ) *relative to the pure liquid at a specified* temperature and pressure;

$$a = \gamma c \tag{11}$$

where c = the liquid concentration (mole/cm^3)

For the one-dimensional example, equation 10 can be integrated to yield

$$F\tau = \int_{C_1}^{C_2} p\gamma \, dc \tag{12}$$

$$= \overline{P\gamma} \, (C_2 - C_1) \tag{13}$$

where τ = film thickness (cm)

$\overline{P\gamma}$ = average reduced permeability coefficient (cm^2/s)

If the diffusing species obeys Henry's law, γ is constant and equation 13 simplifies to

$$F\tau = \overline{P}'\gamma(C_2 - C_1) \tag{14}$$

where $\overline{P}'$ = the average permeability coefficient in the Henry's law case. Eq. 10 and 14 are quite similar, but should not be confused. The differential permeability (P) is a function of position within the paint film, whereas the average permeability $\overline{P}'$ may depend on the conditions, film thickness (τ), concentration (C), etc., of the experiment.

For systems in which the differential permeability coefficient is constant, $\overline{P}' = P$. However, a systematic variation of $\overline{P}'$ with thickness (τ) was observed with several of the paint systems investigated. Most of these systems show increasing permeability coefficients with increasing thickness. One simple model of such systems divides the paint films into two regions of different diffusivity. If one region is thin, as one would expect if a compact air-dried skin formed at the air-paint interface, the following equation can be derived:

$$\frac{a_1 - a_2}{F} = \frac{\tau}{P_b} + \tau_s \left(\frac{1}{P_s} - \frac{1}{P_b} \right) \qquad (15)$$

where $a_1 - a_2 = \Delta a$ = external activity difference (mole/cm^3)

F = steady state flux through the membrane (mole/cm^2-s)

τ = total membrane thickness (cm)

τ_s = skin thickness (cm)

P_b = bulk-phase permeability coefficient (cm^2/s)

P_s = skin-phase permeability coefficient (cm^2/s)

A plot of ($\Delta a/F$) versus membrane thickness is expected to produce a straight line with the slope equal to the reciprocal bulk-phase permeability coefficient. In the special case when the skin is absent $\tau_s = 0$, Eq. 15 reduces to Eq. 14 with $\overline{P}' = P_b$. Whenever enough data were available to make an unambiguous determination of the bulk-phase permeability coefficient, Eq. 15 was used to calculate the water permeability coefficients.

The bulk-phase and/or the average permeability coefficients have been measured at different temperatures. Arrhenius plots of the permeability coefficients generally yield typical, positive activation energies ($0 < E_p < 10$ kcal/mole). Fang (7) has shown, however, that this is not necessarily required, and his argument is repeated here briefly.

The permeability coefficient (P) depends on both the diffusivity (D) and the dimensionless solubility (S):

$$P = DS \tag{16}$$

Over a limited temperature range an exponential temperature dependence is expected:

$$P = P' \exp\ (-E_P/RT) \tag{17}$$

$$D = D' \exp\ (-E_D/RT) \tag{18}$$

$$S = S' \exp\ (-\Delta H_s/RT) \tag{19}$$

where P', D', S' = constants (cm^2/s)

E_P = activation energy for permeability (kcal/mole)

E_D = activation energy for diffusion (kcal/mole)

ΔH_s = heat of solution of solvent in the membrane material (kcal/mole)

R = gas constant (kcal/mole - °K)

T = absolute temperature (°K)

When Eq. 17-19 are substituted into Eq. 16 the following results are obtained:

$$P' = D'S' \tag{20}$$

$$E_P = E_D + \Delta H_s \tag{21}$$

Diffusion is a fundamental kinetic process; therefore, $E_D > 0$, but ΔH_s is a thermodynamic quantity and can take either positive or negative values. It is thus possible for the activation energy for permeation (E_p) to be positive, negative, or zero.

3.2.2 Experimental

The permeability of water through paint membranes has been measured using diffusion cups (ASTM E96-66, procedure BW). In this experiment, liquid water is placed in a glass vessel which is then sealed with the membrane. The vessel is placed in a position such that liquid water always covers the membrane surface inside the vessel. The exterior paint surface is maintained at zero partial pressure of water by contacting with air

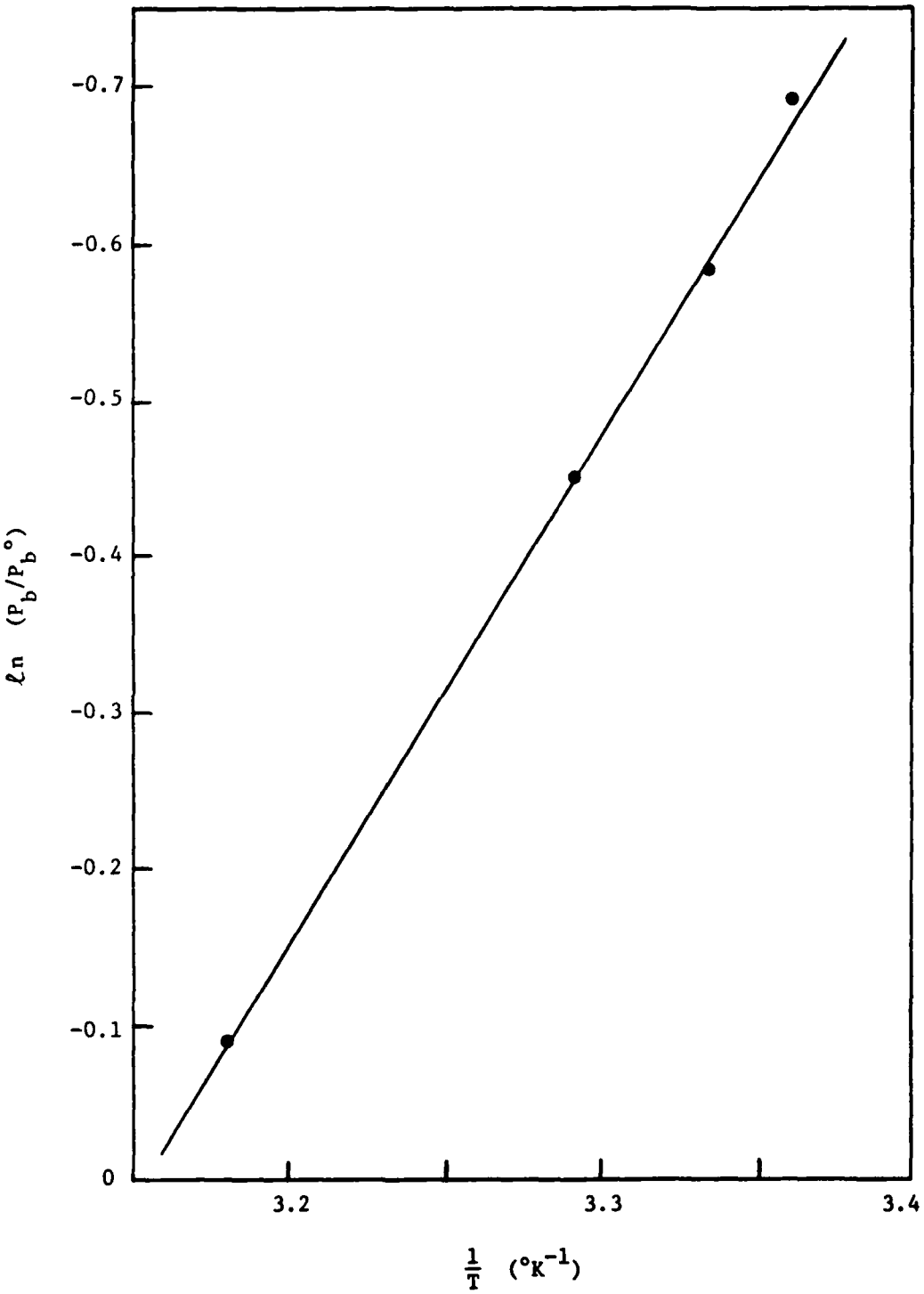

Fig. 13. Natural logarithm of dimensionless permeability coefficient vs reciprocal temperature for water in 0 PUR.

dried by a dessicant and circulated with a fan. The temperature was maintained constant ±2°C by external heating coils. The weight of the diffusion cups was measured daily, and the results plotted as weight loss versus time.

3.2.3 Results and Discussion

3.2.3-1 Old Polyurethane System (System VIII, O PUR)

Water permeability coefficients have been determined at temperatures between $24.5°C < T < 41.3°C$. Thicknesses ranged between 3.5×10^{-3} cm $< \tau < 14.5 \times 10^{-3}$ cm. The glass transition temperature of O PUR is 61°C (1).

Fig. 13 is an Arrhenius plot of the dimensionless bulk-phase permeability coefficient. The activation energy is 6.6 kcal/mole. Based on a least-squares fit of the data the bulk-phase permeability at 25°C is

$$P_b\ (298) = 4.87 \times 10^{-10}\ cm^2/s) \tag{22}$$

Similar manipulations can be performed on the average permeability.

$$\bar{P}'\ (298) = 4.95 \times 10^{-10}\ cm^2/s \tag{23}$$

$$E'_P = 4.34\ kcal/mole \tag{24}$$

The close correlation between $\bar{P}'$ and P_b indicates that the second term on the right in equation 15 is small. This could be the result of either of two conditions,

$$\tau_s << \tau \tag{25}$$

$$\text{or } P_s \cong P_b \tag{26}$$

The fact that the intercept is positive when the data are plotted using Eq. 14 indicates that

$$P_b > P_s \tag{27}$$

The diffusion data obtained with the crystal oscillator indicate that

$$D_b \gtrsim 10(D_s) \tag{28}$$

If the solubilities are not too different,

$$S_b \cong S_s \tag{29}$$

We can calculate that τ_s is on the order of 10^{-4} cm. τ_s thus appears to be a relatively thin compact layer. Other membranes (cellulose acetate) have been shown to possess a similar physical configuration, a dense outer layer supported by a more permeable structure underneath the surface skin (9, 10). Based on the preliminary results obtained in this study, this configuration may represent a rather general feature of high-solvent-content paint systems.

3.2.3-2 New Polyurethane (System VII, N PUR)

The N PUR system has been investigated at temperatures between $26.4°C < T < 38.5°C$, and thicknesses between 2.5×10^{-3} cm $< \ell <$ 3.8×10^{-3} cm. The glass transition temperature for N PUR is 70°C (1). Only three thicknesses of N PUR have been tested. Analysis using Eq. 15 was therefore deemed inappropriate. The complete data are included in Appendix A. The average permeability coefficient at 25°C and activation energy are

$$\bar{P}' \ (298) = 2.61 \times 10^{-10} \ cm^2/s \tag{30}$$

$$E'_P = 5.72 \ kcal/mole \tag{31}$$

If the permeability data are used to generate Arrhenius plots for each film thickness, the activation energies tend to increase with film thickness (≈2 kcal/mole). The magnitude of this change is not great, but it may indicate a changing diffusion mechanism with changing film thickness. The changes could be the result of a changing diffusivity, a changing solubility, or both. From these data, it appears that the water permeation characteristics of N PUR are similar but slightly different from those for the other polyurethane system.

3.2.3-3 Vinyl Resin II (System II, VR2)

The vinyl resin II (VR2) paint system was investigated at temperatures between 23.3°C < T< 37.6°C and thicknesses between 2.13×10^{-10} cm $< \tau < 3.09 \times 10^{-3}$ cm. The glass transition temperature for VR2 is 72°C (1). A complete data summary is presented in Appendix A. The bulk-phase permeability coefficient at 25°C and corresponding activation energy are

$$P_b\ (298) = 5.71 \times 10^{-10}\ cm^2/s \tag{32}$$

$$E_P = 9.98\ kcal/mole \tag{33}$$

The linear correlation coefficients (R) for the reduction of these data according to Eq. 15 are generally greater than 0.8.

The average permeability coefficient at 25°C and activation energy are

$$\bar{P}'\ (298) = 7.79 \times 10^{-10}\ cm^2/s \tag{34}$$

$$E'_P = 4.35\ kcal/mole \tag{35}$$

The average permeability coefficient ($\bar{P}'$) in this case is slightly greater than P_b indicating

$$P_b < P_s \tag{36}$$

This is born out by the Eq. 15 plots which generally produce negative intercepts. As indicated previously, however, the data are somewhat scattered ($R \cong 0.8$), and the results should be considered preliminary.

3.2.3-4 Vinyl Resin III (System III, VR3)

The vinyl resin III system (VR3) has been investigated over the temperature range, 20.8°C < T < 36.2°C, at thicknesses between 2.08×10^{-3} cm $< \tau < 6.58\ cm^{-1}$. The glass transition temperature of VR3 is 46°C.

The experiments determined the permeability coefficient at 36.2°C, close to the glass transition temperature of 46°C. Upon cooling the samples below 36.2°C, it was observed that some irreversible changes had taken place in the membranes. This observation was confirmed later on the VR3 samples tested in the humidity chamber as well as with other paint

types. It appears now that most paint polymers are reasonably reversible with respect to the effect of temperature on permeability coefficients at temperatures far from the glass transition. As the glass transition temperature is approached, permanent changes occur in the permeability, probably indicating a structural rearrangement inside the paint. This is consistent with the observation that the data are more scattered on falling-temperature experiments than when the temperature is rising. Consequently, most data reported here are from rising-temperature experiments. The data reported for this system are an exception; they were taken as the temperature decreased over the specified range.

The bulk-phase permeability coefficient at 25°C and activation energy for VR3 are

$$P_b\ (298) = 3.48 \times 10^{-10}\ cm^2/s \tag{37}$$

$$E_P = 12.92\ kcal/mole \tag{38}$$

Based on the diffusivity (D) calculated from humidity-cell experiments the solubility of water in VR3 is

$$S = 3.16 \times 10^{-3} \tag{39}$$

This is somewhat lower than one might expect based on experience, but compares favorably with the values, $2.6 \times 10^{-3} < S < 5.3 \times 10^{-3}$, obtained from humidity-chamber work. The solubility (Eq. 39) would tend to appear high if the diffusivity is too low, as would be expected if a compact skin is present on the surface of VR3. When Eq. 15 is used to reduce the data, the intercept is small but always positive. This fact indicates that VR3 is a two-layer, composite film. We thus expect the water solubility of VR3 to be quite small. More complete permeability data are given in Appendix A.

3.2.3-5 Vinyl Resin IV (System IV, VR4)

The vinyl resin IV system (VR4) was investigated in the temperature range $25.1°C < T < 42.2°C$, with thicknesses between $3.38 \times 10^{-3} < \tau < 7.70 \times 10^{-3}$ cm. The glass transition temperature of VR4 is not well known ($T_g \geq 45°C$).

The bulk-phase permeability coefficient reduced to 25°C and activation energy for VR4 are

$$P_b\ (298) = 1.05 \times 10^{-9}\ cm^2/s \tag{40}$$

$$E_P = -6.00\ kcal/mole \tag{41}$$

As these figures indicate, VR4 exhibits anomalous behavior based on the other paints studied. The average permeability coefficient is much lower than P_b:

$$\bar{P}'\ (298) = 2.63 \times 10^{-10}\ cm^2/s \tag{42}$$

$$E'_P = 10.25\ kcal/mole \tag{43}$$

The large discrepancy between P_b and $\bar{P}'$ indicate that at least two diffusivity regions are present, and the surface film represents a large fraction of the total film resistance.

The two average permeability coefficients calculated from Hittorf experiments with VR4 are

$$\bar{P}'_H\ (298) = 1.59 \times 10^{-10}\ cm^2/s \tag{44}$$

$$\bar{P}'_H\ (298) = 2.11 \times 10^{-10}\ cm^2/s \tag{45}$$

These agree with $\bar{P}'$ from Eq. 42. Since the Hittorf experiments have a significantly higher average water concentration than the permeability-cell experiments, these results indicate that water permeation in VR4 is not strongly concentration dependent.

Table 6 summarizes all the water permeability results. It is interesting to note that the permeability coefficients lie in the region,

$$2.6 \times 10^{-10} < P(298) < 10.5 \times 10^{-10}\ cm^2/s \tag{46}$$

In spite of this rather narrow range of permeabilities, the activation energies are widely scattered, indicating that different internal processes are affecting permeation. In most cases where sufficient data are available, a position-dependent diffusivity is indicated. The VR2 system is the one possible exception to this statement. Further experiments are planned to investigate the mechanism of water permeation through paint films with the intent of accurately modeling the process.

Table 6

Water Permeability Coefficients and Activation Energies for Five Paints

Paint	P_b (298) (cm^2/s)	E_P (kcal/mole)	$\bar{P}'$ (298) (cm^2/s)	E_P' (kcal/mole)
O PUR	4.9×10^{-10}	6.6	4.9×10^{-10}	4.3
N PUR			2.6×10^{-10}	5.7
VR2	5.7×10^{-10}	10.0	7.8×10^{-10}	4.4
VR3	3.5×10^{-10}	12.9	3.0×10^{-10}	4.3
VR4	10.5×10^{-10}	-6.0	2.6×10^{-10}	10.3

3.3 Ionic Capacity

Ionic capacity (a parameter in the mathematical model of paint films) has been measured for two paint systems, VR4 and O PUR. A total of three experiments have been conducted; therefore, the results are preliminary. The technique has been described elsewhere (11), but briefly; it consists of allowing a paint film to stand in contact with a sodium chloride solution until equilibrium has been attained. The concentrations of sodium or chloride and water are measured both inside the paint and in the external solution. Radiotracer elements (Cl^{36}, Na^{22}, and H^3) were used for this purpose.

A single experiment has been conducted with VR4. The salt concentration was 0.091 N, NaCl. Radioactive sodium and tritiated water were used as tracers. The results indicate the water concentration

$$\overline{C}_w = 5.85 \times 10^{-2} \text{ g } H_2O/\text{g paint} \tag{47}$$

The sodium concentration was also determined:

$$\overline{C}_{Na} = 7.9 \times 10^{-7} \text{ mole/cm}^3 \tag{48}$$

The ionic capacity cannot be determined until a similar experiment has been completed using chloride radiotracer, but a dimensionless solubility can be calculated for sodium ions alone:

$$S_{Na} = 8.7 \times 10^{-3} \tag{49}$$

This value is slightly higher than the value ($S \cong 10^{-3}$) estimated for O PUR (11). Additional data for O PUR have been presented and discussed elsewhere (11).

3.4 Hittorf Experiments

The classic Hittorf method has been used to test paint membranes by passing a current between two chemically identical solutions through the membrane. The solution concentrations were the same on both sides of the paint film. The plane of the paint membrane was horizontal, and the

air side was always down. The solution having the highest radioactivity was always in the bottom compartment, on the air side of the membrane. Voltages were reported relative to the bottom electrode (air side) as ground. Further details of the method have been discussed elsewhere (11, 12). In the past year, six Hittorf experiments have been completed involving two types of paint: system IV (VR4), and system VIII (O PUR). All Hittorf experiments were conducted at 25°C.

Hittorf experiments are designed to yield water and ionic-species permeability coefficients. The basic procedure involves measuring the rate of concentration changes in the two solutions as well as the charge passing through the membrane. The results are reported as transference numbers and permeability coefficients. Permeability coefficients are discussed elsewhere (11, Sect. 3.2).

The transport of each mobile species can be described using a number of transport parameters (2). Transference numbers represent one type of transport parameter. For ionic species, transference numbers represent the fraction of the total current carried by the corresponding ion. The sum of all ionic transference numbers is one.

3.4.1 Results and Discussion

The results of all Hittorf experiments are summarized in Table 7. Detailed experimental data are presented in Appendix A. The two experiments involving VR4 produced minimal results because no detectable quantities of radioactive sodium (Na^{22}) or chloride (Cl^{36}) were found. This has been a persistent problem which has only recently been overcome in experiments conducted with O PUR membranes. Future experiments with VR4 are expected to yield complete results. Water permeability coefficients ($\overline{P}'$) were obtained by measuring the passage of tritium-labeled water through VR4. The results are in fair agreement with those obtained in diffusion cup experiments (Table 7).

Four Hittorf experiments were conducted with O PUR membranes. The most striking feature of these results is that the sum of the sodium and chloride ionic transference numbers is not one. These data indicate that

Table 7

Summary of Hittorf Experimental Results

Exp. #	Paint	Thickness (cm)	Volts (V)	NaCl Conc. (N)	Transference #		Permeability Coefficients		
					t+	t-	H_2O (cm^2/s)	Cl^- (cm^2/s)	Na^+ (cm^2/s)
NR-1	VR4	4.66×10^{-3}	1.52	1.04×10^{-1}			1.59×10^{-10}		
NR-2	VR4	7.06×10^{-3}	-1.55	9.90×10^{-2}			2.11×10^{-10}		
NR-3	O PUR	5.76×10^{-3}	9.5	3.73×10^{-2}		0.362	6.12×10^{-10}	3.1×10^{-13}	
NR-4	O PUR	3.87×10^{-3}	-9.3	9.22×10^{-3}	0.021		5.61×10^{-10}		8.0×10^{-14}
NR-5	O PUR	3.79×10^{-3}	4.4	2.33×10^{-2}		0.268	7.48×10^{-10}	1.0×10^{-14}	
			9.4			0.254		1.1×10^{-14}	
			19.5			0.286		1.7×10^{-14}	
NR-6	O PUR	3.44×10^{-3}	-4.0	2.46×10^{-2}	0.021		4.40×10^{-10}		2.7×10^{-14}
			-9.9		0.105				4.9×10^{-14}
			-19.0		0.009				7.3×10^{-14}

roughly two thirds of the current is being carried by some ionic species other than sodium or chloride. This is particularly interesting in view of the common practice of many researchers to assume the identity,

$$t_+ + t_- = 1, \tag{50}$$

in cases involving a binary salt. Eq. 50 is clearly not justified when modeling ionic transport through O PUR. These results support the hypothesis proposed by Ruggeri and Beck (11, 13) that some dissociation of neutral species is involved. The neutral species could be small impurity compounds present in the paint or some other compound such as water. Water is a small molecule, and can therefore be expected to be highly mobile, but it may not be as concentrated inside the paint as some organic impurities.

The Hittorf data in Table 7 show significant variations between paint films. Similar observations were noticed with the diffusion cup (water permeability) results. The Hittorf water-permeability coefficient ($\bar{P}'$) for O PUR is

$$\bar{P}'_H(298) = 5.9 \times 10^{-10}\ cm^2/s \tag{51}$$

which is within one standard deviation of the value obtained from diffusion cup experiments. This fact again underscores the observation that the diffusion coefficient of water in O PUR is not a strong function of water concentration (Sect. 3.1). This conclusion follows because, in diffusion cup experiments, the average water concentration inside the paint films is about one-half the concentration found in Hittorf experiments. The water permeability results obtained in Hittorf experiments are thus consistent with all permeability data obtained by other means.

Table 7 also shows permeability data for the mobile ions, sodium and chloride. A significant variation between individual paint specimens is indicated, as well as variations of a single membrane with time. Fig. 14 shows sodium activity as a function of total coulombs of charge passed through O PUR (charge increases monotonically with time). The slope of this curve represents the sodium-ion transference number. Fig. 14 clearly

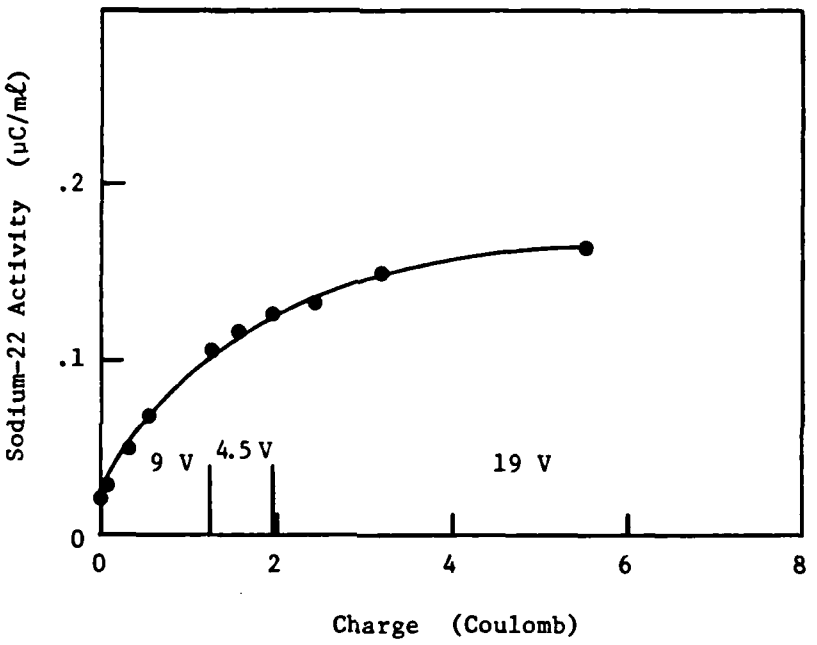

Fig. 14. Sodium-22 activity vs charge for Hittorf experiment No. NR-6, O PUR at 25°C.

illustrates a systematic decrease in sodium-ion transference number as time increases. Despite these time variations, the transference-number data appear to be quite constant, even between paint specimens. A maximum variation of about 40% (between specimens) was observed in chloride transference number, while the same samples produced permeability coefficients differing by a factor of 30.

Another interesting feature of these data is the apparent discrepancy between the sodium and chloride permeability coefficients. Despite the fact that the sodium-ion transference number is roughly one tenth that of chloride, the permeability coefficient for sodium appears to be slightly greater than the chloride coefficient. The discrepancy is probably a result of the previously discussed variations between individual paint specimens.

These Hittorf data for O PUR clearly lead to two conclusions:

(1) Only about 1/3 of the current is carried by the "primary" ions, sodium and chloride,

(2) The differences in transport properties between paint specimens are relatively large.

Both VR4 and O PUR require additional investigation, but the second point is compatible with Mayne's (14-16) position that membrane properties change significantly in the plane of the film. Further investigations are planned to determine which ions are responsible for two thirds of the current, and to verify whether or not Mayne's observations apply to these paint films.

3.5 Transference Numbers

Transference numbers have been calculated by measuring the open circuit potential of the following cell:

$$\begin{array}{ccccccccccc} Ag & | & Ag\,I & | & HI & \Big\} & \text{Membrane} & \Big\} & HI & | & Ag\,I & | & Ag \\ \alpha & & \beta & & \gamma & \Big\{ & \delta & \Big\{ & \gamma' & & \beta' & & \alpha' \end{array} \qquad (52)$$

When the hydrogen iodide concentrations are different in the γ and γ' phases, a potential (U) is developed according to the equation (17):

$$U = E_1 - E_2 = - \frac{\nu}{z_- \nu_-} \frac{RT}{F} t_+ \ell n \frac{A_{\pm 1}}{A_{\pm 2}} \tag{53}$$

where ν = moles of ions per mole of salt

ν_- = moles of negative ions per mole of salt

z_- = negative ion valence

t_+ = positive-ion transference number

$A_{\pm 1}$ = salt activity on side 1 (γ) of the membrane (mole/cm^3)

If the concentration of HI is held constant on side 2 ($A_{\pm 2}$ = constant), the slope of U versus $\ell n(A_{\pm 1})$ is directly related to t_+;

$$t_+ = - \frac{z_- \nu_-}{\nu} \frac{F}{RT} \frac{d(U)}{d \ \ell n \ A_{\pm 1}} \tag{54}$$

Fig. 15 shows transference-number data for O PUR in hydrogen iodide solution. Similar data have been reported elsewhere (11) for O PUR in sodium chloride solution. Both experiments show that, as the solution becomes less concentrated, the potential becomes more erratic. This is possibly due to the increased resistance of the paint membranes at low concentrations. The Keithley 616 electrometer used to measure potentials had a 0.1 second time-constant, and no Faraday cage was used in order to facilitate solution changes. The temperature was recorded but not controlled at 21°C ± 1°C. Fig. 15 shows the same general behavior reported previously. At least two different regions of concentration can be identified. In the concentrated region, $C_1 > 10^{-2}$ N, a family of straight lines is obtained, all of nearly identical slope. Each line represents data obtained with a different side 2 HI activity which was held constant as the side 1 activity varied. Table 8 summarizes the concentrated-region results. These data indicate that that hydrogen ion is the primary mobile species in concentrated HI solution. This is in contrast to the behavior in concentrated sodium chloride solution where $t_+ \cong 0.38$ (11). Fig. 15 clearly illustrates, however, the concentration dependence of the transference numbers. In the low-concentration region O PUR in HI exhibits a $t_+ \cong 0.25$. This is surprisingly close to the value of $t_+ = 0.20$ obtained for O PUR

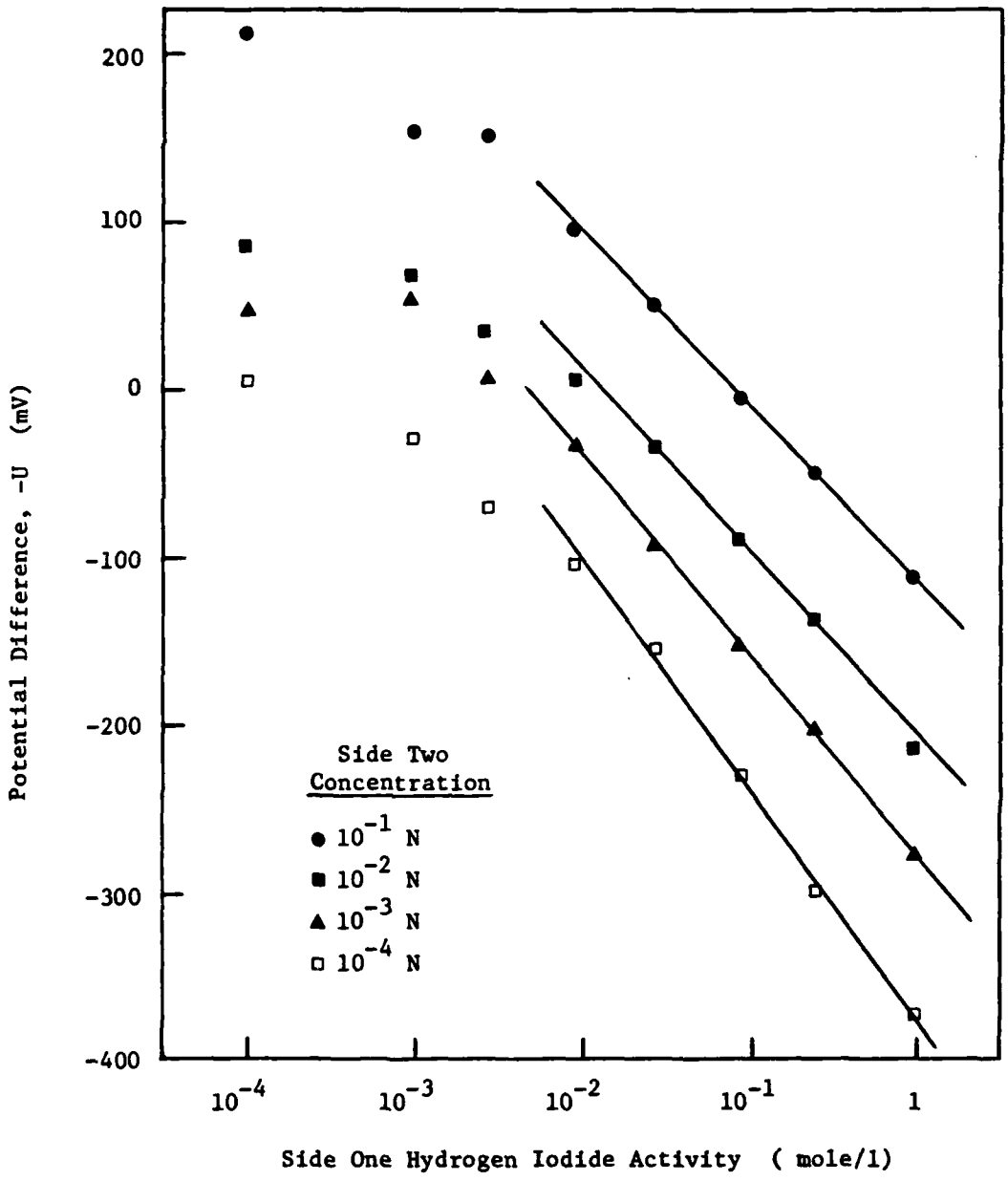

Fig. 15. Potential difference vs logarithm HI activity at four different concentrations on side two of the cell. Points are experimental data. Solid curves are least-squares straight lines through concentrated-region data ($C_1 > 10^{-2}$ N).

Table 8

Hydrogen-Ion Transference Numbers

in 0 PUR at 21°C

HI Constant Concentration	HI Concentration Range	Slope (mV/decade)	t+
10^{-1}	$1 - 3 \times 10^{-2}$	105.5	.89
10^{-2}	$1 - 3 \times 10^{-2}$	116.4	.98
10^{-3}	$1 - 3 \times 10^{-2}$	117.1	.99

in NaCl at similar concentrations. One final comparison between the HI and NaCl results is that the break between the high and low concentration regions occurs at the same concentration, 10^{-2} N.

It would be unwise to rely greatly on these data at this time, but they clearly indicate a changing transport mechanism as the concentration passes through the break point, 10^{-2} N. Similar observations have been presented for the sodium chloride system indicating that the two experiments have elements in common. Furthermore, these data are consistent with an earlier hypothesis that a neutral species, possibly water, contributes ions for conduction at low concentrations. These "secondary" ions are produced by dissociation of the neutral species, but it should be pointed out that Eq. 52 and 53 apply only to systems containing two ionic species. By including the dissociation of water, at least three ionic species are involved, and a more complex theory must be adopted. The computer model is a particularly convenient way to handle these more complex situations in detail, but from the data and discussion presented here, it is clear that some change in the diffusion of ionic species occurs in O PUR as the external solution concentration approaches 10^{-2} N.

3.6 Additional Testing

In addition to the experiments already discussed, several other types of testing have been performed. One of these tests involves the flow of salt solutions through membranes under a pressure gradient. A special apparatus similar to that described by Choi and Bennion (18) has been constructed for these experiments. The experiments consist of forcing a solution of known composition through a paint membrane while measuring the flow rate, potential drop, and filtrate composition. Preliminary tests have been conducted with Teflon and O PUR, but no definitive conclusions can yet be drawn. Qualitatively, the flow of solution through O PUR under a pressure gradient appears to be a reversible process having little effect on the solution concentration. These tests are expected to continue at an increased level in the coming year.

Time-transient-current experiments have been conducted with O PUR in sodium chloride solution at ≈21°C. These experiments measure the current as a function of time after application of a voltage step function. The experiments were complicated by the inability to attain a well-specified initial condition. This is compatible with the Hittorf results in which varying transference numbers were observed as the paint film aged (Sect. 3.4). It appears to be a general observation of these films that the electrical properties exhibit large variations in time as well as between individual specimens (conductivity data, Appendix A). Average values and dimensionless parameters, such as transference numbers, on the other hand vary considerably less. Many time-transient-current experiments were completed, and semi-quantitative results have been presented (11) which indicate that the time constant for current decay is about 1000 seconds.

Finally, the densities of paint films have been measured by weighing samples dry and submerged in water. The scales were accurate to 1×10^{-4} g, and sample weights were generally between

$$50 \text{ mg} < W < 90 \text{ mg} \tag{55}$$

Table 9 summarizes the density measurements.

4.0 PLANNED WORK

Future work in the area of transport parameters will continue to emphasize the quantitative description of mass transport in paint films. Efforts will continue on diffusivity, permeability, Hittorf, and transference-number experiments. Additional high-pressure-flow experiments will be conducted on a series of different paint films. When complete, these experiments will produce enough data to quantitatively describe the diffusion of water and sodium chloride through the paint films. In addition, investigation of oxygen diffusion through these paints under submerged conditions as well as testing the paints for regional diffusivity variations as discussed by Mayne (14-16) is planned.

Table 9

Paint Density. Dry and Submerged Weight Method.
Multiple Entries Represent Different Specimens.

Paint	Density
O PUR	1.1711
	1.1979
	1.1455
VR3	1.3510
	1.3693
	1.3234
VR4	1.323
	1.5424
	1.1202
	1.2507
	1.1512
	1.2806
	1.1601
	1.2094
K Epoxy	1.1568
	1.1475
	1.1394

5.0 REFERENCES

1. T. R. Beck, "Determination of the Effect of Composition, Structure, and Electrochemical Mass Transport Properties on Adhesion and Corrosion Inhibition of Paint Films," Annual Progress Report No. 1, Contract No. N00014-79-C-0021, Naval Ocean Research and Development Activity, Bay St. Louis, Missouri, 1979.

2. R. T. Ruggeri and T. R. Beck, "A Model for Mass Transport in Paint Films," Corrosion Control by Coatings, H. Leidheiser, Ed., Science Press, Princeton, New Jersey, 1979, p 455.

3. J. Crank, The Mathematics of Diffusion, 2nd ed, Clarendon Press, Oxford, 1975, p 47.

4. J. Crank and G. S. Park, Eds., Diffusion in Polymers, Academic Press, New York, 1968, p 16.

5. E. J. Soxman, "Quartz Crystal Film Thickness Relationships and MCD 9000," supplied by Sloan Technology Corp., Santa Barbara, California, 1979.

6. J. Crank and G. S. Park, op. sit., ch 4, ch 8.

7. S. M. Fang, The Permeation of Gases Through Polyethylene Membranes at High Pressure. A "Free-Volume" Model of Permeation, PhD dissertation, Syracuse University, 1975.

8. W. H. King, Jr., Research and Development, p 28, May, 1969.

9. W. Banks and A. Sharples, J. Appl. Chem., 16, 28, 1966.

10. R. J. Riley, J. O. Gardner, and U. Merten, Science, 143, 801, 1964.

11. R. T. Ruggeri and T. R. Beck, "The Transport Properties of Polyurethane Paint," presented at Corrosion Control by Organic Coatings Conference, Aug. 12, 1980, (proceedings to be published).

12. D. A. MacInnes, The Principles of Electrochemistry, Dover, New York, 1961, p 65.

13. R. T. Ruggeri and T. R. Beck, "An Investigation of the Mass Transfer Characteristics of Polyurethane Paint," presented to American Chemical Society, Organic Coatings and Plastics Chemistry, Aug. 24-29, 1980, preprints vol. 43, p 580.

14. C. C. Maitland and J. E. O. Mayne, Official Digest, 34, 972 (1962).

15. J. E. O. Mayne, Anti-Corrosion, p 3, Oct., 1973.

16. J. E. O. Mayne and D. J. Mills, J. Oil Col. Chem. Assoc., 58, 155, (1975).

17. J. S. Newman, Electrochemical Systems, Prentice-Hall, Englewood Cliffs, New Jersey, 1973, p 45.

18. K. W. Choi and D. N. Bennion, Ind. Eng. Chem. Fundam., 14 (4), 296 (1975).

6.0 APPENDIX A

EXPERIMENTAL DATA

Table A-1

Humidity Chamber Results for a VR3 Free Film
3.20×10^{-3} cm Thick

Experiment Number	Relative Humidity %	Temp. (C°)	Days at These Conditions	Diffusivity (cm^2/sec)		Dry Weight (mg)
				Long Time Approximation (eq. 4)	Complete Formula (eq. 2)	
3	77.9	22.5	4	6.23×10^{-8}	7.36×10^{-8}	29.010
4	77.6	23.3	5	5.81×10^{-8}	1.96×10^{-7}	29.010
Mean 3-4	77.8	22.9	4.5	6.02×10^{-8}	1.35×10^{-7}	29.010

Table A-2.1

O PUR Permeability Data (A = 3.46 cm^2)

	26.8°C		30.8°C		41.3°C	
τ (cm)	N (g-cm/s)	$\bar{P}'$ (cm^2/s)	N (g-cm/s)	$\bar{P}'$ (cm^2/s)	N (g-cm/s)	$\bar{P}'$ (cm^2/s)
7.37×10^{-3}	1.95×10^{-9}	5.06×10^{-10}	2.87×10^{-9}	5.95×10^{-10}	5.79×10^{-9}	6.70×10^{-10}
3.81×10^{-3}	1.76×10^{-9}	4.58×10^{-10}				
14.48×10^{-2}	1.93×10^{-9}	5.01×10^{-10}	2.82×10^{-9}	5.83×10^{-10}	7.01×10^{-9}	8.12×10^{-10}
4.32×10^{-3}	1.75×10^{-9}	4.54×10^{-10}				
3.36×10^{-3}	1.54×10^{-9}	4.00×10^{-10}	2.36×10^{-9}	4.89×10^{-10}	6.42×10^{-10}	7.43×10^{-11}

	24.5 °C	
τ (cm)	N (g-cm/s)	$\bar{P}'$ (cm^2/s)
7.37×10^{-3}	2.09×10^{-9}	6.20×10^{-10}
14.48×10^{-2}	1.67×10^{-9}	4.94×10^{-10}
3.56×10^{-3}	1.69×10^{-9}	5.03×10^{-10}

Table A-2.2

N PUR Permeability Data ($A = 3.46\ cm^2$)

	30.5°C		33.4°C		35.6°C	
τ (cm)	N (g-cm/s)	$\overline{P}'$ (cm^2/s)	N (g-cm/s)	$\overline{P}'$ (cm^2/s)	N (g-cm/s)	$\overline{P}'$ (cm^2/s)
2.49×10^{-3}	1.13×10^{-9}	2.36×10^{-10}	1.52×10^{-9}	2.70×10^{-10}	1.77×10^{-9}	2.78×10^{-10}
3.38×10^{-3}	1.63×10^{-9}	3.41×10^{-10}	2.34×10^{-9}	4.16×10^{-10}	2.64×10^{-9}	4.15×10^{-10}
3.81×10^{-3}	1.43×10^{-9}	3.01×10^{-10}	2.01×10^{-9}	4.52×10^{-10}	2.38×10^{-9}	3.75×10^{-10}

	38.5°C		36.5°C		36.3°C	
τ (cm)	N (g-cm/s)	$\overline{P}'$ (cm^2/s)	N (g-cm/s)	$\overline{P}'$ (cm^2/s)	N (g-cm/s)	$\overline{P}'$ (cm^2/s)
2.49×10^{-3}	2.22×10^{-9}	2.99×10^{-10}	1.96×10^{-9}	2.93×10^{-10}	2.32×10^{-9}	3.51×10^{-10}
3.38×10^{-3}	3.35×10^{-9}	4.50×10^{-10}	2.58×10^{-9}	3.86×10^{-10}	2.63×10^{-9}	3.98×10^{-10}
3.81×10^{-3}	3.08×10^{-9}	4.13×10^{-10}	2.13×10^{-9}	3.19×10^{-10}	1.75×10^{-9}	2.65×10^{-10}

	36.5°C		31.2°C		26.4°C	
τ (cm)	N (g-cm/s)	$\overline{P}'$ (cm^2/s)	N (g-cm/s)	$\overline{P}'$ (cm^2/s)	N (g-cm/s)	$\overline{P}'$ (cm^2/s)
2.49×10^{-3}	2.64×10^{-9}	3.95×10^{-10}	1.30×10^{-9}	2.62×10^{-10}	1.18×10^{-9}	3.14×10^{-8}
3.81×10^{-3}	1.91×10^{-9}	2.86×10^{-10}	1.05×10^{-9}	2.10×10^{-10}	8.61×10^{-10}	2.29×10^{-10}

Table A-2.3

VR2 Permeability Data (A = 3.14 cm^2)

	23.3°C		26.1°C		30.9°C	
τ (cm)	N (g-cm/s)	$\bar{P}'$ (cm^2/s)	N (g-cm/s)	$\bar{P}'$ (cm^2/s)	N (g-cm/s)	$\bar{P}'$ (cm^2/s)
2.31×10^{-3}	2.47×10^{-9}	8.69×10^{-10}	3.34×10^{-9}	1.05×10^{-9}	5.47×10^{-9}	1.23×10^{-9}
2.13×10^{-3}	2.00×10^{-9}	7.04×10^{-10}	2.30×10^{-9}	6.67×10^{-10}	2.73×10^{-9}	6.16×10^{-10}
2.33×10^{-3}	2.47×10^{-9}	8.70×10^{-10}	3.01×10^{-9}	8.98×10^{-10}	3.20×10^{-9}	7.23×10^{-10}
3.09×10^{-3}	1.97×10^{-9}	6.93×10^{-10}	2.15×10^{-9}	6.42×10^{-10}	2.78×10^{-9}	6.28×10^{-10}
3.07×10^{-3}	2.29×10^{-9}	7.32×10^{-10}	2.40×10^{-9}	6.48×10^{-10}	2.96×10^{-9}	6.06×10^{-10}

	31.9°C		35.4°C		37.6°C	
τ (cm)	N (g-cm/s)	$\bar{P}'$ (cm^2/s)	N (g-cm/s)	$\bar{P}'$ (cm^2/s)	N (g-cm/s)	$\bar{P}'$ (cm^2/s)
2.31×10^{-3}	7.60×10^{-9}	1.62×10^{-9}	8.45×10^{-9}	1.48×10^{-9}	5.74×10^{-9}	8.93×10^{-10}
2.13×10^{-3}	6.23×10^{-9}	1.33×10^{-9}	7.81×10^{-9}	1.37×10^{-9}	4.62×10^{-9}	7.18×10^{-10}
2.33×10^{-3}	4.41×10^{-9}	9.39×10^{-10}	4.80×10^{-9}	8.41×10^{-10}		
3.09×10^{-3}	3.19×10^{-9}	6.81×10^{-10}	3.76×10^{-9}	6.60×10^{-10}	5.26×10^{-9}	8.18×10^{-10}
*3.07×10^{-3}	3.62×10^{-9}	7.01×10^{-10}	4.39×10^{-9}	6.98×10^{-10}	6.25×10^{-9}	8.81×10^{-10}

*(A = 3.46 cm^2)

Table A-2.4

VR3 Permeability Data ($A = 3.46\ cm^2$)

	36.2°C		35.9°C		29.6°C	
τ (cm)	N (g-cm/s)	$\bar{P}'$ (cm^2/s)	N (g-cm/s)	$\bar{P}'$ (cm^2/s)	N (g-cm/s)	$\bar{P}'$ (cm^2/s)
2.08×10^{-3}	1.95×10^{-9}	2.97×10^{-10}	1.85×10^{-9}	2.86×10^{-10}	1.14×10^{-10}	2.51×10^{-10}
2.90×10^{-3}	2.77×10^{-9}	4.22×10^{-10}	2.88×10^{-9}	4.46×10^{-10}	1.87×10^{-9}	4.12×10^{-10}
3.48×10^{-3}	2.53×10^{-9}	3.84×10^{-10}	2.30×10^{-9}	3.56×10^{-10}	1.30×10^{-9}	2.87×10^{-10}
6.58×10^{-3}	3.64×10^{-9}	5.54×10^{-10}	2.92×10^{-9}	4.52×10^{-10}	1.71×10^{-9}	3.76×10^{-10}

	31.0°C		20.8°C		31.0°C	
τ (cm)	N (g-cm/s)	$\bar{P}'$ (cm^2/s)	N (g-cm/s)	$\bar{P}'$ (cm^2/s)	N (g-cm/s)	$\bar{P}'$ (cm^2/s)
2.08×10^{-3}	1.19×10^{-9}	2.42×10^{-10}	5.39×10^{-10}	2.01×10^{-10}	1.13×10^{-9}	2.30×10^{-10}
2.90×10^{-3}	1.97×10^{-9}	4.00×10^{-10}	1.09×10^{-9}	4.06×10^{-10}	2.04×10^{-9}	4.15×10^{-10}
3.48×10^{-3}	1.42×10^{-9}	2.90×10^{-10}	5.96×10^{-10}	2.22×10^{-10}	1.37×10^{-9}	2.79×10^{-10}
6.58×10^{-3}	1.92×10^{-9}	3.91×10^{-10}	7.16×10^{-10}	2.67×10^{-10}	1.84×10^{-9}	3.74×10^{-10}

	27.6°C		27.6°C	
τ (cm)	N (g-cm/s)	$\bar{P}'$ (cm^2/s)	N (g-cm/s)	$\bar{P}'$ (cm^2/s)
2.08×10^{-3}	9.41×10^{-10}	2.33×10^{-10}	9.41×10^{-10}	2.33×10^{-10}
2.90×10^{-3}	1.80×10^{-9}	4.46×10^{-10}	1.81×10^{-9}	4.47×10^{-10}
3.48×10^{-3}	1.08×10^{-9}	2.68×10^{-10}	1.08×10^{-9}	2.67×10^{-10}
6.58×10^{-3}	1.39×10^{-9}	3.43×10^{-10}	1.40×10^{-9}	3.47×10^{-10}

Table A-2.5

VR4 Permeability Data (A = 3.46 cm^2)

	26.4°C		26.2°C		24.2°C	
τ (cm)	N (g-cm/s)	$\overline{P}'$ (cm^2/s)	N (g-cm/s)	$\overline{P}'$ (cm^2/s)	N (g-cm/s)	$\overline{P}'$ (cm^2/s)
6.63×10^{-3}	9.86×10^{-10}	2.62×10^{-10}	9.75×10^{-10}	2.62×10^{-10}		
6.73×10^{-3}	1.08×10^{-10}	2.86×10^{-10}	1.20×10^{-10}	3.22×10^{-10}	9.82×10^{-9}	2.98×10^{-10}

	29.3°C		28.0°C		26.4°C	
τ (cm)	N (g-cm/s)	$\overline{P}'$ (cm^2/s)	N (g-cm/s)	$\overline{P}'$ (cm^2/s)	N (g-cm/s)	$\overline{P}'$ (cm^2/s)
4.85×10^{-3}	1.66×10^{-9}	3.72×10^{-10}	1.05×10^{-9}	2.53×10^{-10}	1.31×10^{-9}	3.48×10^{-10}

	26.1°C		24.4°C	
τ (cm)	N (g-cm/s)	$\overline{P}'$ (cm^2/s)	N (g-cm/s)	$\overline{P}'$ (cm^2/s)
4.85×10^{-3}	1.42×10^{-10}	3.84×10^{-10}	9.83×10^{-10}	2.94×10^{-10}

Table A-2.6

VR4 Permeability Data ($A = 3.46\ cm^2$)

	36.5°C		29.5°C		33.8°C	
τ (cm)	N (g-cm/s)	$\bar{P}'$ (cm^2/s)	N (g-cm/s)	$\bar{P}'$ (cm^2/s)	N (g-cm/s)	$\bar{P}'$ (cm^2/s)
3.68×10^{-3}	3.47×10^{-9}	0.52×10^{-11}	1.90×10^{-9}	4.21×10^{-10}		
6.63×10^{-3}			1.58×10^{-9}	3.48×10^{-10}	2.29×10^{-9}	3.98×10^{-10}
6.73×10^{-3}			1.93×10^{-9}	4.28×10^{-10}	2.66×10^{-9}	4.62×10^{-10}

	33.6°C		31.3°C		29.4°C	
τ (cm)	N (g-cm/s)	$\bar{P}'$ (cm^2/s)	N (g-cm/s)	$\bar{P}'$ (cm^2/s)	N (g-cm/s)	$\bar{P}'$ (cm^2/s)
6.63×10^{-3}	1.74×10^{-9}	3.06×10^{-10}	1.53×10^{-9}	3.05×10^{-10}	1.06×10^{-9}	2.36×10^{-10}
6.73×10^{-3}	1.90×10^{-9}	3.35×10^{-10}	1.50×10^{-9}	2.99×10^{-10}	1.25×10^{-9}	2.79×10^{-10}

	31.2°C		29.4°C		28.1°C	
τ (cm)	N (g-cm/s)	$\bar{P}'$ (cm^2/s)	N (g-cm/s)	$\bar{P}'$ (cm^2/s)	N (g-cm/s)	$\bar{P}'$ (cm^2/s)
6.63×10^{-3}	1.21×10^{-9}	2.43×10^{-10}	1.19×10^{-9}	2.65×10^{-10}	1.00×10^{-9}	2.42×10^{-10}
6.73×10^{-3}	1.39×10^{-9}	2.80×10^{-10}	1.52×10^{-9}	3.39×10^{-10}	1.11×10^{-9}	2.58×10^{-10}

Table A-2.7

VR 4 Permeability Data (A = 3.46 cm^2)

	28.0°C		27.4°C		26.4°C	
τ (cm)	N (g-cm/s)	$\bar{P}'$ (cm^2/s)	N (g-cm/s)	$\bar{P}'$ (cm^2/s)	N (g-cm/s)	$\bar{P}'$ (cm^2/s)
2.85×10^{-3}	1.02×10^{-9}	2.46×10^{-10}	1.25×10^{-9}	3.12×10^{-10}	1.03×10^{-9}	2.73×10^{-10}
3.68×10^{-3}	1.24×10^{-9}	3.00×10^{-10}	1.51×10^{-9}	3.79×10^{-10}	1.18×10^{-9}	3.13×10^{-10}

	30.5°C		33.4°C		35.6°C	
τ (cm)	N (g-cm/s)	$\bar{P}'$ (cm^2/s)	N (g-cm/s)	$\bar{P}'$ (cm^2/s)	N (g-cm/s)	$\bar{P}'$ (cm^2/s)
2.85×10^{-3}	1.48×10^{-9}	3.09×10^{-10}	2.46×10^{-10}	4.37×10^{-10}	2.92×10^{-9}	4.59×10^{-10}
3.68×10^{-3}	1.77×10^{-9}	3.71×10^{-10}	2.52×10^{-9}	4.47×10^{-10}	2.01×10^{-9}	4.58×10^{-10}

	38.5°C		36.5°C		36.3°C	
τ (cm)	N (g-cm/s)	$\bar{P}'$ (cm^2/s)	N (g-cm/s)	$\bar{P}'$ (cm^2/s)	N (g-cm/s)	$\bar{P}'$ (cm^2/s)
2.85×10^{-3}	4.50×10^{-9}	6.04×10^{-10}				
3.68×10^{-3}	4.11×10^{-9}	5.51×10^{-10}	2.79×10^{-9}	4.18×10^{-10}	2.84×10^{-9}	4.29×10^{-10}

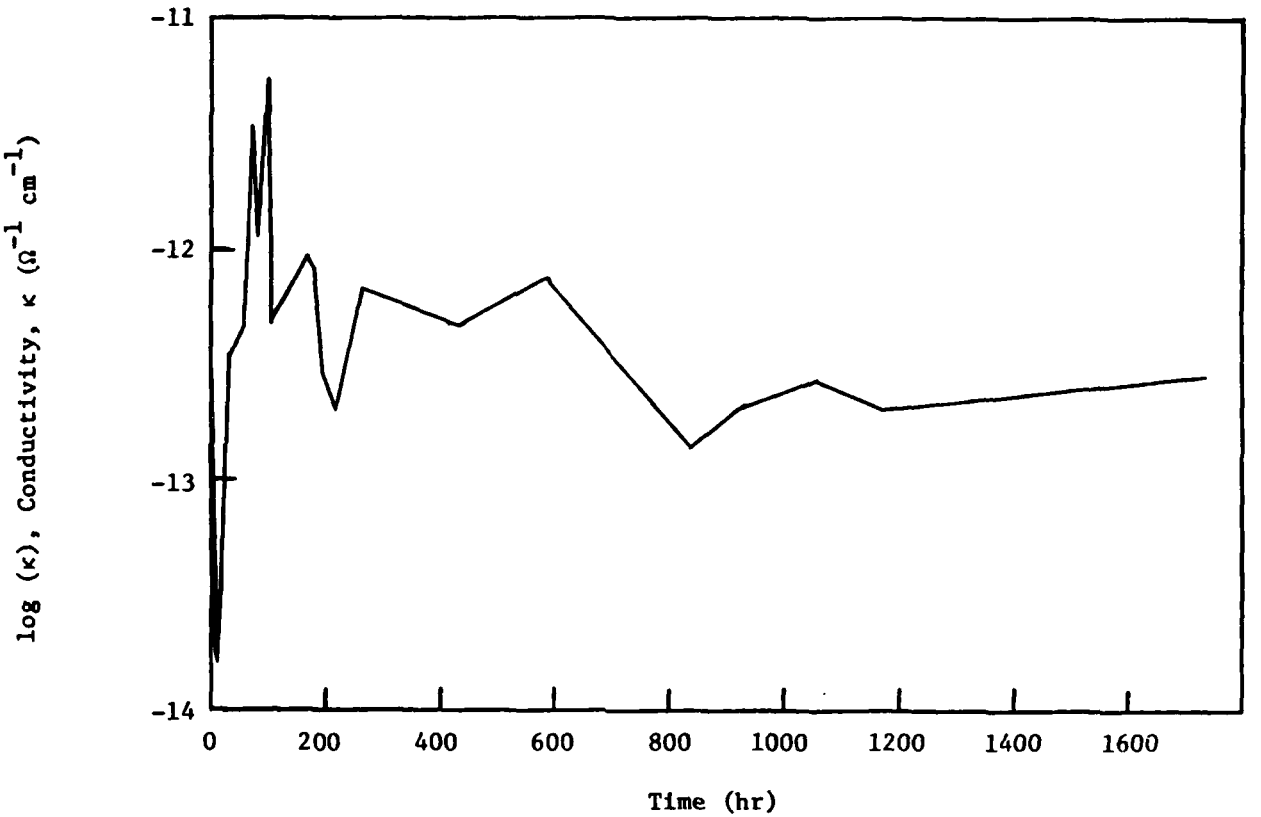

Fig. A-3.1. Logarithm of conductivity vs time for Hittorf experiment No. NR-1, VR4 at 25°C.

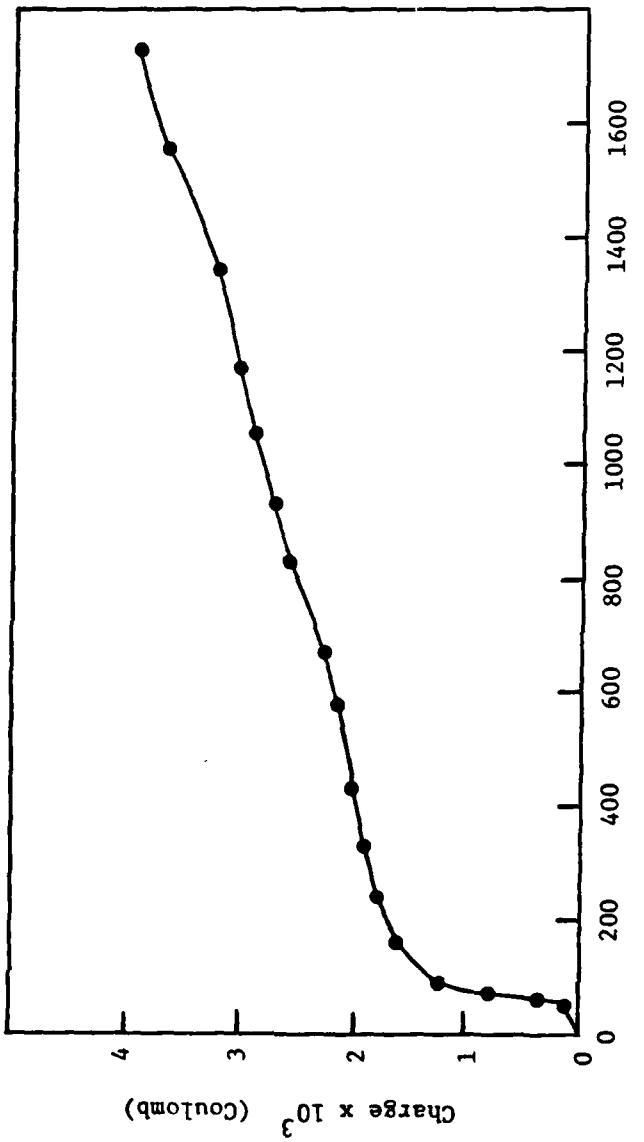

Fig. A-3.2. Charge vs time for Hittorf experiment No. NR-1, VR4 at 25°C.

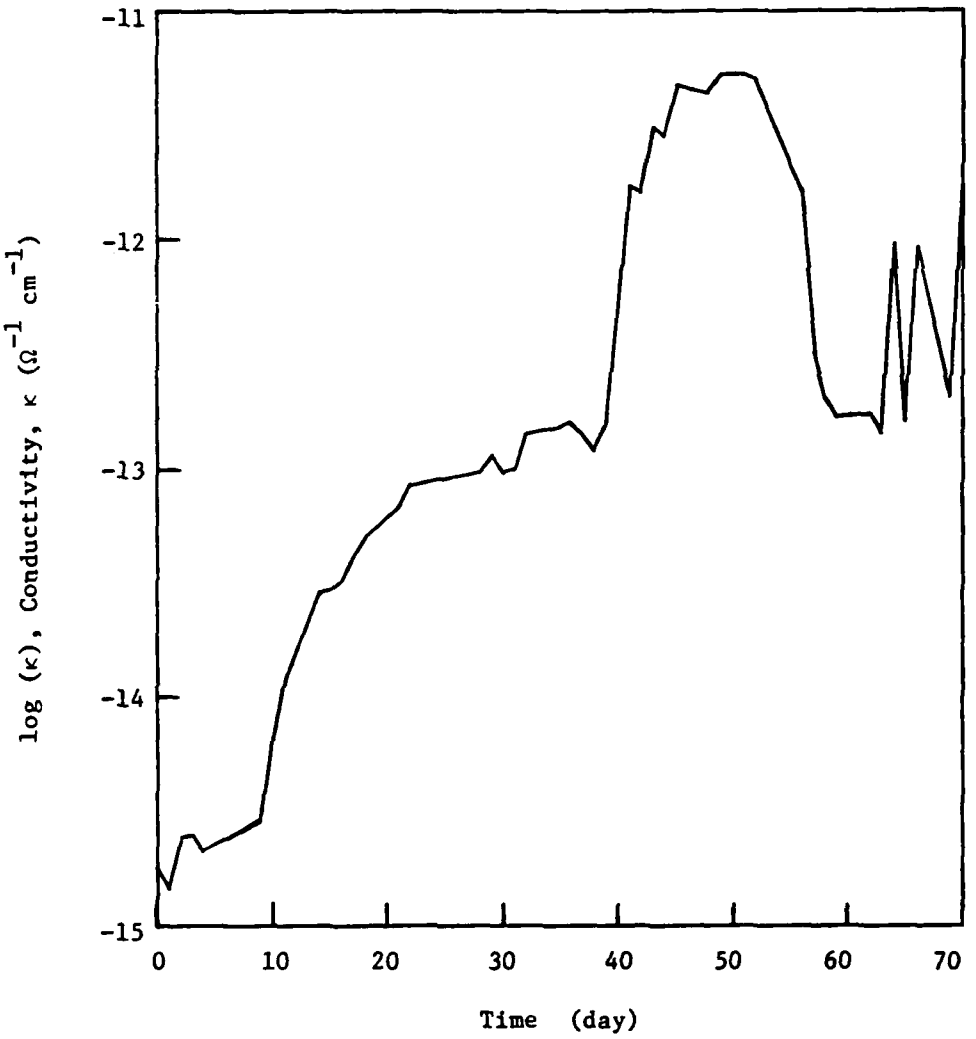

Fig. A-3.3. Logarithm of conductivity vs time for Hittorf experiment No. NR-2, VR4 at 25°C.

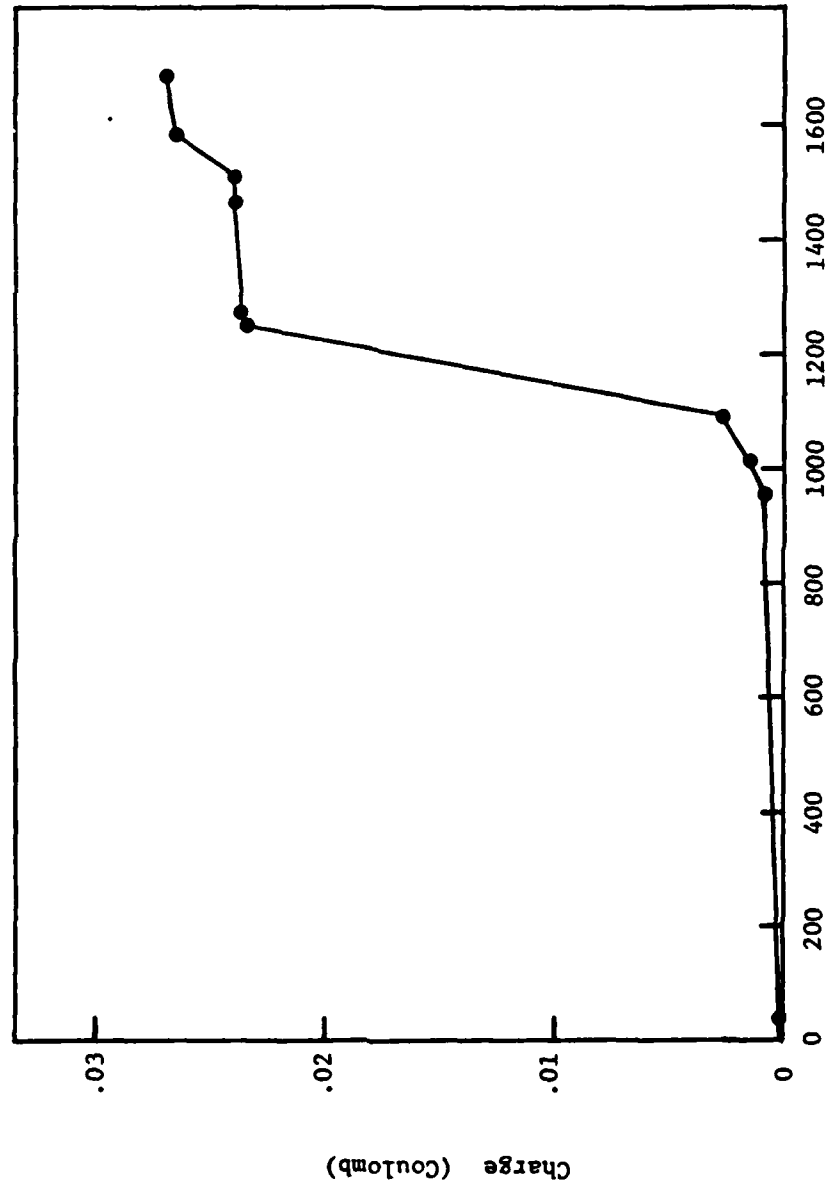

Fig. A-3.4. Charge vs time for Hittorf experiment No. NR-2, VR4 at 25°C.

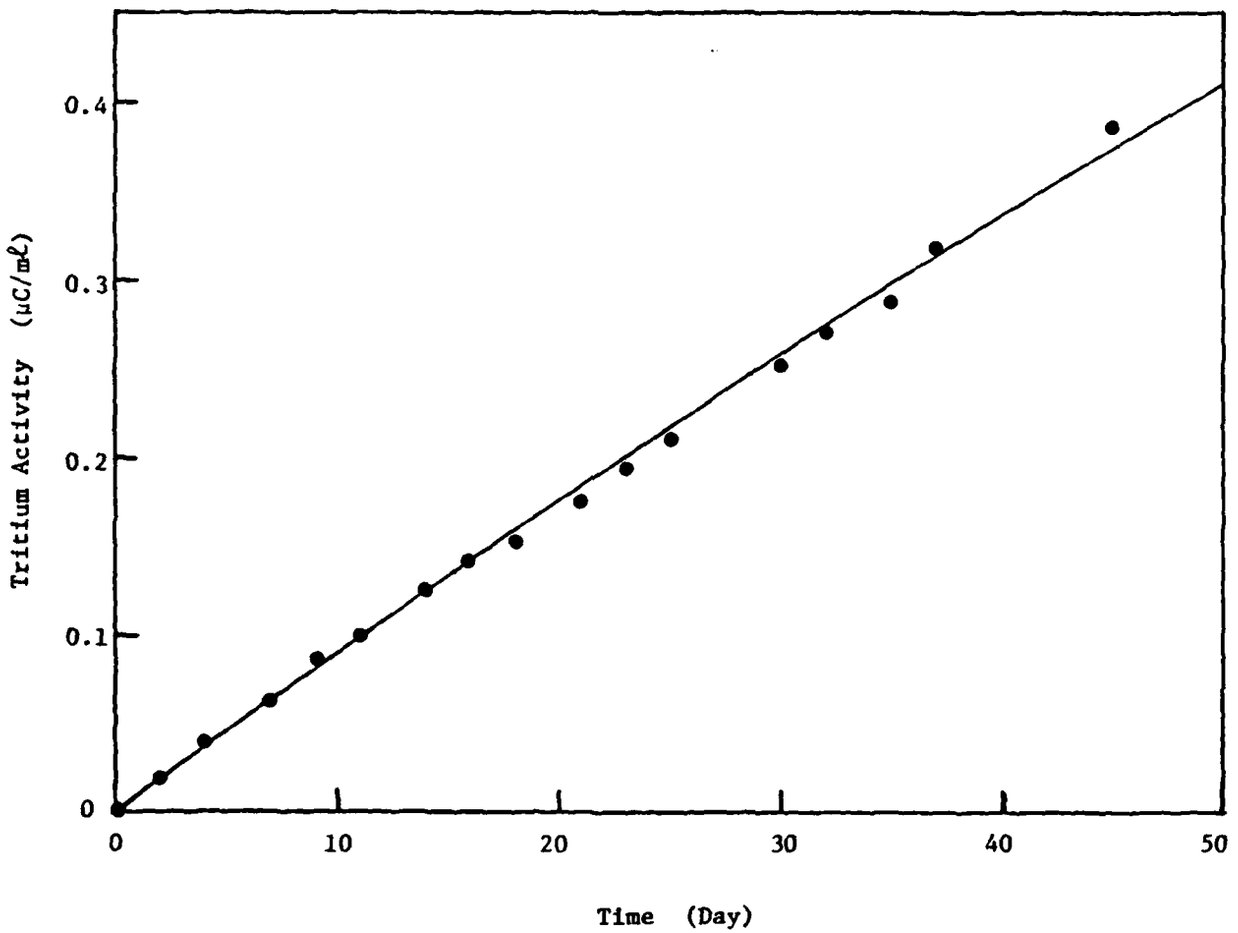

Fig. A-3.5. Tritium (H^3) activity vs time for Hittorf experiment No. NR-2, VR4 at 25°C. Solid curve for theoretical best diffusivity. Points are experimental data.

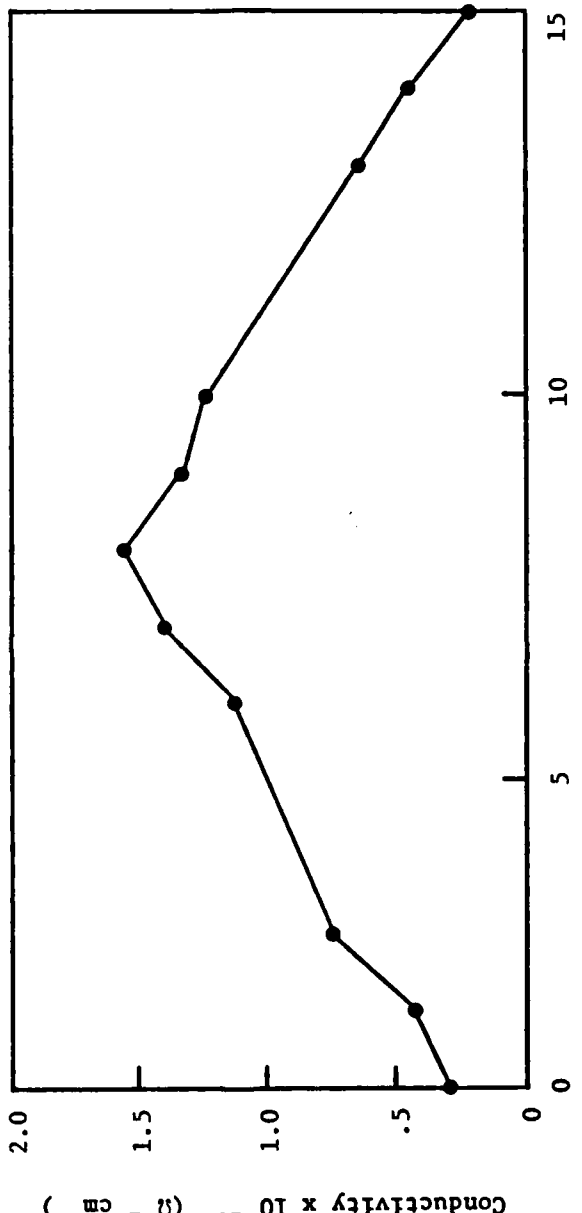

Fig. A-3.6. Conductivity vs time for Hittorf experiment No. NR-3, 0 PUR at 25°C.

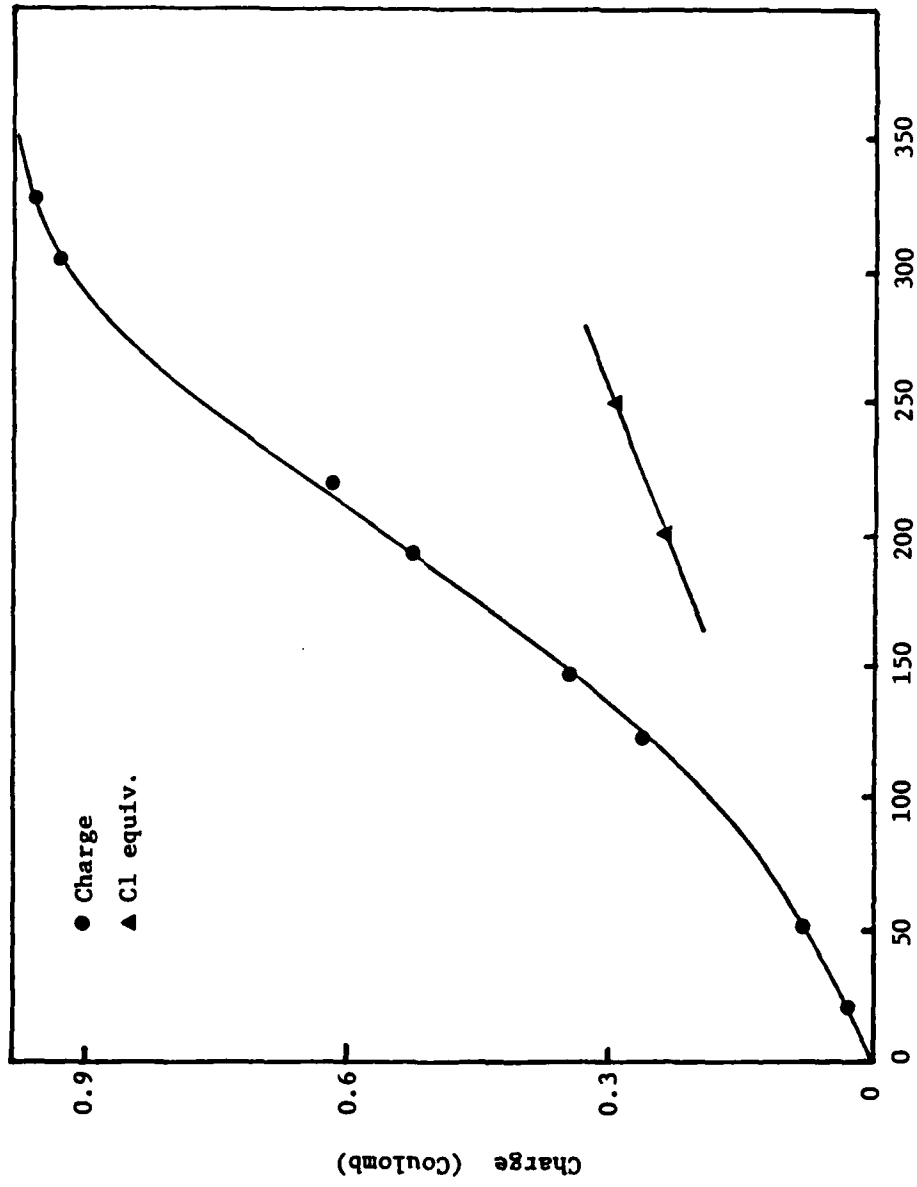

Fig. A-3.7. Charge vs time for Hittorf experiment No. NR-3, O PUR at 25°C. Also shown is the chloride charge equivalent in coulombs.

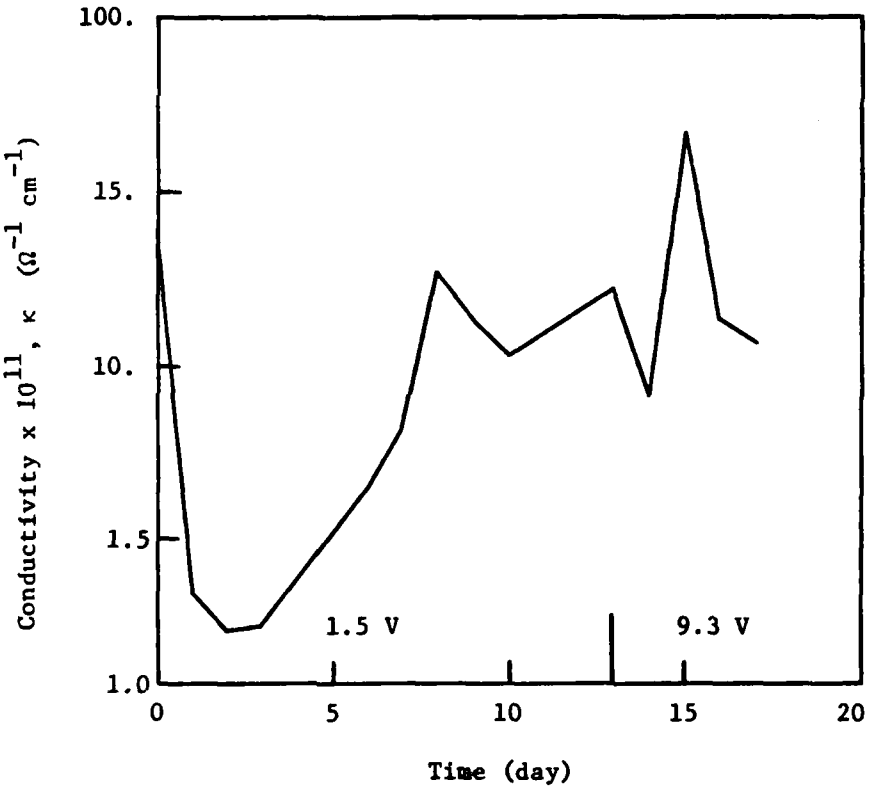

Fig. A-3.8. Logarithm of conductivity vs time for Hittorf experiment No. NR-4, O PUR at 25°C.

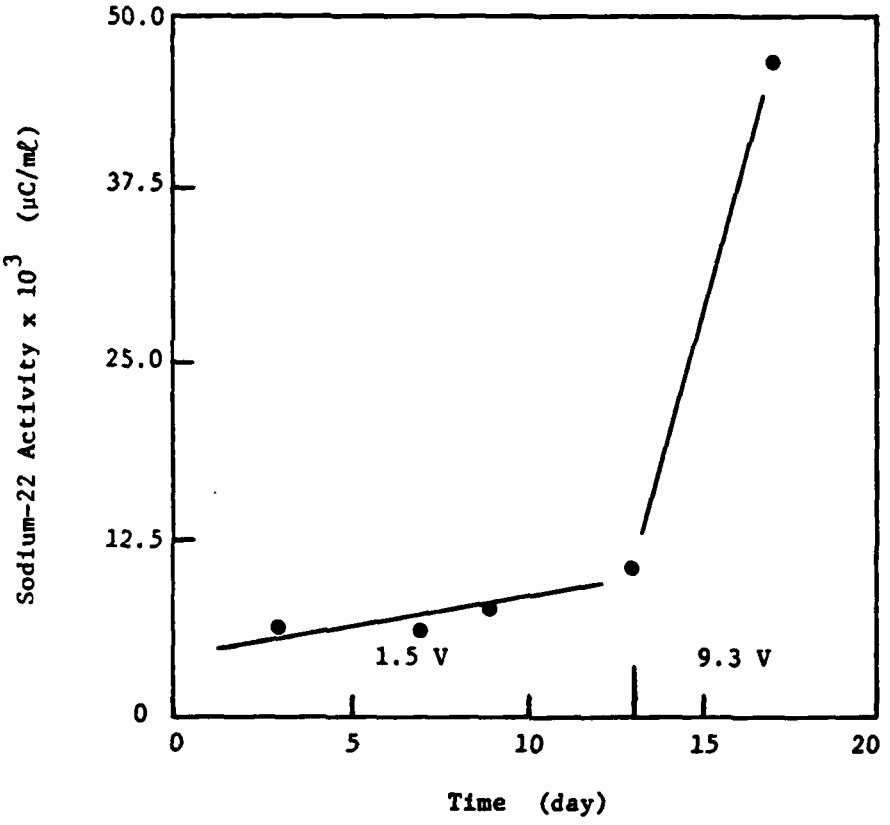

Fig. A-3.9. Sodium-22 activity vs time for Hittorf experiment No. NR-4, O PUR at 25°C.

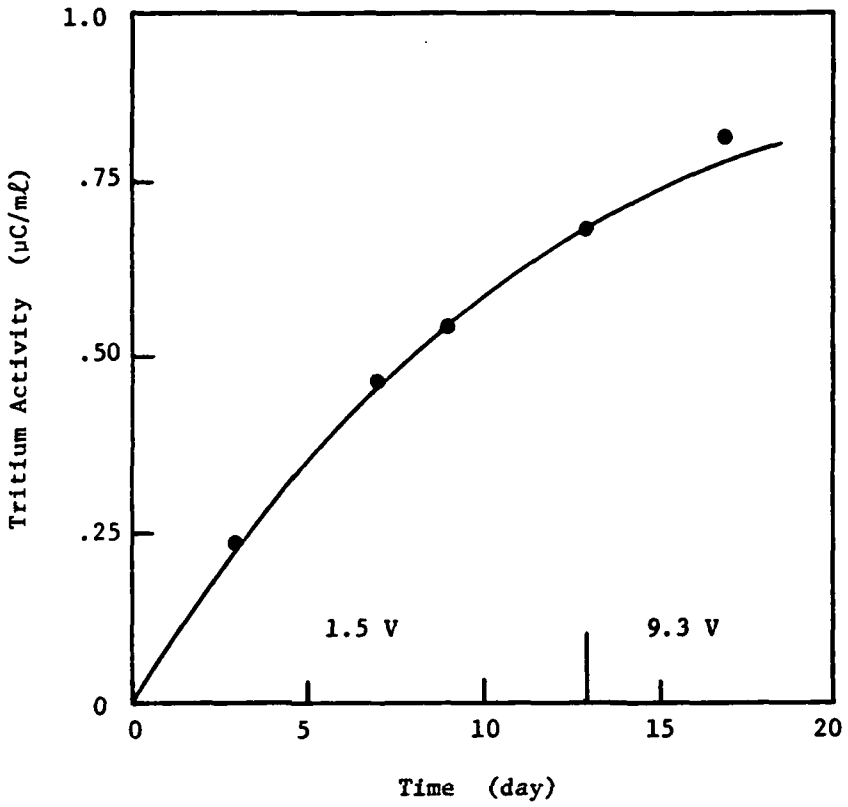

Fig. A-3.10. Tritium activity for Hittorf experiment No. NR-4, 0 PUR at 25°C. Solid curve for theoretical best diffusivity. Points are experimental data.

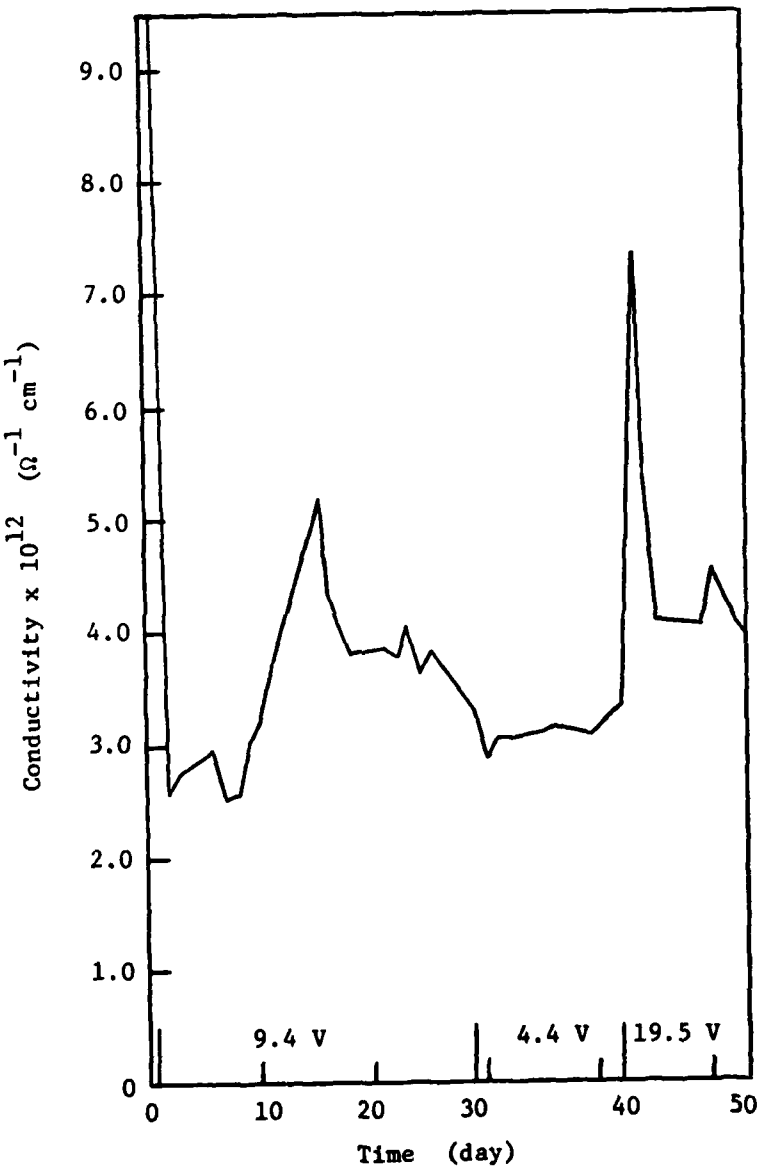

Fig. A-3.11. Conductivity vs time for Hittorf experiment No. NR-5, 0 PUR at 25°C.

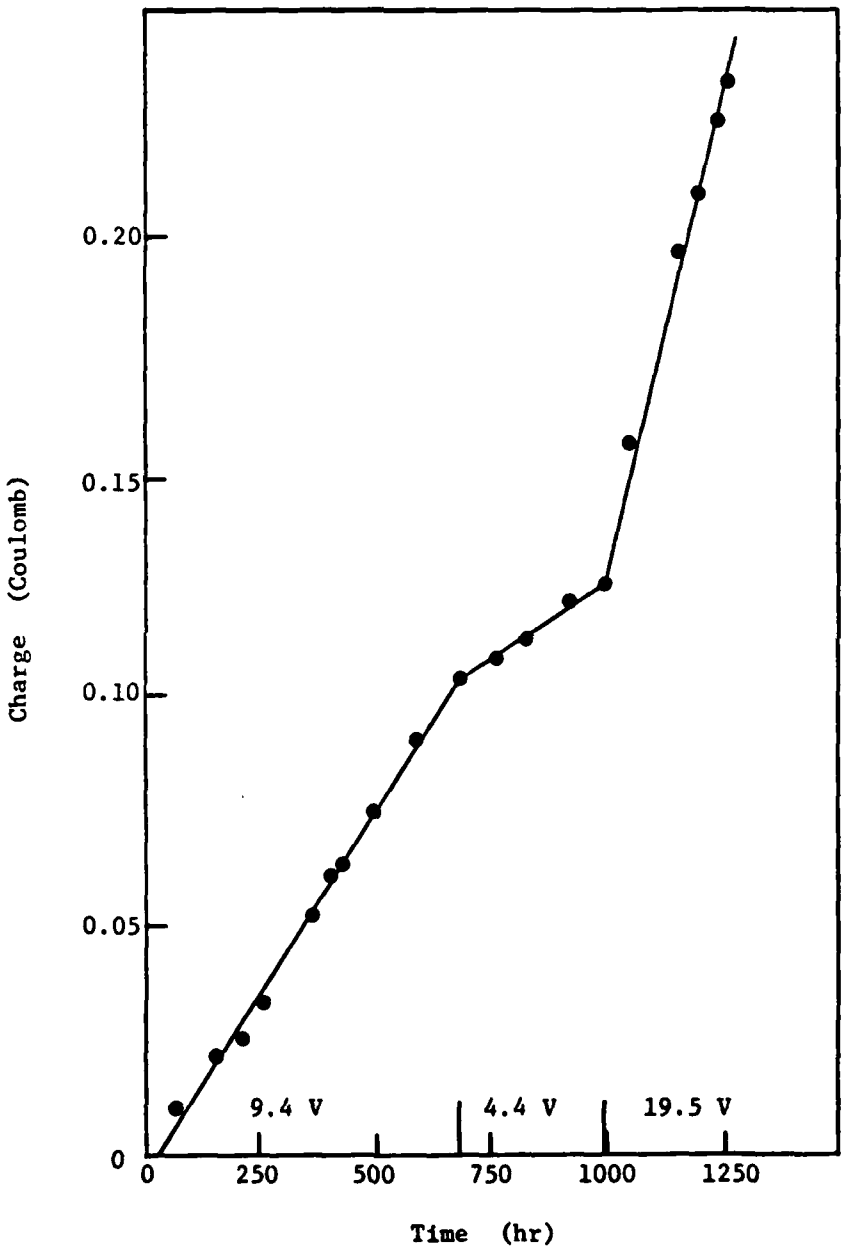

Fig. A-3.12. Charge vs time for Hittorf experiment No. NR-5, O PUR at 25°C.

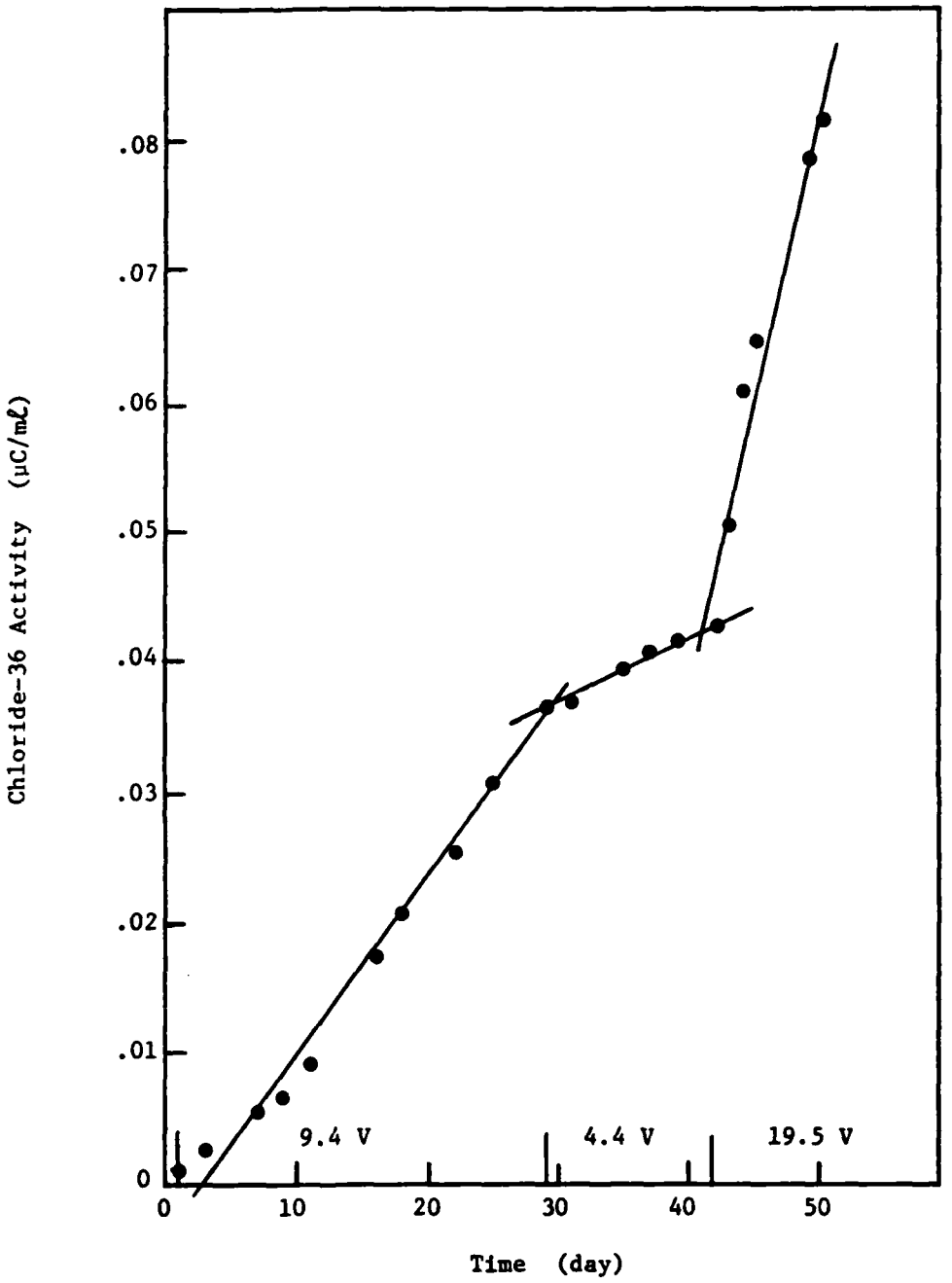

Fig. A-3.13. Chloride-36 activity vs time for Hittorf experiment No. NR-5, O PUR at 25°C.

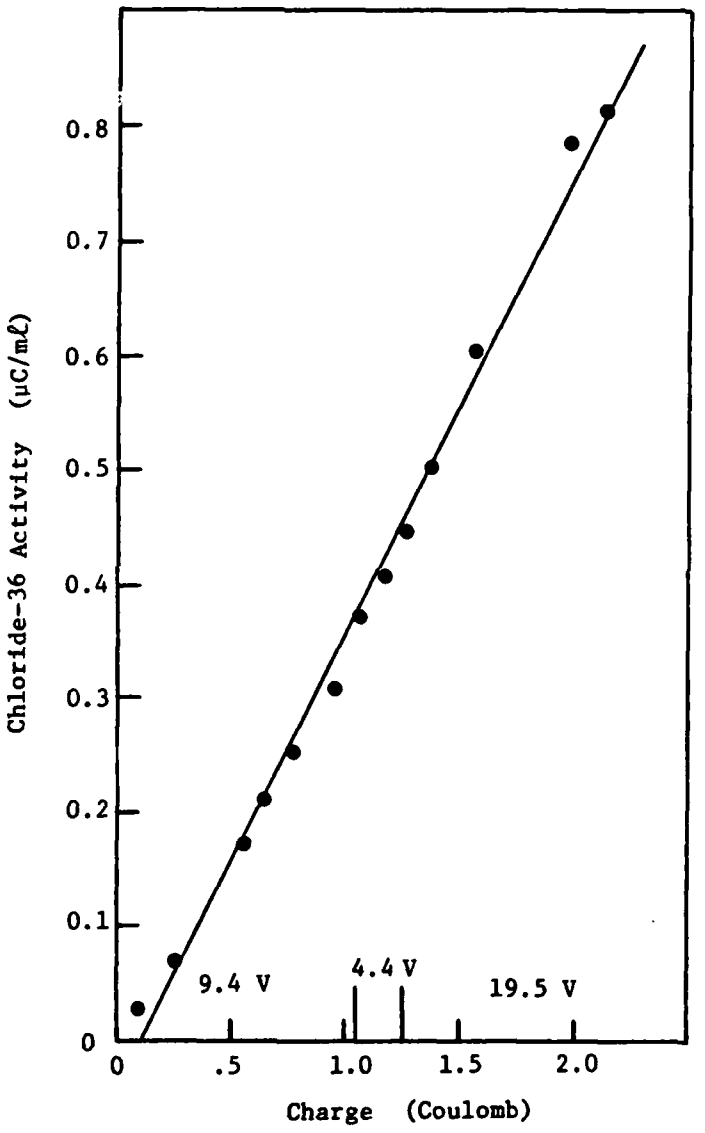

Fig. A-3.14. Chloride-36 vs charge for Hittorf experiment No. NR-5, O PUR at 25°C.

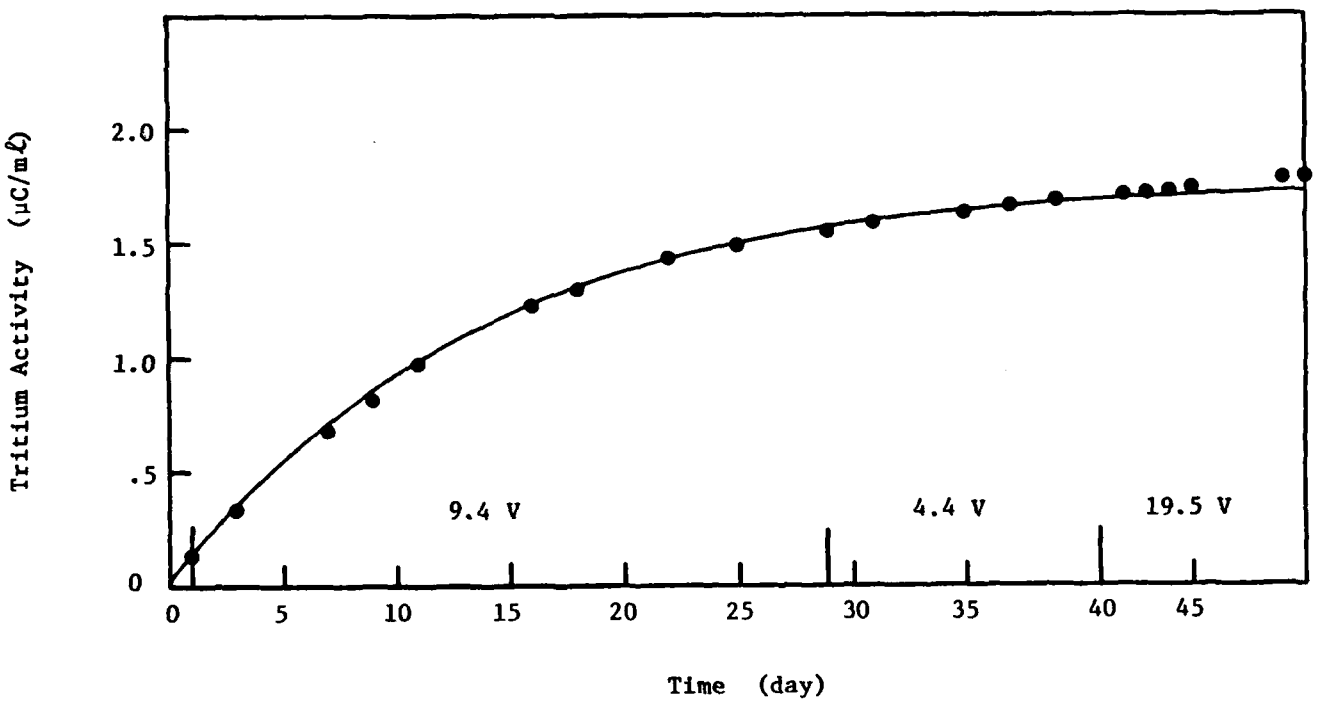

Fig. A-3.15. Tritium (H^3) activity vs time for Hittorf experiment No. NR-5, O PUR at 25°C. Solid curve for theoretical best diffusivity. Points are experimental data.

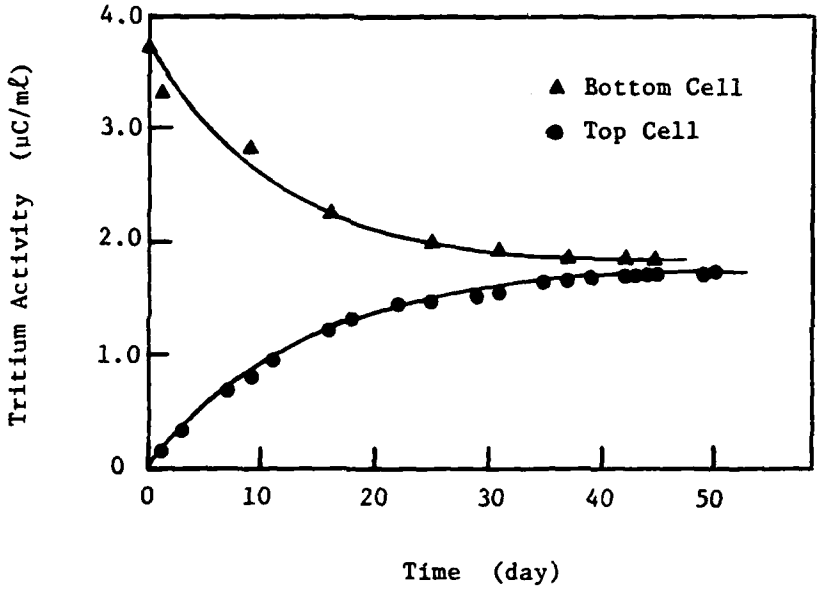

Fig. A-3.16. Tritium activity vs time for Hittorf experiment No. NR-5, O PUR at 25°C. Both bottom and top cell activities are shown.

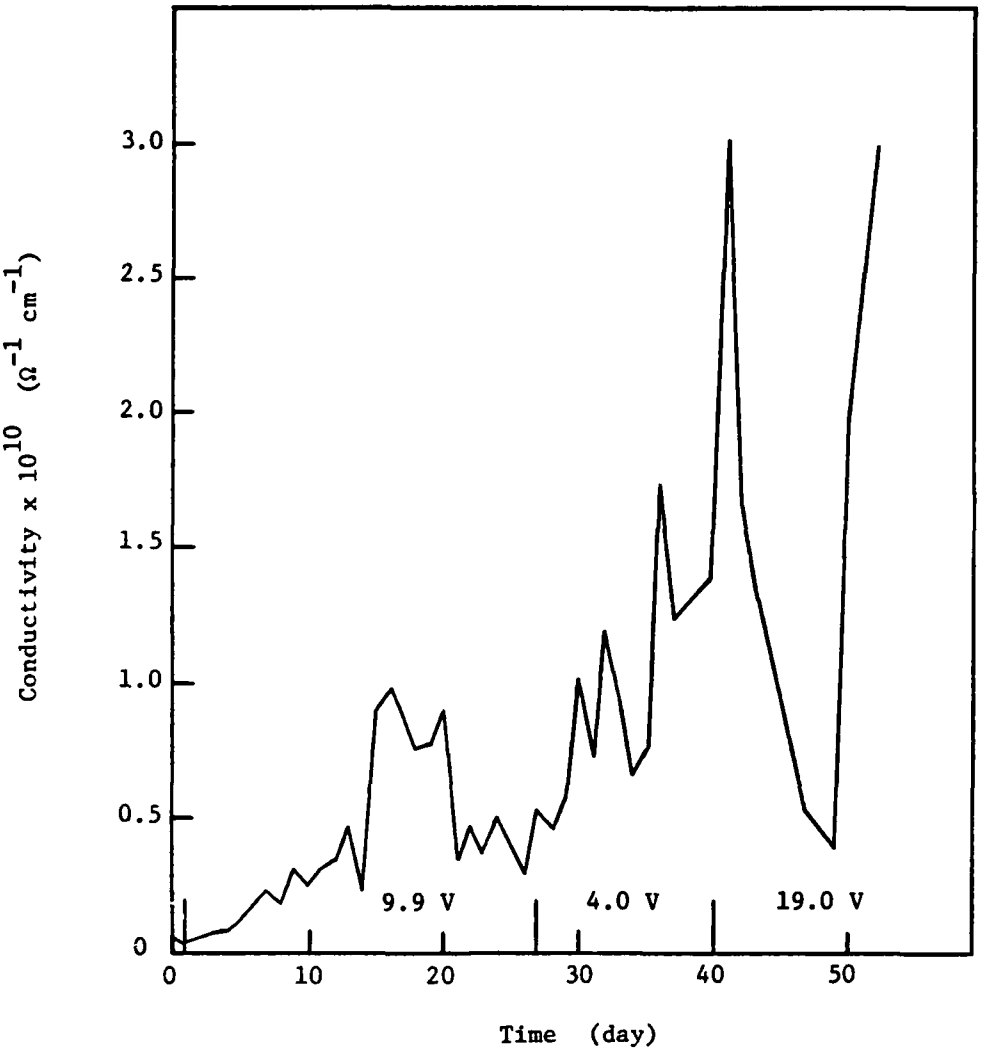

Fig. A-3.17. Conductivity vs time for Hittorf experiment No. NR-6, O PUR at 25°C.

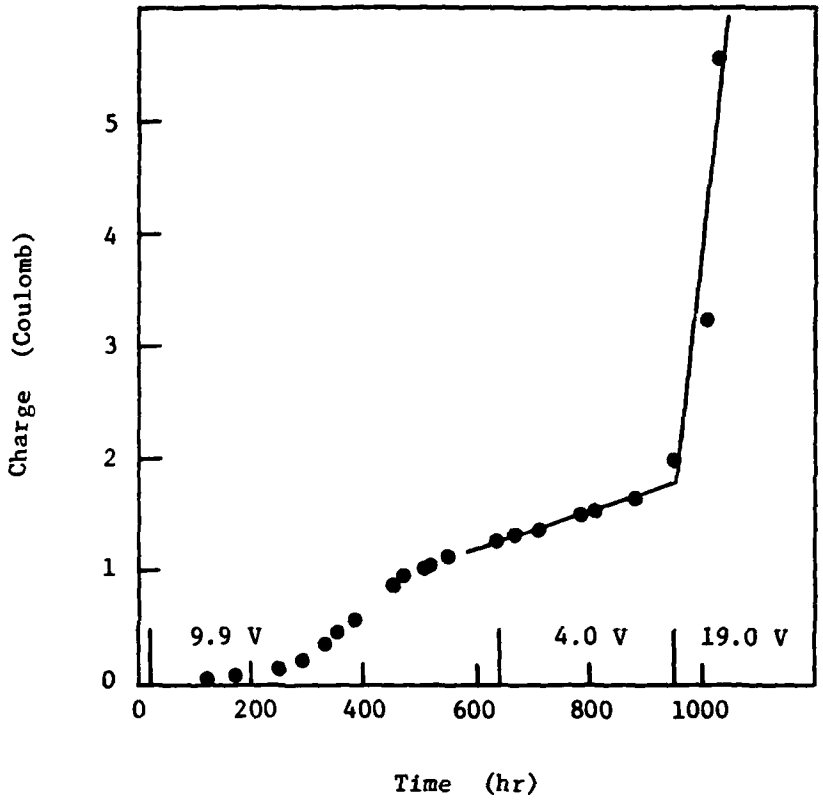

Fig. A-3.18. Charge vs time for Hittorf experiment No. NR-6, O PUR at 25°C.

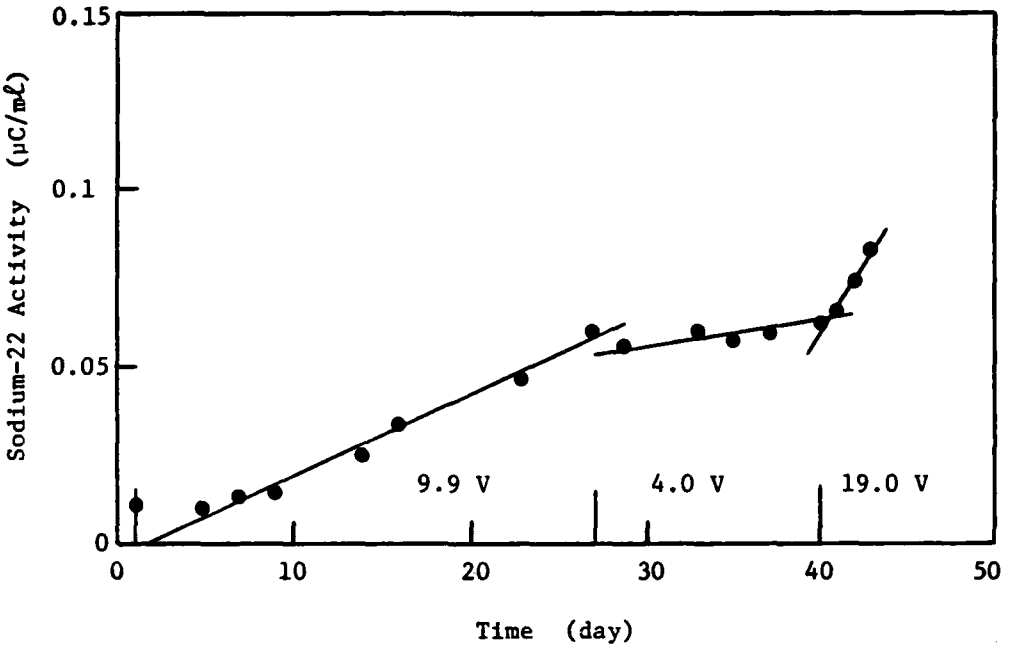

Fig. A-3.19. Sodium-22 activity vs time for Hittorf experiment No. NR-4, 0 PUR at 25°C.

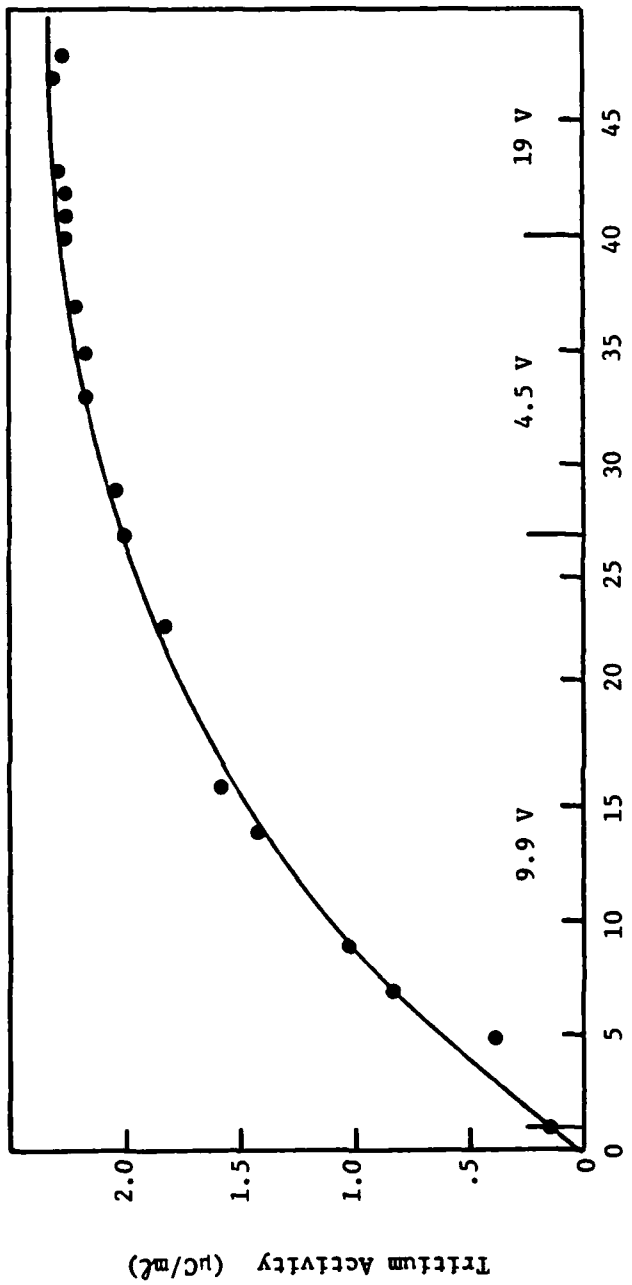

Fig. A-3.20. Tritium (H^3) activity vs time for Hittorf experiment NR-6, O PUR at 25°C. Solid curve for theoretical best diffusivity. Points are experimental data.

Table A-4.1

Cell Potential (mV) for 0 PUR in HI Solution

Reference Solution 10^{-1} N HI

B = Reference Solution on Bottom, T = Reference Solution on Top

Variable Concentration	Reference Position			Mean
	B	T	B	
10^{-4}		-266	160	213
10^{-3}	126	-202	134	154
3×10^{-3}		-151		151
10^{-2}	96	-104	91	97
3×10^{-2}	50		52	51
10^{-1}	-4	2	0	-3
3×10^{-1}	-51	49	-50	-50
1	-116			-116

Table A-4.2

Cell Potential (mV) for O PUR in HI Solution

Reference Solution 10^{-2} N HI

B = Reference Solution on Bottom, T = Reference Solution on Top

Variable Concentration	Reference Position		
	B	B	T
10^{-4}	37	107	-89
10^{-3}	53.2	75	-61
3×10^{-3}		43	-37
10^{-2}	22	2	3
3×10^{-2}	-19	-38	45
10^{-1}	-72	-88	100
3×10^{-1}	-136	-139	151
1	-217		

Variable Concentration	Reference Position		Mean
	B	T	
10^{-4}	113	-74	84
10^{-3}	76	-60	65
3×10^{-3}	38	-26	36
10^{-2}	6	5	4
3×10^{-2}	-36	47	-37
10^{-1}	-88		-87
3×10^{-1}	-128	143	-139
1			-217

Table A-4.3

Cell Potential (mV) for O PUR in HI Solution

Reference Solution 10^{-3} N HI

B = Reference Solution on Bottom, T = Reference Solution on Top

Variable Concentration	Reference Solution B	B	B
10^{-4}	30		76
10^{-3}	99	68	54
3×10^{-3}		26	26
10^{-2}	19	-37	-37
3×10^{-2}	-39	-93	-93
10^{-1}	-115	-159	-151
3×10^{-1}	-195		-211
1	-279		

Variable Concentration	Reference Position T	Mean
10^{-4}	-31	46
10^{-3}	7	54
3×10^{-3}	43	3
10^{-2}	87	-35.5
3×10^{-2}	141	-91.5
10^{-1}	205	-157.5
3×10^{-1}		-203
1		-279

Table A-4.4

Cell Potential (mV) for 0 PUR in HI Solution

Reference Solution 10^{-4} N HI

B = Reference Solution on Bottom, T = Reference Solution on Top

Variable Concentration	Reference Position B	B	Mean
10^{-4}	5	1	3
10^{-3}	-33	-28	-30.5
3×10^{-3}		-73	-73
10^{-2}	-83	-122	-102.5
3×10^{-2}	-124	-190	-157
10^{-1}	-210	-253	-231.5
3×10^{-1}	-291	-309	-300
1	-375		-375

6.0 APPENDIX B

The Transport Properties of Polyurethane Paint

An Investigation of the Mass Transfer Characteristics of Polyurethane Paint

THE TRANSPORT PROPERTIES OF POLYURETHANE PAINT

R. T. Ruggeri and T. R. Beck

Electrochemical Technology Corp.
3935 Leary Way N.W.
Seattle, Washington 98107

ABSTRACT

Unpigmented paints reduce corrosion by inhibiting the rate of mass transfer of reactants toward and products away from metal surfaces. In order to quantitatively describe the mass-transfer processes in polymer paints a new mathematical model of diffusion has been proposed. An experimental investigation of one type of polyurethane has been conducted to evaluate the applicability of the model and determine the required parameters (diffusion coefficients, transference numbers, etc.). A water diffusivity ($D = 3.2 \times 10^{-8}$ cm^2/sec) and dimensionless solubility ($S = 0.015$) have been determined. The concentration of sodium chloride in paint exposed to 0.1 N NaCl solution at 22°C has been measured

$$4.6 \times 10^{-8} < C_i < 1.9 \times 10^{-7} \text{ mole/g-paint}$$

A new hypothesis is presented; hydrogen and/or hydroxyl ions carry the bulk of the current through polyurethane films immersed in dilute sodium chloride solutions.

INTRODUCTION

Paint has been used to inhibit corrosion for a great many years, but a complete quantitative model of paint properties and behavior has not been presented. In an effort to facilitate a more quantitative understanding of how paint protects metals from corrosion, a mathematical model has been developed (1). The model is based on ideas presented by several authors. Mayne (2), for example, has pointed out that unpigmented paints retard corrosion primarily by acting as diffusion barriers. Several authors (2-6) have recognized the importance of the diffusion of ions and have studied the membrane potential of paint films. These studies indicate that paint behaves as a low capacity ion-exchange membrane. Ulfvarson (7-9) and others (10, 11) have measured the ion-exchange capacity of a variety of paints in an attempt to relate it to the protective performance of the paints. The diffusion of water in polymers has been considered by Crank and Park (12). They discuss the two major schools of thought concerning water sorbtion and diffusion: adsorption of water by a porous polymer, or disolution of water into a solid organic-polymer phase. The Brunauer, Emmett and Teller (13) (BET) theory of adsorption has been applied to the porous-media model of paint. Solution theories like those

presented by Flory (14) have been used to describe polymers as single-phase solutions.

The concepts presented by these authors form the basis for the mathematical description of the transport properties of paint films. The model describes paint as a protective layer limiting the mass transfer of reactants toward and products away from the corroding metal. The paint posesses ion-exchange capacity and is treated as an organic solution rather than a porous solid. In this manner the model attempts for the first time to quantitatively describe the movement of mobile species through the paint, and further, to relate the various fluxes stoichiometrically to the corrosion process occurring at the paint-metal interface. In order to describe the diffusion of mobile species through paint, a set of equations has been used which are similar to those proposed by Newman (15, p 239) for diffusion in liquids. Newman's equations are, likewise, similar to the Stefan-Maxwell equations describing diffusion in gases (16). These equations are very general in nature and are consequently widely applicable. A program was written to solve the equations using a digital computer. When the correct set of parameters (diffusion coefficients, transference numbers, etc.) (1) are used, the program calculates all the fluxes and concentrations within the paint as functions of the external conditions (solution concentrations, pressure, etc.). The generality of the diffusion equations represents one advantage of the current model over what has been presented previously. A disadvantage of this model is that the equations used here are not as well known as other descriptions of diffusion, and they have only recently been applied to polymer systems (17). In order to test the application of the equations to paint systems and evaluate the parameters required for the model, an experimental investigation of the diffusion of water and ions (sodium and chloride) through polyurethane was undertaken. The experiments have confirmed many of the basic concepts upon which the model was constructed and have led to a new postulate concerning the passage of current through paint membranes.

EXPERIMENTAL

Hittorf Experiments

The classic Hittorf method (18) has been used in an attempt to determine ionic transference numbers and diffusivities in polyurethane films. Hittorf experiments involved recording the current and electrolyte concentrations as functions of time after the application of a fixed potential across the paint films. The polyurethane (#14-9-3-900, Desoto, Inc., Berkeley, California) is used on commercial airplanes and was obtained from The Boeing Company, Seattle, Washington. The paint meets Mil. Spec. C-83286B, USAF. Free films of the polyurethane were prepared by spray painting sheets of decal paper and subsequent stripping. The paint was dried in laboratory air at room temperature and ambient relative humidity. After the paint had dried, it was aged for a period not less than thirty days at ambient temperature and humidity. The paint was stripped from the decal paper, just prior to use, by soaking in water for a few minutes. The free paint film was rinsed until it no longer felt slippery to the

touch and then given a final rinse in distilled water. The paint film was placed in a Plexiglas Hittorf cell in such a way that it formed the separating barrier between two compartments containing electrolyte solutions of identical concentration. After the paint was placed in the cell, the two compartments were filled and the entire apparatus enclosed in an aluminum box acting as a Faraday cage. A potential was applied across the membrane with two identical silver-silver chloride electrodes. The electrodes were parallel to, the same diameter as, and equidistant from the paint film. Periodically the aluminum box was opened for sampling of the aqueous solutions in the two compartments. The solutions were made from reagent grade laboratory chemicals and distilled water. In some cases radioactive tracers of sodium ($^{22}Na^{+}$) and chloride ($^{36}Cl^{-}$) were used. These radionuclides were purchased as soluble salts from commercial sources and were certified to be 99% chemically pure. No attempt was made to control the carbon dioxide or oxygen content of the solutions. The experiments were run at ambient room temperature (≈23°C).

Transference-Number Experiments

Transference numbers were obtained by measuring the membrane potential (6) in the Hittorf-cell apparatus. The basic measurement involved placing a membrane between two solutions of different composition and recording, with an electrometer, the open-circuit potential between the silver-silver chloride electrodes. Radioactive sodium and chloride were used to trace the diffusion of ionic species, and tritium labled water was used to measure the water flux. Small (10 μℓ) samples were periodically drawn off each aqueous solution, and the radioactive tracer contents analyzed by liquid scintillation counting the beta emissions.

Time-Transient Current

The Hittorf-cell apparatus has also been used to obtain measurements of the current transient after application of a potential step function. The current was measured on a Keithley model 616 digital electrometer which produced a voltage output proportional to the current. For experiments shorter than about 1000 seconds, the output voltage was recorded on a Hewlett-Packard model 7046A XY recorder. For longer experiments (t > 1000 sec) a Hewlett-Packard model 7132A strip chart recorder was used. The time constant of the Keithley electrometer was about 0.1 second while that of the XY recorder was about 0.5 second.

Ionic Capacity

The measurement of the ionic capacity of polyurethane has been attempted employing two different methods: specific-ion titrations and radiotracer counting. The latter technique has been the most successful.

Van der Heyden (10) and Khullar and Ulfvarson (9) have indicated that the ion-exchange capacity of paint varies between about 0.01 m mole/g and 0.5 m mole/g, or from about one percent to fifty percent of the capacity of commercial ion-exchange materials. For materials with this high an exchange capacity, aqueous-titration methods should be appropriate. Such techniques have been applied to polyurethane with little success; the

ion-exchange capacity was measured to be 0.00 ± 0.01 m mole/g.

For the second method, a solution of known sodium-chloride composition was prepared using sodium-22 and chloride-36 radiotracers. A preweighed paint sample was allowed to stand in contact with this solution for two weeks. Small samples of the solution were withdrawn periodically for liquid scintillation analysis. After two weeks the paint sample was removed, rinsed three times (for five seconds each) in distilled water, and dried. The paint was then analyzed for sodium-22 and chloride-36.

The energy of the sodium-22 beta decay is very similar to that of the chloride-36. Liquid scintillation techniques cannot, therefore, be used to distinguish between these two elements; however, sodium-22 emits a positron (β^+) with a decay efficiency of 89.8% (19). Each positron produces two 0.511 Mev gamma rays when it is annihilated in the surrounding medium. This fact allows one to coincidence count the gamma radiation from the sodium-22. The technique involves two gamma ray detectors and a timing mechanism. The clock is started when one of the detectors is activated by a gamma ray. If the second detector is excited within 2×10^{-6} sec, a simultaneous event is assumed and a decay is recorded; otherwise the event is ignored. With such apparatus, the counting efficiency is low ($\approx$7.5%), but the chloride-36 interference is reduced nearly to zero.

Using the coincidence counting technique, the sodium-22 content of paint films has been determined. Liquid scintillation methods were then used to establish the sum of the chloride-36 and sodium-22 present in the paint. The chloride content was calculated by difference. Some difficulties have been experinced using this method. They stem primarily from the low salt content (low radioactive activity) of the paint and the low counting efficiency of the coincidence technique; nevertheless, the order of magnitude of the salt concentration has been determined. Further refinements of the experimental and analytical techniques will reduce the uncertainty.

RESULTS AND DISCUSSION

The flux (J) of a neutral species through a film can be described as follows:

$$J = - \frac{P \Delta C}{\ell} \qquad (1)$$

where P = the permeability coefficient, ΔC = the external solution concentration difference, and ℓ = the film thickness (12, p 5). Application of the concepts illustrated in equation 1 to the flux equation for electrolytes in diulte solutions (15, Eq. 82-3) yields

$$J = -P \frac{\Delta C}{\ell} - \frac{zF}{RT} PC \frac{\Delta \phi}{\ell} \qquad (2)$$

where z = the ionic charge, F = the Faraday constant, R = the gas constant, T = the absolute temperature, and ϕ = the electric potential. Equation 2 can be thought of as a definition of the permeability coefficient.

Hittorf experiments have been performed with polyurethane in aqueous sodium chloride solution. These experiments were designed to establish the fluxes of all mobile species under varying conditions of applied potential and electrolyte concentration. The sodium and chloride fluxes were to be determined by adding known quantities of radioactive tracers

$$(10^3 < a < 10^5 \ \mu\text{Curi/mole})$$

to the solution in one of the Hittorf-cell compartments. The results showed that the ionic species fluxes were below the detectable limit, i.e., the concentration change of radioactive tracers was too small to be determined. In contrast, the transport of tritium labled water was easily determined. The results of several experiments are summarized in Table 1. The maximum permeability coefficients for ionic species are indicated. These coefficients were calculated from the maximum fluxes which in turn were calculated from the detection limits of the appropriate isotopes. It is apparent from Table 1 that the permeability coefficients of all the mobile species are small.

The permeability coefficient can be written in terms of the diffusivity and the dimensionless solubility

$$P = DS \tag{3}$$

where D = the diffusivity, and S = the solubility (12, p 5). The small

Table 1

Permeability Coefficients in Polyurethane Free Films at ≈22°C

Mobile Species	P (cm^2/s)	External Conditions	
		Salt Concentration	Potential Difference
Cl^-	< 6.0 E-14	0.1 N	1.5 V
Cl^-	< 6.0 E-14	0.018 N	1.5 V
Cl^-	< 3.8 E-11	0.018 N	0.0 V
Na^+	< 3.0 E-14	0.1 N	1.5 V
Na^+	< 3.3 E-11	0.09 N	0.0 V
H_2O	1.23 E-10	2.5 N	0.14 V
H_2O	3.28 E-10	0.2 N	0.1 V
H_2O	4.06 E-10	0.1 N	1.5 V
H_2O	3.84 E-10	0.09 N	0.0 V
H_2O	4.56 E-10	0.02 N	1.5 V
H_2O	4.56 E-10	0.02 N	0.0 V

magnitude of the permeability coefficient could, therefore, indicate either a low solubility or a low diffusivity.

The solubility of water in polyurethane has been measured in absorption isotherm experiments and has been found to be 1.5% by weight at about 20°C (20). This information has been used to calculate the diffusivity of water in polyurethane. An average value of

$$D_{H_2O} = \frac{P}{S} = 3.2 \times 10^{-8} \pm 35\% \text{ cm}^2/\text{sec} \quad (4)$$

was obtained. This average includes permeability data obtained from diffusion cup experiments (ASTM E96-66, procedure BW) as well as that listed in Table 1.

Radioactive sodium and chloride have been used to measure ion concentrations in the paint. The procedure was the same as that discussed for measuring the ionic capacitance. The paint was allowed to stand in contact with a solution of known composition for a period of time. Samples of the liquid were withdrawn periodically, and after two weeks the paint was removed from the solution, rinsed in distilled water, and analyzed for radioactive tracers. Conservation of mass requires that the total quantity of radioactive materials in both the paint and the solution remain constant; however, some measurement problems may result because the ion concentrations inside the paint are low. Measurements made on the paint film may suffer from the problems of incomplete phase separation which occur when the paint phase is removed from the solution phase prior to counting the radiotracers (21, 22). Any solution left clinging to the paint after rinsing is counted as though it were absorbed inside the paint. On the other hand, measurements of the changes in solution activity suffer from the classic difficulty of measuring a small difference between large numbers. Despite these problems, the order of magnitude of the ion concentrations have been determined in two different radiotracer experiments, both at about 0.1 N NaCl. The ion concentrations from the first and second experiments were, respectively

$$1.6 \times 10^{-8} < C_i < 1.2 \times 10^{-6} \text{ mole/g-paint} \quad (5)$$

$$4.6 \times 10^{-8} < C_i < 1.9 \times 10^{-7} \text{ mole/g-paint} \quad (6)$$

The first experiment was considered less reliable than the second. If a value of $C_i \simeq 10^{-7}$ mole/g-paint is taken as an average, the solubility is calculated:

$$S \simeq \frac{10^{-7}}{10^{-4}} = 10^{-3} \quad (7)$$

The diffusivity of ions in the paint can then be calculated from the permeability data (Table 1)

$$D_i \simeq 6 \times 10^{-11} \text{ cm}^2/\text{sec} \quad (8)$$

The ionic capacity of several types of paint has been measured previously (7-11). In these studies fairly high values of ionic capacity were obtained by conventional titration techniques. Measurement of the ionic capacity for this type polyurethane has been attempted using these same methods. The technique has a sensitivity of about 10^{-2} m mole/g-paint, but no detectable ion-exchange capacity was observed. This is consistent with the results of Khullar and Ulfvarson (9) who reported the ion-exchange capacity of another polyurethane as zero at pH values below seven. At a pH of eight they observed a moderate ion-exchange capacity (0.35 m mole/g-paint). Higher capacity at high pH was not observed in this investigation. Although the ion-exchange capacity has not been determined, an upper bound of about 10^{-2} m mole/g-paint can be established from these results. This upper bounding value is also consistent with the ion content of the paint determined by radiotracer experiments

$$C_i \leq 1.9 \times 10^{-4} \text{ m mole/g-paint } (0.19 \text{ mole/m}^3) \quad (9)$$

Current transients have been recorded after the application of a potential step function across a polyurethane film. These data were analyzed to obtain two pieces of information: the time constant for current decay and the apparent steady-state conductivity. The conductivity of the paint film was expected to be qualitatively similar to that for an ion-exchange material. Fig. 1 shows the steady-state conductivity for a polyurethane free-film in sodium chloride solution. Activity coefficients were calculated from the data of Robinson and Stokes (23). The shape of the curve is as predicted, with a conductivity plateau at low solution concentrations and a slope of one at high concentrations. The solid curve represents a mathematical model best fit of the conductivity data. The conductivity becomes constant at low concentrations

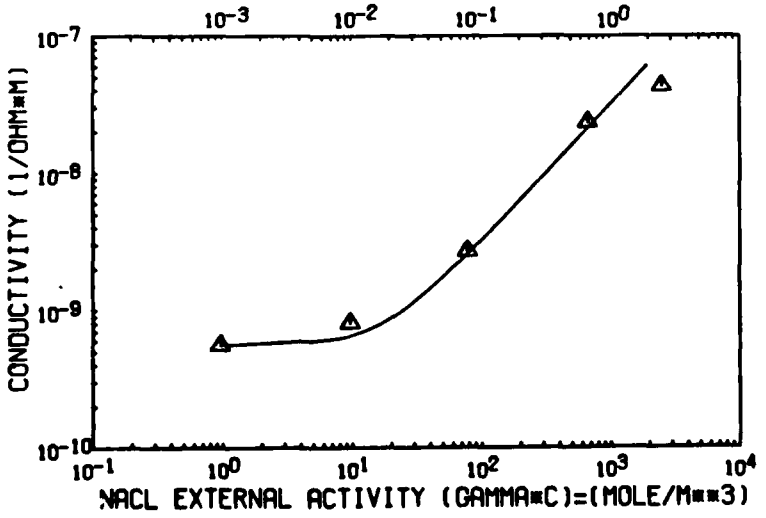

Fig. 1 Polyurethane conductivity in aqueous NaCl at 22°C. Top scale units are mole/ℓ. Symbols represent experimental data. Solid curve is the computer calculated "best fit."

when the ion content of the paint is limited by the membrane ionic capacity. Donnan exclusion is operating in this concentration region. At higher salt concentrations the ion concentration in the membrane is determined primarily by the external solution concentration and the ionic distribution coefficients.

The second body of information available from the transient-current experiments centers around the determination of the time constant for decay of the transient. Interpretation of these data is complicated by the fact that the results are highly erratic. Similar observations have been previously reported for measurements of other dynamic properties of polymers (12). The measured properties appear to be related to the history of the polymer. Thus, attempts were made to achieve a uniform condition of the paint prior to testing, but the erratic behavior was unaffected. One of these attempts involved conditioning the paint in the test solution for various lengths of time up to three days (72 hours). Other attempts included conditioning in various solutions (distilled water, for example) at temperatures up to about 55°C, and conditioning in methanol (a water soluble, non-aqueous solvent) then test solution. Despite the failure of these conditioning procedures to eliminate the experimental noise, enough experiments have been conducted to allow qualitative, and even semi-quantitative evaluation of the current-transient results.

The analysis of the transient current passing through a free film of polyurethane shows that several phenomena are taking place. Fig. 2 qualitatively illustrates the current as a function of time after application of a potential step function. The time scale can be divided

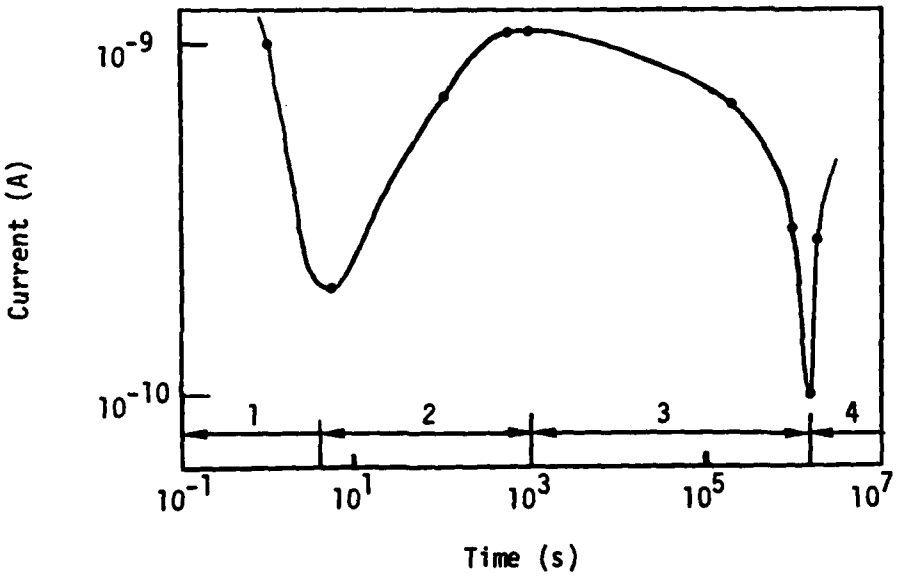

Fig. 2 Qualitative transient current through polyurethane immersed in NaCl solution following the application of a 1 V step function.

into four regions representing four types of transient behavior. In region 1 ($t < \approx 4$ sec) the paint film-solution-electrode circuit can be analyzed as a parallel resistor-capacitor network in series with a second resistor. This equivalent circuit indicates that the current is expected to be high immediately after the step potential and decay rapidly to a low level. The increasing current in region 2 (4 sec < t < 1000 sec) cannot be explained by the R-C network unless the resistance values change. In this region the conductivity of the paint is increasing resulting in an increased flow of current which eventually reaches an apparent steady-state at about one thousand seconds. The reasons for the increasing conductivity of the paint in region 2 are not entirely clear, but must be related to the uptake of either salt or water from the external solution. In either case, the rate of change of concentration inside the paint is expected to be diffusion limited. The time constant for diffusion is thus related to the observed changes of current in region 2. An explanation of the decreasing current in region 3 (1000 sec < t < $\approx 10^6$ sec) is not yet available, but in this time range molecular rearrangements within the polymer are possible. Thus such phenomena as stress relaxation or creep may be important. This is also the region which corresponds with the time constant for ionic diffusion ($\tau = \ell^2/D_i = 4.2 \times 10^5$ sec). In region 4 ($t > 10^6$ sec) physical and chemical changes within the polymer are possible. Tests of the quasi-equilibrium properties of paints conducted at this laboratory have shown plasticizer concentrations change in this time region. Also, the diffusivity of water obtained from diffusion cup experiments changes on this time scale. Our understanding of processes occurring throughout the time range studied is incomplete, but clearly more variables enter the analysis at longer times. In an effort to minimize the unknown factors it is desirable to conduct studies over short time intervals. The current transients in region 1 were largely lost because of the relatively slow response of the recording equipment. Further discussions will thus be limited to region 2 where the current is expected to be limited by the diffusion rates of mobile ions.

Crank (24) has described the diffusion of neutral species across a membrane under the influence of a concentration gradient. He shows that for this type of diffusion the fluxes can be described by an infinite series involving a single dimensionless parameter

$$\frac{Dt}{\ell^2} \qquad (10)$$

where D = the diffusion coefficient, t = time, and ℓ = the membrane thickness. In concentrated solutions, when Donnan exclusion is not operative, the diffusion fluxes depend on the same parameter (Eq. 10) for the case of ions diffusing through paint under the influence of a potential gradient. Crank has also presented a mathematical description of the average concentration of diffusing species in the membrane as a function of the same dimensionless parameter. Thus, one can expect the quasi-steady-state current (region 2) to be related to the diffusivity of mobile ions through an equation similar to that presented by Crank. This being the case, an analysis of the transient current can be expected to produce information

about the diffusivities of ions in the paint phase.

Time constants for the decay of the quasi-steady-state current have been measured using the formula

$$\frac{i_\infty - i}{i_\infty - i_o} = e^{-\frac{t}{\tau}} \tag{11}$$

where i_∞ = the current at "infinite" time ($10^3 < t < 10^4$ sec), i_o = the current at time zero, i = the current at time = t, and τ = the time constant. Current-decay time constants for polyurethane in sodium chloride solutions have been found to be about 1000 sec for 5×10^{-3} cm thick paint films. By equating the time constants of diffusion and current decay, an ionic diffusivity can be calculated

$$D = \frac{\ell^2}{\tau} \tag{12}$$

where ℓ = the paint thickness. For a 5×10^{-3} cm thick paint film, and τ = 1000 sec, a diffusivity

$$D = 2.5 \times 10^{-8} \text{ cm}^2/\text{sec} \tag{13}$$

is calculated. It is interesting to note that this is three orders of magnitude higher than the ionic diffusivity estimated previously (Eq. 8), but it is nearly identical to that measured for water (Eq. 4).

The fact that the current-transient time constant (τ = 1000 sec) is small compared to that estimated previously ($\ell^2/D_i = 4.2 \times 10^5$ sec) is not entirely surprising. The ionic diffusivity (D_i, see Eq. 8) was estimated from the maximum ionic flux and a measured value of the ionic concentration. The concentration measurement was subject to a possible error resulting from incomplete phase separation (21, 22). The error would tend to make the ionic concentration appear too high, and this in turn would produce a low diffusivity (Eq. 3). It is not likely that these experiments are subject to a three-orders-of-magnitude error, as would be required to resolve the discrepancy between the two estimates of the ionic diffusivity. The measurement of the ionic concentration in polyurethane has been repeated three times using a single paint sample, and the results were reproduced within $\pm$ 10%. This consistency is unlikely when incomplete phase separation is a problem. The data indicate, then, that although the apparent ionic diffusivity may be slightly low, a large discrepancy is unlikely, and the ionic diffusivity is much too low to explain the observed time constants for current decay.

A second explanation of the difference between the two time constants should be explored; the presence of additional mobile ions. Only reagent grade (99.8% NaCl) sodium chloride solutions have been investigated in this study. It appears unlikely that a salt impurity could be present and

possess a selectivity coefficient high enough to appear in significant concentrations within the paint film. Another possibility exists; hydrogen and/or hydroxyl ions are carrying the current. These ions are fundamentally different from those of a completely-dissociated salt like sodium chloride. They are the dissociation products of a neutral molecule, water, which is known to be present in the paint. The fact that the electrical resistance of some paint films increases with the activity of water has been previously observed (25, 26) and is consistent with this possibility. Dissolved carbon dioxide is another neutral molecule which exists in equilibrium with ionic species. Thus, ambiguity exists over which compound, carbon dioxide or water, is providing the ions at low salt concentrations. Experiments have not been performed in a carbon-dioxide-free atmosphere making elucidation of the ambiguity impossible at this time. Further research will clarify the point, but for the purposes of this discussion, only the water equilibrium will be considered.

This view of the role water plays in affecting current conduction in paints is further supported by the transference-number data illustrated in Fig. 3. The cell potential is shown as a function of sodium chloride activity for experiments in which a polyurethane film separates two solutions containing different concentrations of sodium chloride. In these experiments the concentration on side two was held constant while the side-one concentration was varied. The experimental data are symbol plotted, and the solid curves represent the computer solution of the mathematical model for the case when the paint behaves as a conventional ion-exchange membrane. All the computer generated curves illustrated in both Figs. 2 and 3 were calculated using one set of relevant parameter values. The curve through the conductivity data was constructed first by adjusting the parameters to obtain a good fit. Once the conductivity data had been successfully

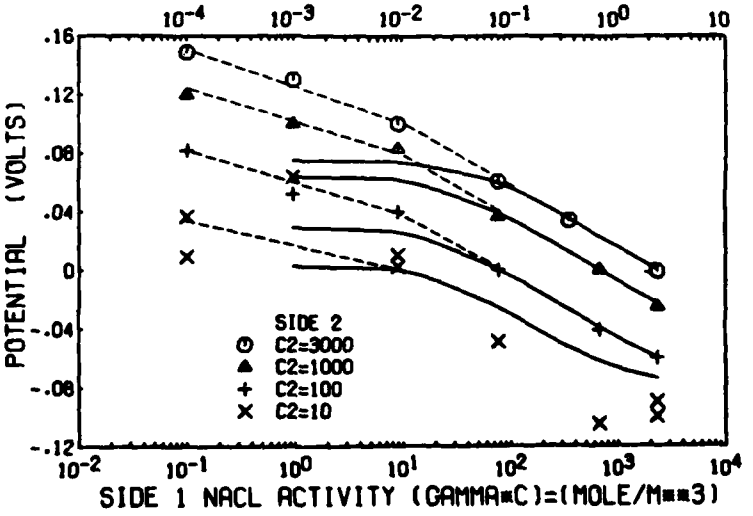

Fig. 3 Transference number data for polyurethane in NaCl solution. Top scale units are mole/ℓ. Symbols are experimental data. Solid lines are the computer simulation of an ion exchange membrane. Dashed straight line segments are compatable with the three-transference-number mechanism.

modeled, only one parameter, the ionic diffusivity ratio (D+/D-) for sodium chloride, was varied to obtain the four "computer curves" shown in Fig. 3. Fig. 3 shows that when the paint is modeled as an ion-exchange membrane the slope approaches zero at low concentrations. Alternatively, when the conductivity results from water dissociation, one can expect the potential to depend on three transference numbers (Newman (15), section 17). The exact nature of this dependence cannot be predicted without solving the diffusion equations for this new model, but the equations indicate that, just as in the ion-exchange case, two concentration regions can be identified. At high salt concentrations the membrane will behave as before with the potential falling as the concentration on side one increases. The slope of the potential versus concentration curve in this region is determined primarily by the sodium-ion transference number. In the low concentration region the slope of the curve depends most on the hydroxyl-ion transference number. Thus the slope in the dilute region does not go to zero as for the ion-exchange membrane, and if the concentration dependence of the transference number can be ignored, straight lines can be expected. The dashed lines drawn through the data in Fig. 3 illustrate this point. Parallel lines are to be expected in both the low and high concentration ranges if the three-transference-number mechanism is operative, but are more difficult to explain if the slope changes because the ionic diffusivities are concentration dependent. With the exception of the experimental series having the lowest side-two concentration (C_2 = 10 mole/m^3), the data appear to be well represented by two straight lines. When the side-two concentration was dilute (C_2 = 10 mole/m^3), the data were erratic and subject to considerable experimental error. Despite this difficulty, these dilute side-two data can also be approximated by two straight line segments. Thus the majority of these data qualitatively support the conclusion that the conductivity of polyurethane films exposed to dilute salt solutions is determined primarily by ions resulting from the dissociation of neutral species within the paint. A quantitative check of this new mechanism is planned employing an updated version of the original mathematical model.

The hypothesis that two ionically dissociating species (NaCl and H_2O) are present within the polyurethane membrane is supported by the results of two different types of experiments: time-transient current, and transference-number experiments. The time-transient-current experiments yield low time constants, and hence ionic diffusivities which are three orders of magnitude higher than the best estimates based on NaCl ionic flux and solubility data. These experiments represent dynamic measurements and suffer from the classic difficulties associated with the effects of polymer history. The transference-number experiments, on the other hand, represent steady-state measurements and appear to be much less affected by polymer history. The transference-number experiments indicate that two ionically dissociating species (at least three ionic species) are present within the paint, and that the primary current-carrying ions change with concentration. The presence of a significant concentration of a second salt is unlikely. One is thus forced to conclude that water itself represents the most likely second ionicically dissociating species. This conclusion is supported qualitatively by Mayne (25) and by the data of Kittelberger and Elm (27).

The hypothesis is also consistent with the results of the Hittorf, ionic-capacity, and conductivity data obtained in this laboratory. It should be noted, however, that a limited number of experiments have been performed at this time, and although the results are encouragingly consistent, further tests will be required to verify the hypothesis.

CONCLUSIONS

The following conclusions are based on mass transport and supporting experiments carried out on a commercial, unpigmented, polyurethane paint meeting Military Specification C-83286B(USAF):

1. The diffusivity of water in polyurethane is about 3.2×10^{-8} cm^2/sec.

2. The concentration of mobile ions in polyurethane exposed to 0.1 N NaCl solution at 22°C is

   $$C_i < 1.2 \times 10^{-6} \text{ mole/g-paint},$$

   and is probably close to

   $$C_i \simeq 10^{-7} \text{ mole/g-paint}.$$

3. The permeability of polyurethane to sodium and chloride ions is low.

   $$P \leq 6 \times 10^{-14} \text{ cm}^2/\text{sec}$$

   under the exposure conditions investigated

   $$C = 0.1 \text{ N NaCl}$$

   $$\Delta\phi = 1.5 \text{ V}$$

4. The mechanism of ionic conduction in polyurethane changes as the external electrolyte concentration changes. At high concentrations the conductivity increases as the electrolyte concentration increases, indicating conduction by soluble ionic salts. At low concentrations, the membrane conductivity appears to be determined by the concentration of ions resulting from dissociation of neutral species, such as water.

ACKNOWLEDGMENT

This work was supported by Air Force Office of Scientific Research Contract No. F49620-76-C-0029, and by Naval Ocean Research and Development Agency Contract No. N00014-79-C-0021. Thanks also to William P. Miller, Assistant Director of Reactor Operations, Nuclear Reactor Laboratory,

University of Washington, for his assistance with the coincidence counting experiments.

REFERENCES

1. R. T. Ruggeri and T. R. Beck, "A Model for Mass Transport in Paint Films," Corrosion Control by Coatings, Henry Leidheiser, Ed., Science Press, Princeton, 1979, p 455.
2. J. E. O. Mayne, J. Oil and Colour Chem. Assoc., 32, 481 (1949).
3. E. M. Kinsella and J. E. O. Mayne, Proc. Third Int. Congress on Metallic Corrosion, Vol 3, p 117, Moscow, 1966 (1969).
4. W. W. Kittelberger and A. C. Elm, Ind. Eng. Chem., 44 (2), 326 (1952).
5. C. A. Kumins, Official Digest, 34, 843 (1962).
6. C. A. Kumins and A. London, J. Polymer Sci., 46, 395 (1960).
7. U. Ulfvarson and M. Khullar, J. Oil Col. Chem. Assoc., 54, 604 (1971).
8. U. Ulvarsson, J. L. Khullar, and E. Wahlin, J. Oil Col. Chem. Assoc., 50, 254 (1967).
9. M. L. Khullar and U. Ulfvarson, IX FATIPEC Congress, 1968, Section 3, p 165.
10. L. A. van der Heyden, XI FATIPEC Congress, 1972, p 475.
11. W. U. Malik and L. Aggarwal, J. Oil Col. Chem. Assoc., 57, 131 (1974).
12. Diffusion in Polymers, J. Crank and G. S. Park, Eds., Academic Press, New York, 1968.
13. Catalysis, P. H. Emmett, Ed., Reinhold, New York, 1954, p 31.
14. P. J. Flory, Principles of Polymer Chemistry, Cornell University Press, New York, 1953, p 495.
15. J. S. Newman, Electrochemical Systems, Prentice-Hall, New Jersey, 1973.
16. R. B. Bird, W. E. Stewart, and E. N. Lightfoot, Transport Phenomena, John Wiley, New York, 1960, p 570.
17. W. B. Sunu and D. N. Bennion, Ind. Eng. Chem. Fundam., 16 (2), 283 (1977).
18. D. A. MacInnes, The Principles of Electrochemistry, Dover, New York, 1961, p 65.
19. L. Slack and K. Way, Radiations from Radioactive Atoms in Frequent Use, U.S. Atomic Energy Commission, Washington, DC, 1959.
20. T. R. Beck and R. T. Ruggeri, "A Study of Transport Processes and Initiation of Corrosion Under Paint Films," Final Report for Air Force Office of Scientific Research done under Contract No. F49620-76-C-0029, Washington, DC, 1979.
21. G. E. Boyd and K. Bunzl, J. Am. Chem. Soc., 89, 1776 (1967).
22. E. Glueckauf and R. E. Watts, Proc. Royal Soc. (London), A268, 339 (1962).
23. R. A. Robinson and R. H. Stokes, Electrolyte Solutions, Butterworths, London, 1959.
24. J. Crank, The Mathematics of Diffusion, 2nd ed., Clarendon Press, Oxford, 1975.
25. J. E. O. Mayne, J. Oil Col. Chem. Assoc., 40, 183 (1957).
26. C. C. Maitland and J. E. O. Mayne, Official Digest, 34, 972 (1962).
27. W. W. Kittelberger and A. C. Elm, Ind. Eng. Chem., 39 (7), 876 (1947).

AN INVESTIGATION OF THE MASS TRANSFER CHARACTERISTICS OF POLYURETHANE PAINT

R. T. Ruggeri and T. R. Beck

Electrochemical Technology Corp.
3935 Leary Way N.W.
Seattle, WA 98107

INTRODUCTION

Mechanisms of corrosion protection by organic paint films are not yet quantitatively understood even though paints have long been employed as corrosion inhibiters. A review of the literature shows that many variables are involved in the protective performance of paints. However, prior investigators have attempted to correlate protective performance with only one or two of these variables at a time. The result has been imperfect correlation and incomplete understanding of the protection mechanisms.

Evaluation of a comprehensive mass transport model is described in this paper. A model proposed for use with different paint systems must be flexible and consider a large number of physical parameters (potential, concentration, pressure, etc.). Certain concepts concerning the nature of paint and corrosion have been developed in order to formulate this model in which the paint film is assumed to be a continuous-phase diffusion barrier and metal surface reaction kinetics are described mathematically through boundary conditions. A series of experiments has been performed, and the results compared to those predicted by the model. From these comparisons important conclusions have been drawn indicating that several of the basic concepts forming the foundation of the model are correct. Experimental data are incomplete, however, and a complete evaluation of the model cannot be made at this time.

MATHEMATICAL MODEL

Ambient temperature corrosion of metals involves electrochemical oxidation in the presence of oxygen and an electrolyte (1). The overall reaction rate is generally limited by either diffusion or reaction kinetics. Although electrode reaction kinetics and equilibrium cell potentials are the most widely used tools for studying corrosion, in practical systems local concentration and potentials are usually determined by mass transport. A corrosion model has therefore been developed for painted metals which emphasizes the mass-transfer aspects of the corrosion process. The basic rate-limiting step is either diffusion of a reactant toward, or of a product away from the corroding metal surface through a paint-phase electrolyte.

The question of whether the paint can be treated as a continuous-phase (solution) or would be more accurately represented as a porous medium has been addressed. (Guggenheim (2) has discussed the continuously varying properties of a continuous-phase.) The solubility of water in polymers has historically been treated either as adsorption onto a porous solid, or as dissolution in a single-phase solution. An adsorption theory, like that developed by Brunauer, Emmett, and Teller (3), applies to the former while the work of Flory (4) has been applied to the latter. For the porous-media model, Mayne (5, 6) has concluded that the maximum pore radius is near 1000 angstroms. Large holes ($r \approx 1000$ Å) in a paint are considered here as macroscopic defects, and any smaller-radius pathways, occurring randomly throughout the paint, are treated by application of a continuous-phase model. This view was confirmed, on theoretical grounds, by Kedem (7) who showed that by proper choice of parameters the equations describing a general continuous-phase membrane model reduce to the same form as those based on diffusion through porous media.

In addition to modeling the paint as a solution, the nature of the

solution must be considered. In general, a polymer can contain ionizable sites. The concentration (C_m) of these sites is a property of the paint which must be determined, but for any non-zero C_m, paint posesses the fundamental characteristic of an ion-exchange resin. Although the ion-exchange capacity of paint has been recognized by some authors (5, 8-10), it is not widely discussed in the literature. Inclusion of C_m in the model represents an example of the flexibility discussed in the introduction because the paint phase loses its ion-exchange character as C_m goes to zero. This model is thus capable of describing a wide range of cases representing different ion-exchange characteristics of paint.

The flexibility of the model is increased by including a variable ion-exchange capacity (C_m). Flexibility can be further achieved by using general equations to describe the diffusion and migration of mobile species through the paint. Such a system of equations is proposed by Newman (11) for aqueous electrolytes and has been adapted here to represent diffusion through the paint phase (12). Sunu and Bennion (13) have presented a similar set of equations to describe ionic transport in cellulose acetate membranes. All of these equation sets (diffusion models) are based on, and are similar to, the Stefan-Maxwell equations which describe diffusion in gases (11, 14). The diffusion equations describe the flux of each mobile species as a linear combination of all the driving forces, in this case the gradients of all the electrochemical potentials. Although the form of these equations is fixed by the theory, the values of the coefficients of the driving forces are unknown and must be evaluated from experimental data. For a system containing n mobile species there are in general $\frac{1}{2}n(n + 1)$ unknown coefficients (7). This large number of coefficients is a consequence of the general nature of the Stefan-Maxwell equations and represents one cost of using a flexible model.

Despite its complexity, the model posesses the advantages of generality and is capable of correlating a large number of experimental observations related to diffusion through membranes. The large number of coefficients raises one question; can the model be inappropriately made to fit nearly any experimental observation? The large number of coefficients can be deceiving in this regard because the functional form of the Stefan-Maxwell equations is fixed. Furthermore, a large number of diverse phenomena are to be described, including diffusion under concentration gradients as well as under potential or pressure gradients. Although it is possible to accurately model a single type of diffusion by taking advantage of the number of coefficients, the subsequent use of those coefficients to describe a second or third type of diffusion invariably fails unless the original model posesses the correct functional form. Thus, the best test of this model is the simultaneous description of several diverse experiments. Such a test is in the process of completion, and the preliminary experimental results support several of the basic concepts upon which the model is based, thereby indicating the validity of the model.

EXPERIMENTAL

Using the mathematical model as a guide, a series of experiments has been undertaken to determine the diffusional rate parameters (coefficients) for a particular polyurethane paint (Mil. Spec. C-83286B, USAF). This polyurethane (#14-9-3-900, Desoto, Inc., Berkeley, Calif.), used on commercial airplanes, was obtained from The Boeing Company, Seattle, Washington. Clear, unpigmented, free films were used for all experiments. The films were formed by spray painting sheets of decal paper. After the films dried, the paint was easily removed by soaking the paper in water for a few minutes.

All experiments were made in the same apparatus consisting of a Plexiglas cell in which a free film of polyurethane separates two compartments containing aqueous solutions. Potentials in the aqueous solutions were measured by two identical silver-silver chloride electrodes, and provisions were made for sampling the solution compositions as time passed. Both aqueous solutions were stirred with Teflon coated magnets.

Three types of experiments are commonly used to investigate diffusion in

membranes: Hittorf, concentration gradient, and pressure gradient. In the Hittorf experiments, the current and concentrations are monitored as functions of time while a fixed potential is applied across the membrane. The concentration changes are recorded by using radioactive isotopes of sodium (Na^{22}) and chloride (Cl^{36}). The primary driving force is related to the externally-specified potential difference. By measuring the total current and potential difference, the steady-state conductivity can be determined, and by measuring concentration changes, the ionic transference numbers can be calculated. Electrical time-transient experiments have also been conducted in an Hittorf cell. The current-time transients were monitored after the application of a potential step change. Concentration changes were not measured, although the primary driving force was still the applied potential difference.

The primary driving force in the second type of experiment is a concentration gradient. In these transference-number experiments the membrane separates two solutions of different composition. Usually the open-circuit potential and concentrations are monitored as functions of time. If the mobile species concentrations within the membrane are known, or can be assumed or calculated, measurement of the open-circuit potential yields ionic transference numbers.

The third type of experiment involves the diffusion of mobile species under the influence of a pressure gradient. These experiments require more-complicated apparatus than the first two types, and remain to be conducted.

In addition to the diffusion-type experiments, water absorption isotherms have been obtained to establish the solubility of water in polyurethane. These experiments are conducted by exposing paint samples to constant-humidity atmospheres and measuring the weight change with a Cahn (gram) electrobalance. Constant humidities are maintained with saturated solutions of various salts. Only one temperature has been thoroughly investigated at this time (20°C ± 3°C).

RESULTS AND DISCUSSION

Hittorf experiments have been used to measure the steady-state conductivity while monitoring mobile species fluxes with radiotracers. The flux of a neutral species can be written as follows:

$$J = \frac{P\Delta C_{ex}}{\tau} \qquad (1)$$

where ΔC_{ex} = the external concentration difference across the membrane, τ = the thickness, and P = the permeability coefficient. A similar expression holds for ionic species, but an additional term expressing the effect of a potential difference is required. Equation 1 can be used to calculate the permeability coefficients from flux measurements. Analysis of Hittorf data using tritium labled water has allowed the permeability coefficient of water to be determined. Similar techniques have been unsuccessful for determination of the ionic fluxes because the fluxes of both sodium and chloride have been below the detectable limit. Despite this uncertainty, the detection limit of the radiotracer method can be used to establish an upper bound on the ionic fluxes and permeability coefficients. The permeability data from several experiments is shown in Table 1.

The permeability data in Table 1 indicate that the ionic species permeate the paint much more slowly than does water. Even at the potential difference of 1.5 V the ionic flux is less than the water flux ($\Delta C_w = 10^{-8}$ M). These observations at first seem to support Mayne's contention that ionic transport is the rate limiting step (1, 5, 6). However, another possibility for corroding metal is that no ions actually diffuse through the paint film. In this case the ions present at the metal surface before painting are simply covered over by the paint, and the corrosion mechanism is not limited by ionic diffusion but by oxygen or water transport. In any case the low permeability coefficients in Table 1 indicate that, for unpigmented poly-

urethane, the assumption that diffusion is the rate-limiting step was justified.

Absorption isotherms for the polyurethane-water system obtained at 20°C are not particularly well modeled by any of the five Brunauer, Emmett and Teller (BET) type isotherms. The isotherms show slight upward curvature as the partial pressure of water increases, but have a definite weight fraction at the saturation pressure. One can fit the data quite well, however, by including a linear term in the activity coefficient expansion. Thus

$$\gamma_{H_2O} = H + Af_w \qquad (2)$$

where H and A are constants and f_w = the weight fraction of water. This is exactly the behavior commonly encountered when describing ordinary liquid solutions. Similar results were found when the membranes were equilibrated with saturated sodium chloride solution before performing the absorption isotherm experiment. These data indicate that the paint phase can be treated as a homogeneous solution rather than a porous solid, thereby supporting the assumption made about the nature of the paint phase.

Fig. 1 illustrates the variation of conductivity of a polyurethane free film with external electrolyte activity. Fig. 1 shows a plateau at low salt activity. This is exactly the form expected if the membrane posesses fixed ionic species, i.e., the membrane is an ion-exchange material. This form of the conductivity versus concentration curve is difficult to explain on the basis of a solution containing a single electrolyte, i.e., if the paint does not posess ion-exchange capacity.

The curve through the conductivity data of Fig. 1 is the model prediction based on an optimized value of the polyurethane ionic capacity (C_m). The conductivity data are adequately modeled. Fig. 2 compares the model predictions (solid curves) to transference-number experimental results (symbols). The same set of transport coefficients and C_m were used in modeling both types of experiments. The transference-number experiments were conducted by holding the sodium chloride concentration on side two of the membrane constant and varying the concentration on side one while recording the potential difference across the film. Agreement between the model and the experimental results is quite good at high salt activities, but when one side of the membrane is at a low activity the experimental results become erratic, and the model fails to agree.

One possible explanation of this descrepancy is that the ionic diffusivities are concentration dependent. This explanation seems likely in view of the fact that the most commonly used models of diffusion in polymers are based on free-volume theories, and most of these theories predict an exponential dependence of the diffusivity on concentration (15). Although the mathematical model is quite capable of incorporating this additional complexity, the results illustrated in Fig. 2 were calculated assuming constant diffusivities for all mobile species.

Another possible explanation of the discrepancy might be the presence of additional mobile ions. These ions might be H^+ or OH^- in aqueous systems. The presence of ions other than chloride or sodium is further supported by some Hittorf conductivity data. The total Hittorf current passed is greater than that calculated for the upper bound ionic fluxes, indicating an additional ionic species is carrying current. If these species are H^+ and OH^- it is clear that their concentrations in the paint phase are important. The ion concentrations are determined by the chemical equilibrium with water, and consequently the water content of the paint. This may explain Mayne's (6) conclusion that when paint resistance is high (low conductivity) it is controlled by water uptake rather than external electrolyte concentration. Either of these two explanations of the transference-number results may eventually prove to be correct. In either case the model will remain acceptable; is can describe both situations. This fact again illustrates the flexibility and generality of the model.

CONCLUSIONS

The following conclusions are based on mass transport and supporting experiments carried out on a commercial, unpigmented, polyurethane paint meeting Military Specification C-83286B(USAF):

1. Mass transfer of various molecular and ionic species through this paint film limits the corrosion rate of painted metal surfaces.
2. The polyurethane paint phase is more adequately described as a solution than as a porous medium.
3. This polyurethane is a weak ion-exchange medium.
4. In general, ion-exchange capacity must be included in a mass transport model for paint films.
5. The increased complexity of the proposed mathematical model is justified in terms of the increased flexibility and accuracy obtained.

ACKNOWLEDGMENT

This work was supported by Air Force Office of Scientific Research Contract No. F49620-76-C-0029, and by Naval Ocean Research and Development Agency Contract No. N00014-79-C-0021.

REFERENCES

1. Mayne, J.E.O., Trans. Inst. Metal Finishing, 29, 146 (1953).
2. Guggenheim, E.A., Thermodynamics, North-Holland, Amsterdam, 1957.
3. Emmett, P.H., Catalysis, Vol. 1, Reinhold, New York, 1954.
4. Flory, P.J., Principles of Polymer Chemistry, Cornell Univ. Press, Ithaca, N.Y., 1953.
5. Mayne, J.E.O., Br. Corrosion J., 5, 106 (1970).
6. Mayne, J.E.O., J. Oil and Colour Chem. Assoc., 40, 183 (1957).
7. Kedem, O. and Katchalsky, A., J. Gen. Physiol., 45, 143 (1961).
8. Ulfvarson, U., and Khullar, M., J. Oil Color Chem. Assoc., 54, 604 (1971).
9. Malik, W.U. and Aggarwal, L., J. Oil Color Chem. Assoc., 57, 131 (1974).
10. van der Heyden, L.A., XI FATIPEC Congress, 475 (1972).
11. Newman, J.S., Electrochemical Systems, Prentice-Hall, New Jersey, 1973.
12. Ruggeri, R.T. and Beck, T.R., Corrosion Control by Coatings, H. Leidheiser, Ed., Science Press, Princeton, 1979, p. 455.
13. Sunu, W.G. and Bennion, D.N., Ind. Eng. Chem. Fundam., 16 (2), 283 (1977).
14. Hirschfelder, J.O., Curtiss, C.F., and Bird, R.B., Molecular Theory of Gases and Liquids, Wiley, New York, 1954.
15. Fang, S., The Permeation of Gases through Polyethylene Membranes at High Pressures. A "Free-Volume" Model of Permeation, Ph.D. thesis, Syracuse Univ., 1975.

Table 1

Permeability Coefficients in Polyurethane Free Films at ≈22°C

Mobile Species	P (cm^2/s)	External Conditions	
		Salt Concentration	Potential Difference
Cl^-	< 2.0 E-12	0.1 N	1.5 V
Cl^-	< 1.3 E-12	0.018 N	1.5 V
Cl^-	< 3.8 E-11	0.018 N	0.0 V
Na^+	< 1.1 E-12	0.1 N	1.5 V
Na^+	< 3.3 E-11	0.09 N	0.0 V
H_2O	1.23 E-10	2.5 N	0.0 V
H_2O	3.28 E-10	0.2 N	0.0 V
H_2O	4.06 E-10	0.1 N	1.5 V
H_2O	3.84 E-10	0.09 N	0.0 V
H_2O	4.56 E-10	0.02 N	1.5 V
H_2O	4.56 E-10	0.02 N	0.0 V

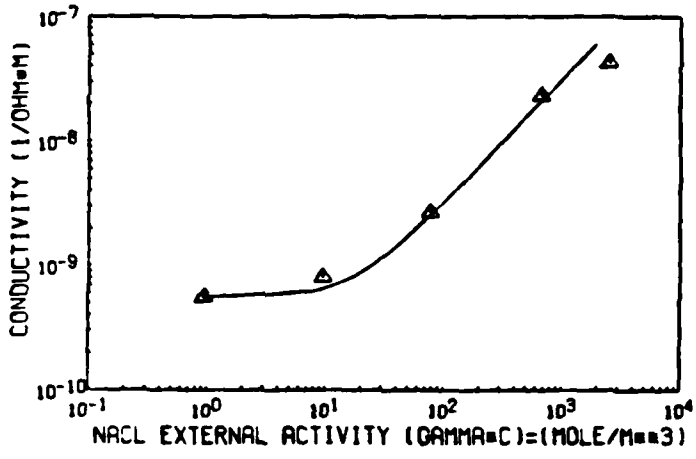

Fig. 1 Polyurethane conductivity in aqueous NaCl at 22°C.

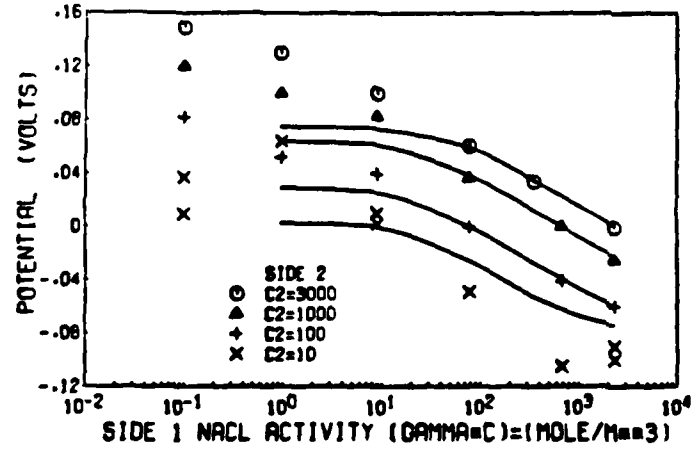

Fig. 2 Polyurethane transference-number data in aqueous NaCl at 22°C.